Addis Ababa University

Addis Ababa Institute of Technology

School of Civil and Environment Engineering

Optimization Of Retaining Wall Types For Deep Excavation Of Addis Ababa Clay Soil

A Thesis in Geothechnical Engineering

BY

MUNIK ABRAR

May,2020

Addis Ababa, Ethiopia

A Thesis submitted to school of Graduate Studies of Addis Ababa Institute of Technology in partial fulfillment of the requirements for the Degree of Master of Science in Geotechnical Engineering.

Advisor

Henok Fikre (Dr.-Ing)

The undersigned have examined the thesis entitled **"Optimization of Retaining Wall Types for Deep Excavation of Addis Ababa Clay Soil"** presented by **Munik Abrar** , a candidate for the degree of **Master of Science** and hereby certify that it is worthy of acceptance.

Henok Fikre (Dr.-Ing)	_____	_____
Advisor	Signature	Date
Tezera Firew (Dr.- Ing)	_____	_____
Internal Examiner	Signature	Date
Samuel Taddesse(Dr.-Ing)	_____	_____
External Examiner	Signature	Date
_____	_____	_____
Chair Person	Signature	Date

DECLARATION

This thesis is presented in partial fulfillment of the requirements for master of degree at Addis Ababa University. Following this I grant the University the nonexclusive royalty free to archive, reproduce, distribute and display the thesis in any and/or all forms, including electronic format, via any digital library maintained by AAU/AAiT.

I certify that research work titled "**Optimization of Retaining Wall Types for Deep Excavation of Addis Ababa Clay Soil**" is my own work. The work has not been presented elsewhere for assessment. Whereas, material and sources used for research, have been properly acknowledged / referred.

Munik Abrar Awol

Signature: _____

amunik1984@gmail.com

ABSTRACT

Construction of retaining wall type for deep excavation is always anticipated in urban areas especially in Addis Ababa where construction is highly growing due to the limited availability of land. The most common type of retaining wall for deep excavation in the city is contiguous bored pile wall. This retaining method may not be effective in terms of various parameters like soil type, embedment depth, size of the wall and construction cost. Thus other alternative retaining systems should be considered and analyzed to select a best option. The results presented in this paper are for specific types of retaining structures. i.e. diaphragm and contiguous bored piles. Actual site selected for this study was around commercial college of Addis Ababa University, Addis Ababa.

In this research, diaphragm wall and contiguous bored pile have been considered for the analysis. by employing the finite element software Plaxis 2D. The primary goal of this thesis was to study the effects of the two walls for deep excavation in terms of wall deflections and cost incurred. The effects of wall stiffness, embedment depth and no of Anchors have been investigated for that purpose in detail.

The Finite element results shows for both DW and CBP, an increase in stiffness (size of the wall), decrease deformation.BS 8002 recommends, the wall displacement is to be limited to 0.5% of the wall height. Because of this those wall sections above 600mm fulfill the requirement. Similarly, when increasing the embedment depth, the deformation increase, However, it is only to some extent because of wall friction deformation decrease when embedment depth increases. Since the adjacent structure in the research area is road, embedment depth require is at a shallow depth of 7m is enough.

Based on comparison of cost incurred, Diaphragm wall require minimum cost for installation than contiguous bored pile walls. Finally, based on the results of this Research the optimized wall type for the selected site is Diaphragm wall with thickness of 600mm with embedment depth of 7m.

Key Words: Optimization, Retaining Walls, Embedment depth

ACKNOWLEDGEMENTS

I am grateful to my advisor Dr.-Ing Henok Fikre, for his close supervision and constructive suggestions during my research work. I would also want to forward my special thanks to Prof.Im Soo Been and Mr. Jemal Jibril who gave me valuable comments on this thesis.

I would like to express my deepest gratitude to my family and my colleague Muhamed Mulat for their unlimited support.

Table of Contents

DECLARATION iii
ABSTRACT iv
ACKNOWLEDGEMENTS v
Table of Contents vi
List of Table viii
List of Figure ix
NOMENCLATURE xiii
I. Chapter One: Background of the Study 1
1.1. Introduction 1
1.2 Statement of Problem 2
1.3 Purpose of the Study 2
1.4 Objective of the Research 3
1.4.1 General Objective 3
1.4.2 Specific Objective 3
1.5 Methodology 4
1.5.1 Data collection 4
1.5.2 Methodology 4
1.6 Scope of the Research 5
1.7 Outline of the Research 5
II. Chapter Two: Literature Review 6
2.1. Deep Excavations 6
2.2. Types of Retaining Walls 7
2.2.1. Contiguous Bored Piles 7
2.2.2. Diaphragm Wall 8
2.3 Stress and Deformation Analysis 9
2.4 Design Methods 10
2.4.1 Analytical Methods 10
2.4.2 Computational or Numerical Methods 11
2.5 Model Details and Simulation Process 13
2.6 Basic Principles 16

2.6.1 Plane Strain Elements 17
2.6.2 Bar Elements 17
2.6.3 Beam Elements 18
2.6.4 Interface Elements 18
2.6.5 Mesh Generation 19
2.6.6 Boundary Condition 20
2.7 Optimization 21
2.8 Design of Data for Optimization 23
2.9 Design and Displacement of Retaining Walls 25
III. Chapter Three: Data Collection and Modeling 26
3.1 Research Area 26
3.2 Ground conditions 27
3.2.1 Interpreted Sub Soil and Geological Profile 27
3.2.2. Description of the Geological Layers 29
3.2.3. Ground Water Monitoring 31
3.3 Soil Strength 31
3.4 Design Parameters 31
3.5 Anchor properties 32
3.6 Wall Properties 34
3.6.1 Diaphragm wall 34
3.6.2. Contiguous Bored pile 35
3.7 Surcharge 36
3.8 Proposed Scheme 36
3.9 Base Model Generation 36
3.10 Justification for all PLAXIS figure output results 37
IV. Chapter Four: Analysis of Result and Discussion 42
4.1. Optimization for Contiguous Bored Pile Walls 42
4.1.1. Effect of Wall Stiffness 42
4.1.2 Effect of Wall Embedment Length 47
4.1.3 Effect of Number of Anchor 51
4.2. Optimization for Diaphragm Walls 54
4.2.1. Effect of Wall Stiffness 54
4.2.2 Effect of Wall Embedment Length 58
4.3 Cost Analysis 61

V. Chapter Five: Conclusion and Recommendation 65
5.1 Conclusion 65
5.2 Recommendation 66
5.3 Recommendation for Further Studies 66
VI. References 67
VII. Appendix-One 70
VII. Appendix-Two 83
Unit cost breakdown for cost analysis 83

List of Table

Table 3. 2: Coordinate and Depth of Boreholes 28
Table 3. 3: Soil layer cross-section 30
Table 3. 4: Soil parameters 32
Table 3. 5: Recommended Maximum Allowable Anchor Forces 33
Table 3. 6: Diaphragm Wall Parameters (Fahmi (2012)) 34
Table 3. 7: Contiguous Bored Pile Properties (Fahmi (2012)) 35

Table 4. 2: contiguous Board Pile Wall BOQ Shoring Works with thickness 600mm 62
Table 4. 3: Diaphragm Wall BOQ shoring Works with thickness 600mm 63
Table 4. 4: summary of cost Analysis 63

Table 7. 2: Direct Cost Analysis of contiguous Board Pile wall pilling work sheet one 83
Table 7. 3: Direct Cost Analysis of contiguous Board Pile wall pilling work sheet two 84
Table 7. 4: Direct Cost Analysis of contiguous Board Pile wall pilling work sheet three 85

Table 7. 5: contiguous Board Pile wall Bill of Quantity Concrete work 86
Table 7. 6: Direct Cost Analysis of Diaphragm wall pilling work sheet one 87
Table 7. 7: Diaphragm Wall BOQ shoring Works with thickness 600mm 88
Table 7. 8: Diaphragm wall Bill of Quantity concrete work 89
Table 7. 9: CBP Shoring pile Concrete Take-off..... 90
Table 7. 10: Diaphragm Wall Shoring pile Concrete Take-off 91

List of Figure

Figure 2.1: contiguous bored pile wall. 8
Figure 2.2: Diaphragm wall (Fahmi (2012))..... 9
Figure 2.3 Finite Element Analysis of an Excavation: (a) Plan and (b) Meshes of the Section A-A(Fahmi (2012)) 16
Figure 2.4 Nodes Element(Fahmi (2012)) 17
Figure 2.5 Two-Node Bar Element (Fahmi (2012)) 18
Figure 2.6 Two-Node Beam Element (Fahmi (2012))..... 18
Figure 2.7 Interface Element (Fahmi (2012)) 19
Figure 2.8 Finite Element Meshes: (a) Bad Mesh and (b) Good Mesh (Fahmi (2012))..... 20
Figure 2.9 Boundary Condition: Allowed With Rollers (Fahmi (2012)) 21

Figure 3.1: Retaining wall study area location (Google Map)..... 26
Figure 3.2 Geological map of the project and surrounding areas 28
Figure 3.3 Geological Sample co-ordinate axis for all PLAXIS figure output results (3m embedment depth)..... 37

Figure 3.4 Geological Sample co-ordinate axis for all PLAXIS figure output results (5 m embedment depth) 38
Figure 3.5 FE Base Model for 2 Anchor (at 3m and 9m) 38
Figure 3.6 FE Base Model for Anchor at 3m 39
Figure 3.7 FE Base Model for Anchor at 9m 39
Figure 3.8 FE Base Model, phreatic line at assumed water level 40

Figure 4.1 Bending Moment Diagram for CBP 43
Figure 4.2 Lateral Wall Deflection for CBP 44
Figure 4. 3 shear Force Diagram for CBP 46
Figure 4.4 Bending Moment Diagram for CBP 48
Figure 4.5 Lateral Wall Deflection Diagram for CBP 49
Figure 4.6 Shear Force Diagram for CBP 50
Figure 4.7 Bending Moment Diagram for CBP 52
Figure 4.8 Bending Moment Diagram for DW 55
Figure 4.9 Lateral Wall Deflection for DW 56
Figure 4.10 shear Force Diagram for DW 57
Figure 4.11 Bending Moment Diagram for DW 58
Figure 4.12 Lateral Wall Deflection Diagram for DW 59
Figure 4.13 Shear Force Diagram for DW 61

Figure 7.2 Bending Moment Diagram of CBP for 600mm diameter (a) 3m depth& (b) 5m depth 70
Figure 7.3 Bending Moment Diagram of CBP for 600mm diameter (a) 9m depth& (b) 11m depth 70
Figure 7.4 shear force Diagram of CBP for 600mm diameter (a) 3m depth& (b) 7m depth 71
Figure 7.5 shear force Diagram of CBP for 600mm diameter (a) 9m depth& (b) 11m depth 71

Figure 7.6 Lateral wall deflection Diagram of CBP for 600mm diameter (a) 3m depth& (b) 7m depth..... 72
Figure 7.7 Lateral wall deflection Diagram of CBP for 600mm diameter (a) 9m depth& (b) 7m depth..... 72
Figure 7.8 Bending Moment Diagram of CBP for 800mm diameter (a) 5m depth& (b) 7m depth 73
Figure 7.9 Bending Moment Diagram of CBP for 800mm diameter (a) 9m depth& (b) 11m depth 73
Figure 7. 10 shear force Diagram of CBP for 800mm diameter (a) 5m depth& (b) 7m depth 74
Figure 7. 11 shear force Diagram of CBP for 800mm diameter (a) 9m depth& (b) 11m depth .. 74
Figure 7. 12 Lateral wall deflection Diagram of CBP for 800mm diameter (a) 5m depth& (b) 7m depth..... 75
Figure 7. 13 Lateral wall deflection Diagram of CBP for 800mm diameter (a) 9m depth& (b) 11m depth..... 75
Figure 7.14 Bending Moment Diagram of DW for 600mm diameter (a) 3m depth& (b) 5m depth 76
Figure 7.15 Bending Moment Diagram of DW for 600mm diameter (a) 7m depth& (b) 9m depth 76
Figure 7.16 shear force Diagram of DW for 600mm diameter (a) 3m depth& (b) 5m depth 77
Figure 7.17 shear force Diagram of DW for 600mm diameter (a) 7m depth& (b) 9m depth 77
Figure 7. 18 Lateral wall deflection Diagram of DW for 600mm diameter (a) 3m depth& (b) 5m depth..... 78
Figure 7.19 Lateral wall deflection Diagram of DW for 600mm diameter (a) 7m depth& (b) 9m depth..... 78
Figure 7.20 Bending Moment Diagram of CBP for 1Anchor @ 3m..... 79
Figure 7.21 Bending Moment Diagram of CBP for 1Anchor @ 9m..... 79
Figure 7.22 Shear Force Diagram of CBP for 1Anchor @ 3m 80
Figure 7.23 Shear Force Diagram of CBP for 1Anchor @ 9m 80
Figure 7.24 Lateral Wall Deflection Diagram of CBP for 1Anchor @ 3m..... 81
Figure 7.25 Lateral Wall Deflection Diagram of CBP for 1Anchor @ 9m..... 81

Figure 7.26 Shear Force Diagram of CBP for 600mm diameter 82
Figure 7.27 Bending Moment Diagram of CBP for 600mm diameter 82

NOMENCLATURE

The Nomenclature in this report comprise of abbreviations and symbols used in equations, longer naming, acronyms, representation of quantities and parameters.

Abbreviations

AAU…….…. Addis Ababa University

AAiT…….… Addis Ababa Institute of Technology

BOQ……... Bill of Quantity

CBP ……... Contiguous Bored Pile

DW……..... Diaphragm Wall

FEM ……... Finite Element Method

2D……Two Dimensional

.

I. Chapter One: Background of the Study

1.1. Introduction

Excavation support systems are structures that have fundamental influences on safety, quality, speed, and profitability of construction projects that require deep excavations. There is far less technical guidance available for the design of excavation support systems than for permanent structures. Designers and builders of excavation supports rely heavily on past experience as well as company-specific design and construction guidelines to perform their work. This leaves owners and general contractors somewhat in the dark when it comes to making decisions about excavation support systems.

Retaining wall for deep excavation is anticipated in urban areas especially in Addis Ababa where construction activities are highly growing. The design of retaining walls and support systems involves careful analysis, design and monitoring system. This is due to the sensitivity of ground movement that can cause damage to the adjacent buildings, roads, utilities and others.

During excavation, some soil types pose greater problems than others. Sandy soil is always considered dangerous even when it is allowed to stand for a period of time after a vertical cut. Vibration from blasting, traffic and heavy machinery movement, and material loads near the cut can also cause earth to collapse in sandy soils. The instability can be caused by moisture changes in the surrounding air or in the water table. Clayey soils in general, present less risk than sandy soils; however, soft clay can prove to be very treacherous. Silty soils are also unreliable and require the same precautions and support provision as sandy soils. Fahmi (2012).

This study focuses on optimization of retaining wall types for deep excavation. This has been done by employed finite element method using the ground data taken from the 4B+G+30 Zemen Bank S.C head quarter building project.

1.2 Statement of Problem

Excavation support systems have a fundamental influence on the safety, quality, speed and profitability of construction projects that require deep excavations. But due to using of similar support system for different types of soils may not be economical and it may affect work speed since the excavation work, erection of pile, casting concrete for different soils need different time schedule. Also, the effect to adjacent soil mass may vary with respect to the load, soil property; the material will be used and the ground water table. Thus, the selection of the wall must be carefully considered during design and construction stages for deep excavation.

In Addis Ababa the most common type of retaining wall for deep excavation is Cantilevered or Anchored contiguous bored pile wall. This retaining method may not be relatively effective in terms of various parameters. Thus other alternative retaining systems should be analyzed and proved to identify the best options.

The results presented in these thesis are for a specific type of retaining structure (Diaphragm and contiguous bored pile) because contiguous bored pile are common type of retaining wall in Addis Ababa and Diaphragm wall are types of retaining wall applicable for clay soil from different papers written.

The overall cost is a major consideration in the retaining wall as it is essential that operations can be fully justified in an economic basis. Therefore, it is essential that all items of retaining wall costs are optimized taking into consideration their intended use.

1.3 Purpose of the Study

This research will have practical implications on the design and construction of deep excavations. Deep excavations in urban areas are increasingly becoming a necessity in different projects from high-rise buildings to subway systems. One challenging problem in deep excavation is the need to prevent damage to adjacent buildings. To achieve, it is necessary to eliminate or reduce excessive settlement caused by the wall deflection in excavation. Hence, the

selection of the appropriate method, sequence of construction, wall type and support system are important to minimize the ground movement and to achieve economic design and construction.

Therefore, by doing this research, multitude of benefits and advantages are realized through the better understanding of reduction of excessive settlement caused by wall deflection in excavation and minimum cost could be attained. Therefore, the significances of research accounted in better understanding of the parameters, their correlation and effect on the retaining walls and cost

Therefore, the main purpose of the study is to come up with optimum retaining wall type by using the numerical analysis for specific ground condition.

1.4 Objective of the Research

Design optimization for retaining wall types in deep excavation is important that the cost of installation gets higher this time. To accomplish the study, the following general and specific objectives are set: -

1.4.1 General Objective

The main objective of this research is to come up with optimum retaining wall type by optimizing and identifying the effect and performance of Diaphragm and contiguous bored pile retaining walls for clay soils at selected site in Addis Ababa.

1.4.2 Specific Objective

The specific objective of this research will be

- Compare the retaining wall types by their stiffness, embedment depth, settlement and number of anchors.
- Identify optimum wall type selected according to their cost effectiveness and less deformation

1.5 Methodology

To perform this research, the following procedures and resources were used.

1.5.1 Data collection

- This study used the data obtained from site investigation works for Zemen Bank S.C Head Quarter Building project.

1.5.2 Methodology

The methodology used to implement the research is purely numerical, using finite element method analysis with different parameter combinations based on design of data for optimization. Analyses of walls were conducted to obtain the most suitable wall to be adopted at the site. The wall must fulfill the criteria which have less deflection hence less ground surface settlement, and will lead to cost saving.

- The step-by-step procedure used is outlined as follows :

1. FE modeling and analysis using Plaxis 2D

    - Modeling the retaining wall both for contiguous bored pile wall and diaphragm wall
    - Running FE analysis for optimization approach by varying wall types, size of the wall and embedment length.
    - Extracting displacement from FE analysis output which has been used as function for the optimization process.
    - Finding the optimum wall section.

2. Cost Analysis for the optimum wall section

- Detail cost analysis for wall section by varying the embedment depth and wall thickness.
- Compare the cost for the wall types in different embedment depth.

1.6 Scope of the Research

The primary objective of this thesis is to optimize retaining wall in deep excavation for the wall types of Contiguous bored pile and Diaphragm permanent retaining walls for clay soil at selected research area.

The modeling and analysis of the wall and support system was carried out using Plaxis 2D geotechnical finite element software, secondary data were used as input for running the analysis.

1.7 Outline of the Research

This thesis presented in five chapters. The arrangement of the thesis is described below.

- Chapter 1 gives a brief introduction to the research and arrangement of the thesis. The objective, the scope and the research methodology are found in this chapter.
- Chapter 2 Provides literature Review on retaining wall types. The conceptual background related to the topic is reviewed including the recent studies.
- Chapter 3 deals about data collection and modeling in finite element method
- Chapter 4 presents results and discussion. on the different parameters and results of the analysis carried out.
- Chapter 5 in this final chapter the topic has been concluded and further research area has been suggested.

II. Chapter Two: Literature Review

2.1. Deep Excavations

Deep excavation is a complex subject in geotechnical engineering and has been studied using various methods, e.g. theoretical and empirical methods, laboratory tests, field measurements, and more sophisticated numerical analysis. In Addis Ababa the construction of deep excavations is a technically challenging problem. When deep excavation is anticipated, the adjacent building can get damaged if the construction cause excessive ground movement. If damage to the adjacent building occurs, the owner of the building has the right to claim for repair work from the contractor or consultant that is responsible for the construction. Thus, careful considerations during design and construction stages are necessary so that these problems can be minimized.

Performance of deep excavations is related to both stability and deformation. Deep excavations are designed to be stable and to limit deformations within acceptable levels. A stable deep excavation is an excavation whose walls do not collapse, whose adjacent soil doesn't settle excessively and whose base does not heave uncontrollably. Finno and Bryson (2002) found that the settlement of a building outside the excavation follows the development of lateral movement of the soil and the secant pile wall as a result of undrained deformations in saturated clay, and the reduction of wall stiffness and creep also resulted in larger building settlement. Ground deformations around excavations can damage adjacent buildings, streets, and utilities. The severity and extent of damage depends on the magnitude and pattern of ground movements around the excavation. Stability and deformation are related. Thus, prediction of deep excavation performance involves analysis of both stability and deformation. Experience has shown that stability can be evaluated with sufficient accuracy using simple limit equilibrium calculations. Deformations, however, are significantly more difficult to predict, and finite element analyses are often used for this purpose when ground movements are particularly important.

The purpose of a deep excavation support system is to provide lateral support for the soil around an excavation and to limit movement of the surrounding soil. Support systems for deep

excavation consist of two main components. The first is a retaining structure. The second component is the support provided for the retaining structure. Many types of supports have been used in deep excavations. The common types of supports are diaphragm wall (structural slurry), sheet pile, soldier piles, tangent piles, and contiguous piles. The principal types of supports are struts (braces), rakers, and tieback anchors.

2.2. Types of Retaining Walls

There are many types of retaining wall that can be adopted in deep excavation as a permanent basement wall. In deep excavation works, stability of the wall is one of the main important factors that need to be considered. The types of retaining wall are listed below Fahmi (2012):-

1. Contiguous bored pile
2. Secant piles
3. Tangent bored pile walls pile
4. Diaphragm wall
5. Sheet piles
6. Soldier pile

2.2.1. Contiguous Bored Piles

Contiguous bored piles wall can be constructed as basement wall in order to avoid excessive bulk excavation and help to control ground movements. The bored pile has various ranges of sizes ranging from 600mm to 2000mm diameter. It is constructed with gaps in between the pile. Thus, the gap in the structural wall has exposed the soil. Hence, this option is suitable where the retained soil is usually firm to stiff (not generally granular). This is the most economic option and normally the fastest method to construct. Fahmi (2012)

Figure 2.1: contiguous bored pile wall.

2.2.2. Diaphragm Wall

Diaphragm walling is a technique of constructing a continuous underground wall from the ground level. These reinforced concrete diaphragm walls are also called Slurry trench walls due to the reference given to the construction technique where excavation is made possible by filling and keeping the wall cavity full with bentonite-water mixture during excavation to prevent collapse of vertical excavated surfaces. Typical wall thickness varies between 0.6 to 1.1m. The wall is constructed panel by panel in full depth. Panel width varies from 2.5m to about 6m. Short widths of 2.5m are selected in less stable soils, under very high surcharge or for very deep walls. It must be remembered that Diaphragm walls are constructed as a series of alternating primary and secondary panels. Alternate primary panels are constructed first which are restrained on either side by stop-end pipes. Before the intermediate secondary panel excavation is taken up, the pipes are removed and the panel is cast against two primary panels on either side to maintain continuity. The major disadvantage of Diaphragm wall is it requires massive equipment, long construction period, and huge cost. Fahmi (2012)

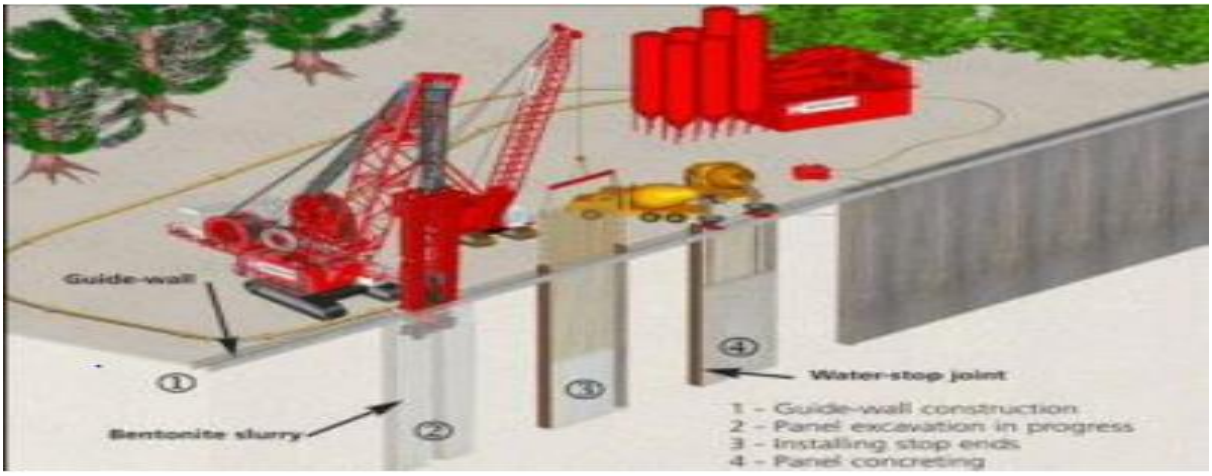

Figure 2.2: Diaphragm wall (Fahmi (2012))

2.3 Stress and Deformation Analysis

There are many different ways to analyses earth retaining structures. Computer software has become more important in order to analyses complex analysis so that more accurate and faster result can be obtained. Finite element and finite difference formulation methods is common tool to calculate the nonlinear analysis nowadays. A complex soil constitutive behavior, actual construction sequences, structural and support details, and consolidation and groundwater effects can be modeled by using a finite element method. Ground movements, wall movements, bending moments and prop loads are well calculated but may be of limited value unless a well-developed soil constitutive model has been used and the results "calibrated" against reliable measurements of well monitored comparable excavations and wall systems. Fahmi (2012)

Nowadays, there are many powerful computer programs which are able to calculate distributions of active and passive pressures, given basic data such as strata thickness and soil parameters. One of the good geotechnical software that available in the market at the moment is Plaxis2D. Plaxis2D is a finite element package that is able predicts deformation and stability in geotechnical engineering projects. The simple graphical input procedures enable a quick generation of complex finite element models, and the enhanced output facilities provide a

detailed presentation of computational results. The calculation itself is fully automated and based on robust numerical procedures. This concept enables new users to work with the package after only a few hours of training.

Plaxis is a finite element package intended for analysis of deformation, stability and groundwater flow problems in geotechnical engineering (Brinkgreve et al. 2004). It is widely used in practice because of its simplicity, user-friendliness and reliability. Plaxis is equipped with features to deal with deep excavation supported with diaphragm wall.

2.4 Design Methods

There are three distinct approaches to arriving at solution to rock and soil mechanics problems and these have been utilized in the design of retaining walls, namely :

1. Analytical methods
2. Computational or numerical methods
3. Empirical methods

2.4.1 Analytical Methods

Osman and Bolton (2006) proposed an analytical solution for estimating ground deformation around excavation in 'undrained' clay. The basic idea of this solution follows early study on using 'mobilized strength' to predict ground strain and hence displacement. A simplified deformation mechanism of excavation was assumed in the mobilized strength design (MSD) method. Ground deformations are linked to stress via stress-strain data from soil tests on undisturbed samples taken from representative elements. This approach has the advantage that one can use a single stress-strain curve from a single soil test, together with a simple hand calculation, to estimate both stability and soil deformation. However, the solution ignored structural energy stored in the retaining system. Ground deformation due to dissipation of excess pore water pressure during and after excavation is not taken into account. Moreover, the solution considers the total energy terms starting from the beginning of excavation. Therefore, the

progressive accumulation of mobilised shear strain at different excavation depths is not considered.

Lam (2010) made further improvement of the MSD method developed by Osman and Bolton (2006), using observed ground deformation mechanisms from a series of centrifuge tests of multi-propped excavations in soft clay. In the improved MSD method, structural energy stored in the retaining system is considered. Progressive accumulation of mobilised shear strain at different excavation depths is also taken into account. Ground deformations calculated by the improved MSD method are compared with those computed by an advanced MIT-E3 model. In general, the predictions fell within 30 % of the finite element computed results.

2.4.2 Computational or Numerical Methods

Mana and Clough (1981) carried out numerical parametric study to investigate effects of wall stiffness, prop spacing, prop stiffness, prestress and elastic soil stiffness on ground deformations due to excavation. It was revealed that ground deformations decreases with increased wall bending stiffness or decreased prop spacing. This effect is more significant when factor of safety against basal heave is relatively low. Ground deformations decrease with increased prop stiffness, with a decreasing rate at high stiffness. Moreover, ground deformations are also significantly affected by soil modulus. Higher modulus leads to smaller movement. Based on results from numerical parametric study (by finite element analysis), Clough et al. (1989) developed a design chart. The chart correlates lateral wall displacement of excavation in soft to medium clay to system stiffness and factor of safety against basal heave. The factor of safety against basal heave used in the figure is derived by Terzaghi (1943).

For wide excavations ($B/H_e > 1$), factor of safety against basal heave is given as:

$$F_s = CubN_c/\left(H\left(\gamma - \frac{CuU}{0.7B}\right)\right) \quad \text{Equation 2.1}$$

For wide excavations where there is a strong stratum near the base of the excavation, the factor of safety is given as:

$$F_s = CubN_c/\left(H\left(\gamma - \frac{CuU}{D}\right)\right) \quad \text{Equation 2.2}$$

where C_{ub} and C_{uu} are undrained shear strength below and above formation level of excavation, respectively; He denotes final excavation depth; B is width of excavation; γ is bulk density of clay; D is distance from the bottom of the excavation to a relatively hard stratum; N_c represents stability factor, which is equal to:

$$N_c = {\gamma H_e}/{C_u} \qquad \text{Equation 2.3}$$

It should be noted that this design chart does not take effect of diaphragm walling into account. The chart illustrates that for a given system stiffness, a lower factor of safety against basal heave results in a larger lateral wall displacement after excavation. For excavations in soft clays, where the factor of safety against basal heave is low, a larger stiffness of the support system results in a smaller lateral wall displacement.

Clough and O'Rourke (1990) conducted a series of finite element parametric studies on excavations in stiff clay. The computed results show that parameters such as wall stiffness and prop spacing have only a small influence on deformations around excavations in stiff clay. This is because the model soils are stiff enough to minimize the need for stiff retaining systems. It was found that soil modulus and coefficient of lateral earth pressure have a more significant impact on the ground movements, compared to stiffness of retaining systems. Clough and O'Rourke (1990) also pointed out that base instability is usually not concern for excavations in stiff clays.

Addenbrooke (2000) proposed a new term, displacement flexibility, $\Delta = {h^5}/{(EI)}$, to quantify overall stiffness of a retaining system. Dependency of lateral wall displacement on the displacement flexibility was confirmed by computed results from a series of elastic-perfectly plastic finite element analyses. Correlation of the displacement flexibility to lateral wall displacement was checked by extensive case histories worldwide.

Mana and Clough (1981) conducted a two-dimensional numerical parametric study to investigate effects of excavation geometry such as excavation width and depth of the underlying firm layer on ground deformations due to excavation. It was revealed that ground deformations increase with excavation width and depth to an underlying firm layer.

Hashash and Whittle (1996) carried out a series of two-dimensional numerical parametric studies to study effects of wall embedment depth and prop spacing on ground deformations due to multi-propped excavations. Constitutive model (MIT-E3) adopted in the numerical analyses is capable of considering anisotropic stress-strain relationship, stress path dependency and strain dependency of clay. Computed results show that wall length has a minimal effect on the pre-failure deformation for excavations in deep layers of clay, but does have a major effect on the location of failure within the soil. Use of very depth wall can improve base stability. However, large bending moment can be resulted and may cause flexure failure of the retaining wall. Not only is basal affected by final excavation depth, but also influenced by vertical prop spacing. Larger vertical prop spacing can result in additional basal heave.

Jen (1998) carried out numerical parametric studies to study effects of excavation geometry, retaining system and stress history of clay on ground deformations due to excavation. The computed results reveal that distribution of ground deformation is significantly affected by depth of hard stratum below soft clay. While magnitude of ground deformation is governed by excavation width, excavation depth and stress history of clay. Based on the computed settlement troughs behind the wall, new design charts are proposed to correlate ground settlement to excavation depth, wall length, depth of hard stratum and soil profile.

2.5 Model Details and Simulation Process

2D simulations (i.e. plain strain and axisymmetric analysis) have been widely used to approximate real deep excavations in the design process and for research purposes due to the limitation of software capabilities and computational resources available.

The advances in hardware and software nowadays have enable the application of fully 2D analysis in deep excavations, which can include more geotechnical and structural details (e.g. ground profile, excavation geometry, retaining system, and construction sequence) and deal with large scale case studies. The geometry and distribution of retaining structures such as the diaphragm wall, the sheet pile wall, joints between diaphragm wall panels, the soldier piles, and horizontal struts, were represented properly in the analyses. The results were promising in these

analyses, and the agreement with field measurement was reasonably good considering the uncertainties and complexities involved in the analysis.

In most analyses, the wall installation process was modelled by the Wished-In-Place (WIP) method which is not able to consider the installation effect on the ground movement and subsequent excavation behavior. However, the excavation for diaphragm wall panels or bored piles is certain to result in significant in situ total stress relief which will alter the level of horizontal total stress applied to the retained side of a wall, and can therefore be expected to influence the actual values of prop or anchor forces and of the maximum bending moment in the wall. Substantial ground movement and reduction of in situ lateral stress have been observed in the field measurements during the construction of embedded retaining walls. The installation effects of bored piles and diaphragm walls have been investigated using numerical analyses in 2D.

The initial stress state in the ground prior to the construction is related to the vertical effective stress and the coefficient of lateral earth pressure at rest. Potts and Fourie (1984) conducted a series of plain strain analyses of a single propped retaining wall at the top in drained condition using two values of (0.5 and 2.0), and found that the value of has a large influence on the excavation behavior such as the wall displacements and bending moments, the prop force, the ground movements, the stress state and stress path in the soil, and earth pressure on the wall. Potts and Fourie (1984) assumed two totally different types of construction method, excavated and backfilled, and found that the excavation behavior was largely different.

Potts and Fourie (1985) found that the wall stiffness has a large effect on the wall displacements, earth pressures on the back of the wall, wall bending moments, and prop forces. Strut prestressing was found to affect considerably the deflection of the upper portion of the wall while virtually no significant change is evident at the bottom of the wall, and the ground settlement also reduces with the increase in the magnitude of strut pre-stress.

The dewatering and consolidation process are usually neglected in the analyses by assuming undrained conditions, but they can be considered in the analysis straightforwardly. Dewatering of the site can be simulated by controlling the pore pressures at specific locations, and consolidation can be modelled using displacement-pore pressure coupled analysis. In practice, however, the

undrained assumption is usually reasonable because the permeability of the soil is small (on the order of) and the construction period is relatively short (e.g. 1 or 2 years). The excess pore water pressures generated during the construction will dissipate after the completion of the construction, and drained conditions are normally assumed to represent a long-term situation in the design and analysis.

Conventional soil models (e.g. Mohr-Coulomb, Soil Harding model) have been used frequently and extensively in the numerical analyses of deep excavations, but they tend to generate unrealistic ground movements, e.g. upward ground movement rather than settlement in the retained area outside the excavation, and larger than expected basal heave inside the excavation, because the small-strain stiffness nonlinearity is not considered in these models.

Clough and Hansen (1981) demonstrated that the strength anisotropy of the clay has large influence on the excavation behavior due to the stress reorientation in the field, whereas the stiffness anisotropy has a relatively smaller influence on the excavation behavior. Finno, Harahap et al. (1991) used both isotropic and anisotropic bounding surface models in the analysis, and showed that the isotopic soil model produced smaller sheet-pile wall displacement and ground settlement than the anisotropic model and underestimated the observed behavior. Ng, Leung et al. (2004) investigated the effects of inherent stiffness anisotropy of the soil on the excavation behavior, using a linear elastic model based on a hypothetical plane strain multistage excavation under fully drained conditions, but they found a relatively small difference (1- 2mm) of computed ground settlement and wall deflection between the isotropic and anisotropic analyses. However, it may be worth investigating the anisotropic effects by using a more advanced soil model which can consider the stiffness and strength anisotropy of the soil, e.g. the MIT-E3 model.

2.6 Basic Principles

In this section the basic principles of the finite element method will be explained. Based on the Figure 3, the central section in most cases is always chosen. Then take the profile of this section and divide the soils and structures within the excavation influence range into many meshes, each of which is called an element.

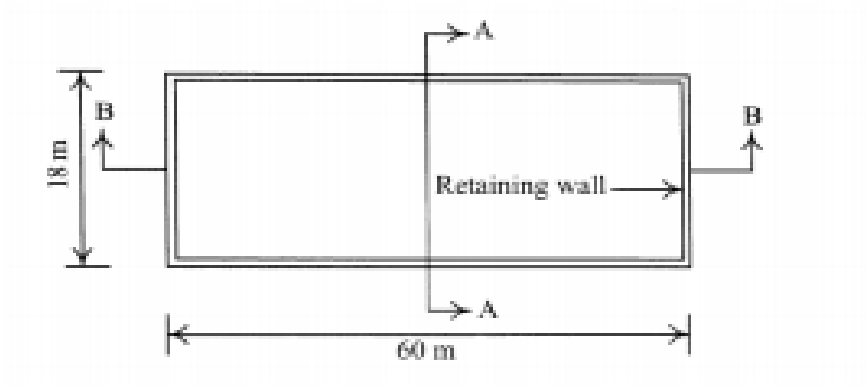

(a)

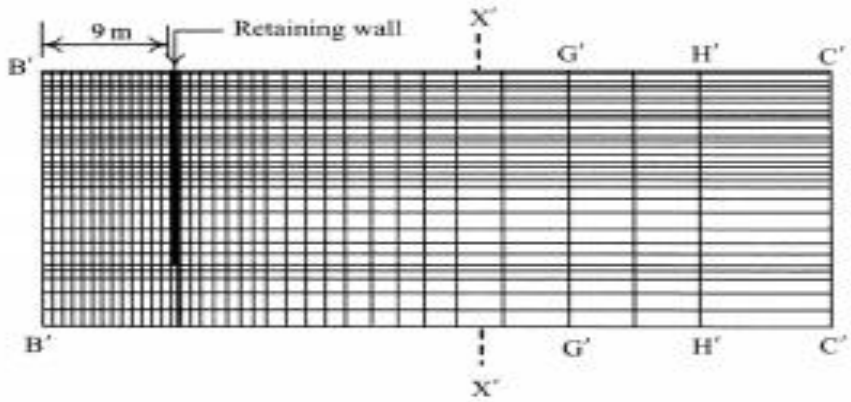

(b)

Figure 2.3Finite Element Analysis of an Excavation: (a) Plan and (b) Meshes of the Section A-A(Fahmi (2012))

2.6.1 Plane Strain Elements

In terms of shape, plane strain elements are usually categorized into triangular elements and quadrilateral elements as shown in Figure 4. For Plaxis2D, there are two options available which either to use 6 nodes or 15 nodes. Element with 15-node can provides more accurate calculation of stresses and failure loads. However, 6-node triangles can offer more quick calculation.

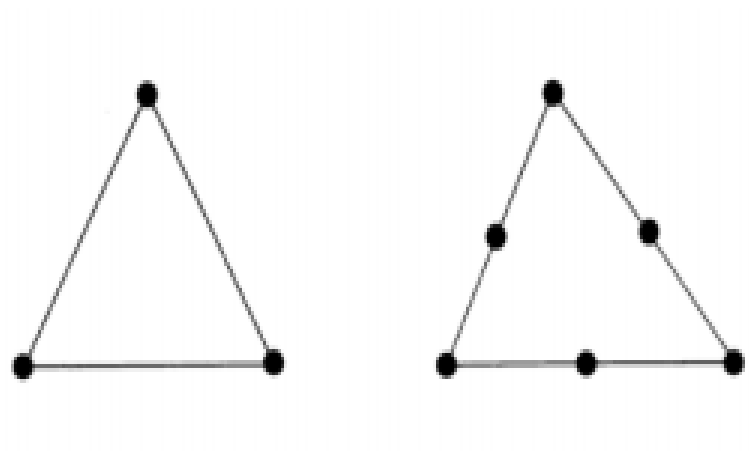

Figure 2.4 Nodes Element(Fahmi (2012))

2.6.2 Bar Elements

Bar elements in Plaxis2D can be used to simulate struts, anchors, or other members bearing only axial stress, as shown in Figure 5. Each node of a bar element has only one degree of freedom. A bar element of low order has two nodes while one of high order has three nodes. In general excavation analyses, two node bar elements can achieve good accuracy.

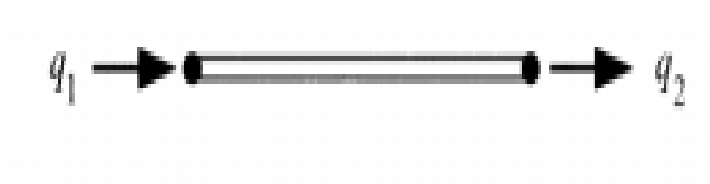

Figure 2.5 Two-Node Bar Element(Fahmi (2012))

2.6.3 Beam Elements

Members subjected to moment can be simulate by using beam elements, or also known as flexural elements, as shown in Figure 6. Each node of a beam element has two degrees of freedom. A beam element of low order has two nodes while one of high order has three nodes. In general excavation analyses, the two node beam element can achieve good accuracy.

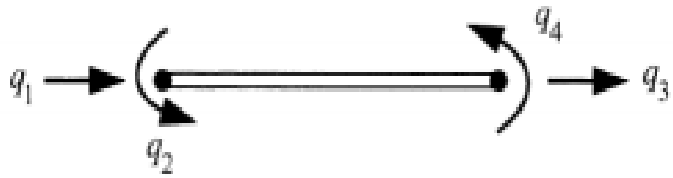

Figure 2.6 Two-Node Beam Element(Fahmi (2012))

2.6.4 Interface Elements

Retaining walls that used in excavation are stiff while the adjacent material which is soil is relatively soft. When the retaining wall deforms, relative displacement may be generated between the soil and the wall. To simulate the relative displacement between soil and structures during excavation, interface elements are sometimes used in analysis. As shown in Figure7, an interface element is an element connecting structures and soil, with or without thickness, which

has a quite large normal stiffness but relatively small shear stiffness so that it can simulate the relative displacement between soil and structures.

Though interface elements can rationally simulate the relative displacement between soil and structures, since extra parameters, which are not easily obtained from conventional soil tests, will be introduced, and numerical instability during analysis often occurs, they have to be used especially carefully. If interface elements are not being adopted, the soil in the vicinity of the structure can be considered to divide into fine elements. When the retaining wall is deformed, these fine soil elements can easily attain the plastic state, which will then produce larger deformation. Therefore, a rational analysis result is also attainable.

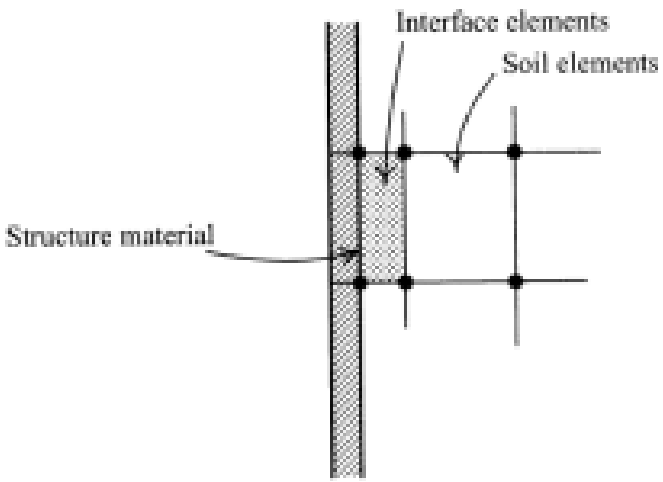

Figure 2.7Interface Element(Fahmi (2012))

2.6.5 Mesh Generation

The shape of the element used in an analysis can strongly affect the results obtained. Density of mesh is one of the main factors than can affect the result. In deep excavation work, the mesh in the area of stress concentration, of rapid strain changing, the crucial areas, and the object zones should be finer. Density of mesh for soil closest to the retaining wall should be finer than the soil further away from the retaining wall.

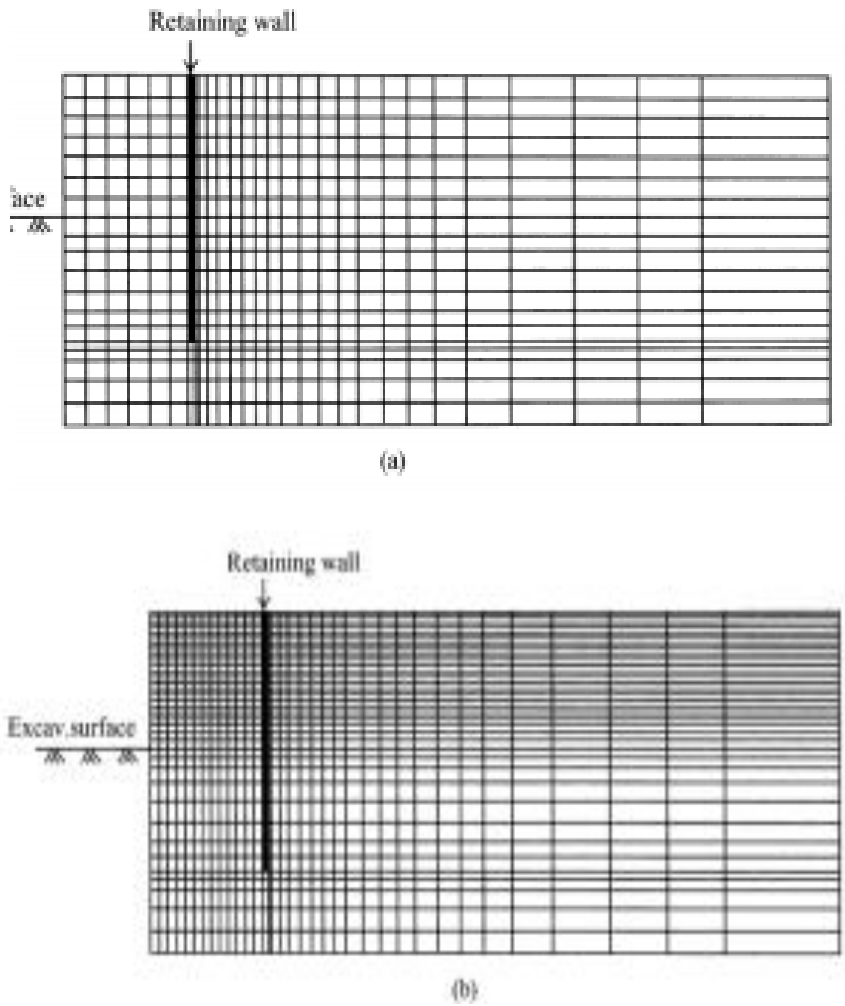

Figure 2.8 Finite Element Meshes: (a) Bad Mesh and (b) Good Mesh(Fahmi (2012))

2.6.6 Boundary Condition

If considering the symmetry of an excavation and taking a half for analysis as shown in Figure 9, the symmetric boundary should be equipped with rollers to restrain the lateral displacement and allow vertical displacement. According to Ouand Shiau (1998), to analyze movement in an excavation, rollers will be more efficient than hinges placed.

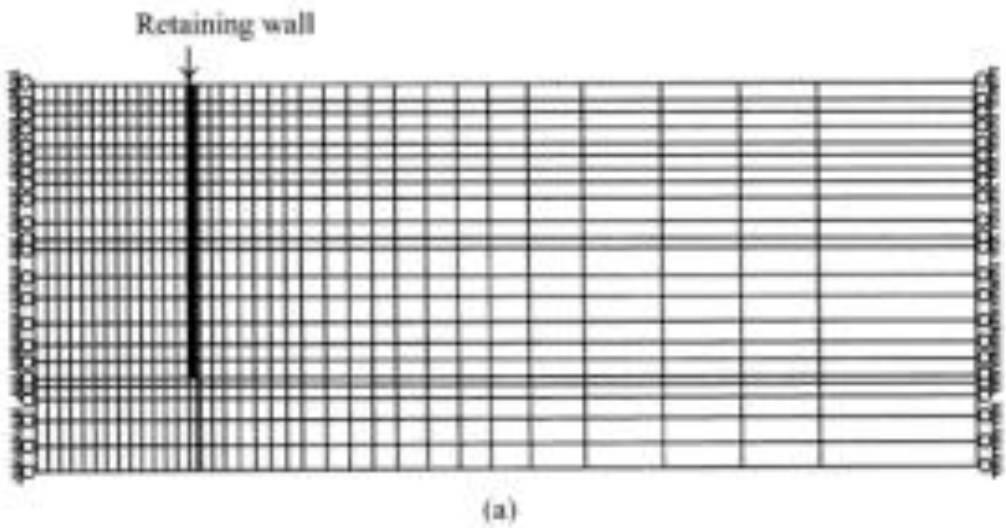

Figure 2.9 Boundary Condition: Allowed With Rollers(Fahmi (2012))

2.7 Optimization

In the theory of optimization, two major classes of optimizations could be identified, based on the number of objective functions used for optimization, as single –objective optimization and multi- objective optimization. In a single –objective optimization, simple searching for the best will be made based on a single objective function, where as in multi-objective optimization the searching is needed to be supported by pareto dominance. And in the sense of mechanics, structural engineering or civil engineering. There are two main categories of optimizations. Which are those of structural optimizations and non –structural optimizations. In general however, both the categories involve searching algorithms, in one way or another, operating on a collection of design spaces. Further, structural optimization is classified into shape-optimization and topology-optimization. **(**Fahmi, 2012)

Design optimization is an important engineering design activity. In general, design optimization determines values for design variables such that an objective is optimized while performance and other constraints are satisfied (Arora, 2004). The use of design optimization in engineering

design continues to increase, driven by more powerful software packages and formulations of new design optimization problems motivated by the decision- based design (DBD) framework.

Teparaksa (2019) studied the comparison between predicted values of diaphragm wall deflection during construction by FEM analysis and by field measurement. Two cases were considered: the new BOT head office and the Rosewood Hotel, which had a maximum excavation depth of 15.8 m and 24.0 m, respectively. In these two projects, the method of construction was different, although a diaphragm wall was used as a retaining wall in both projects. A top-down construction method was employed in the case of the new BOT head office because it is located close to historical palaces. Comparatively, the Rosewood Hotel project used a bottom-up construction technique. The behavior of the diaphragm wall was predicted using FEM analysis with Mohr–Coulomb soil modeling to simulate all the construction sequences. In terms of deflection shape, the predicted values agreed well with the field measurements. However, construction time was fast in the case of Rosewood Hotel. Thus, field measurement wall movements were considerably less than predicted.

Ashok et al. (2016) Study aims to find an optimal section for a diaphragm wall considering variations in many of its design parameters to suit the soil conditions and depth of excavation. The effects of variations of these design parameters will be compared to get an optimized section. The parameters which are selected for the study are panel shape, panel thickness, and maximum panel length and panel width and soil conditions. Comparison has to be done with the bending moment and head displacement for different diaphragm wall shapes, panel width and panel thickness using SAP2000 software. 1st studied the effect of diaphragm wall by changing panel length as 2.5m, 3.5m, 4.5m and 5.5m and panel thickness as 0.6m, 0.8m and 1.1m for both rectangular section and T section. 2nd study is about the effects while changing the depth of the web in the T section.

Godavarthi et al. (2011) A detailed design methodology of an excavation supporting system is furnished in this study. A case study on the Contiguous pile wall retaining system for supporting a deep excavation at a town center is presented. Lack of inadequate space at town centers goes

for deep vertical excavations, which require supports that are designed to consume minimum construction space. Various excavation supporting systems are presented in this study. Contiguous pile wall is one good choice of earth retention systems in the urban context. The detailed analysis and design of a contiguous pile wall is explained by a Case study which uses contiguous pile wall as an excavation supporting system at an urban center.

Emam (2013) Describes a new construction method for a diaphragm wall built in Egypt using a continuous horizontal reinforcement. Significant data related to the construction system were documented, and the difficulties encountered during construction were highlighted. In addition, evaluation of the new system was carried out based on terms of cost and schedule. Industry professionals involved in this field may find the description of the new construction method and the evaluation results of practical value. From evaluation of the system, the following conclusions were drawn: The elimination of using a shoring system or ground anchors reduces the construction time and cost for the new wall system., a cost comparison between the new and traditional wall systems in this particular job revealed that the cost increases by about 18% when continuous horizontal reinforcement is used. However, such comparisons may not yield the same results for other jobs under different circumstances. and the construction progress rate for both new and traditional wall systems indicates close similarity in this particular job.

2.8 Design of Data for Optimization

Design of data experiments was invented by Ronald A. Fisher at Rothamsted Experimental Station, an agricultural research station 25 miles north of London. In Fisher's first book on design of experiments he showed how valid conclusions could be drawn efficiently from experiments with natural fluctuations such as temperature, soil condition, and rain fall, that is, in the presence of nuisance variables, the known nuisance variables usually cause systematic biases in groups of results (e.g., batch-to-batch variation). The unknown nuisance variables usually cause random variability in the results and are called inherent variability or noise.

The fundamental principle in design of experiments is solution to the problems in experimentation posed by the two types of nuisance factors and serve to improve the efficiency of experiments. Those fundamental principles are ,as it is shown and described in (Telford ,2007) the fundamental principle in design of experiments are solutions to the problems in experimentation posed by the two types of nuisance factors and serve to improve the efficiency of experiments. Those fundamental principles are , as it is shown and described in (Telford,2007). These are randomization, replication, blocking, orthogonally and factorial experimentation. There are two common tools available to the practitioner for assisting with the problem statement. These are not actually problem-solving tools but rather are problem identification tools. Although these tools were originally developed for the manufacturing environment, they can easily be adapted to other sectors of industry. These tools are (Christopher, 2004)

- Fishbone chart
- Pareto chart

The Fishbone chart- the purpose of this chart is to identify the cause of the problem or effect of interest. The Fishbone chart looks similar to the bones of a fish. The head of the fish is labeled with the problem or effect. Each major bone coming out of the spine is a possible source or cause of the problem (Christopher, 2004).

The first thing to do in parameter identification is to find a cause-effect relationship which could be realized through the utilization of fish-bone diagrams, in a very smart way. Using the fish bone diagram the cause effect of the tunnel design elements is listed. From those the highest effect on retaining wall design safety and cost. Consequently, the parameters that affect are identified.

The Pareto chart – it may turn out that there are several sources or causes of the problem or problems of interest. The concept of the Pareto chart was developed by the Italian economist Wilfredo Pareto, who postulated that only a few factors are the cause of many problems. This is frequently referred to as the 80-20 rule. The 80-20 rule states 80% of the problem is caused by 20% of the factors. The 80 and the 20 are not magic numbers but seem to be approximately observed in many instances (Christopher, 2004).

2.9 Design and Displacement of Retaining Walls

The design of earth retaining structures using BS 8002 (1994) is based on a design philosophy of limit state design and the analyses are largely made using limit equilibrium methods. BS 8002 acknowledges that soil deformations with 100% (full) mobilization of shear strength in the surrounding soil are generally large in comparison with the normally acceptable strains in service. Therefore, a mobilization factor M is proposed to limit the proportion of available strength that will be mobilized in service. With the mobilization factor the induced strains in the soil would be low enough to assure that excessive ground and structure deformations would be prevented.

Specifically, BS 8002 recommends mobilization factors of 1.5 for designs using total stress parameters and 1.2 for designs using effective stress parameters if the wall displacements are to be limited to within 0.5% of wall height for medium dense or firm soils. Mobilization factor should be larger than 1.5 for clays which require large strains to mobilize if the wall displacements are required to be limited to within 0.5% of wall height. A more detailed analysis of displacement should be performed where tighter criteria are to be applied or soft to loose soils (BS 8002).

III. Chapter Three: Data Collection and Modeling

3.1 Research Area

The project site is located in central Addis Ababa around Addis Ababa University School of Commerce Campus. The project site is characterized by flat topography with an average elevation of 2362m a.s.l. (hand held GPS reading).

Figure 3.1: Retaining wall study area location (Google Map)

3.2 Ground conditions

3.2.1 Interpreted Sub Soil and Geological Profile

Addis Ababa city is situated in western margin of the main Ethiopia Rift and represents a transitional zone between the Ethiopian plateau and rift with poorly defined escarpment.

The geology of Addis Ababa area is represented by four volcanic units dominated in the lower part by basaltic lava flows (Addis Ababa basalt), followed by a pyroclastic sequence, mainly formed by Ignimbrites (Addis Ababa Ignimbrite), followed by central composite volcanoes (Central volcanoes unit) , and finally small spatter cones and lava flows (Akaki unit)

Based on the Geological map of Addis Ababa city (Mulugeta H/Mariam et.al, 2007), the following volcanic formations are predominantly found in the project and surrounding area:

1, Quatemary Basalt (Qb) : Extensively crops out around the project site and is the youngest unit in the area, it predominantly constituted by olivine phyric vesicular Basalt.

2, Repi Basalt (Tb3) : extensively crops out east of the project area and predominantly constituted by alkaline and olivine Basalt.

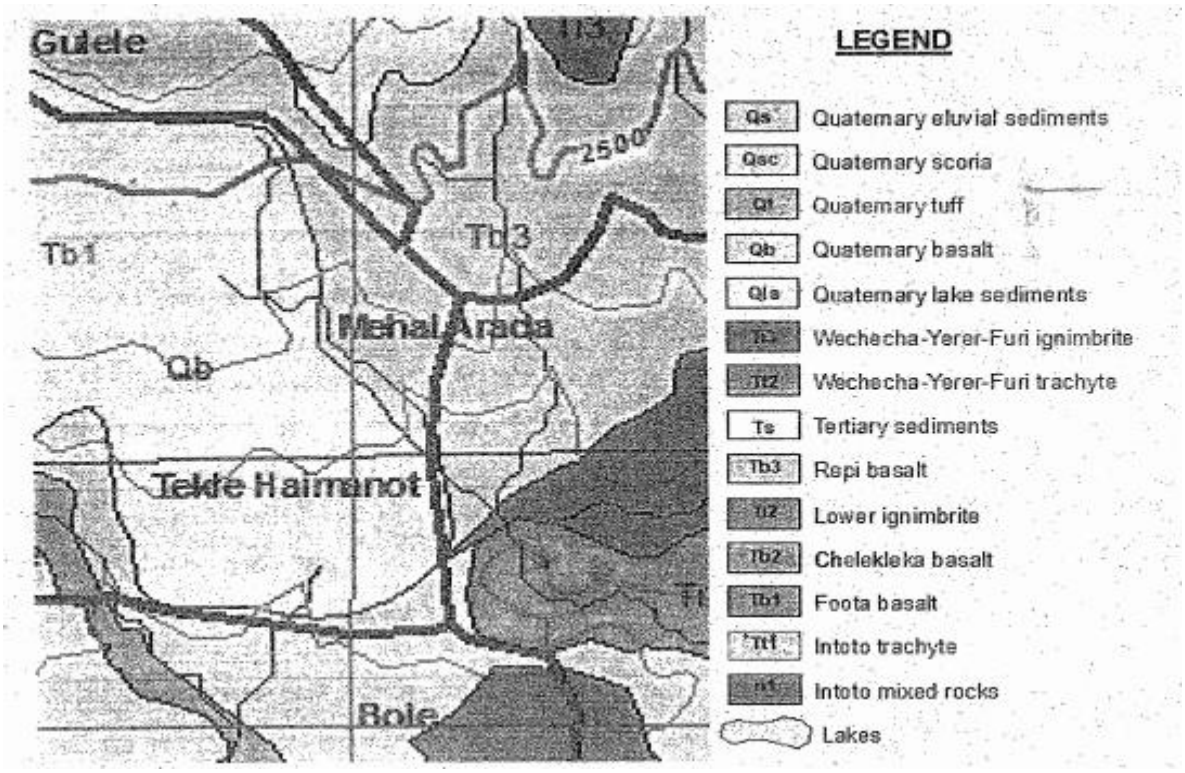

Figure 3.2Geological map of the project and surrounding areas

The field geotechnical investigation has been performed by the help of core drilling, sampling, insitu and laboratory testing. A total of four boreholes were drilled around the area and the co-ordinates, and depth sunk of the exploratory boreholes is presented in Table 3.2. (Best consulting engineers Plc, foundation investigation (2013))

Table 3. 1: Coordinate and Depth of Boreholes

No	BH-ID	Easting	Northing	Elevation	Depth drilled (m)
1	BH-01	0472386	0996250	2362	50.00
2	BH-02	0472392	0996266	2362	50.00
3	BH-03	0472408	0996252	2362	50.00
4	BH-04	0472413	0996267	2362	50.00

3.2.2. Description of the Geological Layers

Layer 1

This is the top firm, covered by gravely silty clay extends to an average depth of 3m below the natural ground level. The average standard penetration test (SPT) performed gave N- value of the layer is 7.5 for 30cm penetration.

Layer 2

This layer is Moderately weathered basalt rock. The layer is found within average depth interval of 3m to 9m below the ground level and has an average thickness of 6m. The average standard penetration test conducted in the layer gave N- value is 45 for 30cm penetration.

Layer 3

This layer is stiff clayey silt and extends average depth interval of 9 m to 16 m below ground level and has average thickness of 7m. the average SPT gave N-value of 30 for 30cm penetration.

Layer 4

This layer is sandy clayey silt and extends average depth interval of 16 m to 22 m below the ground level and has average thickness of 6 m. the average SPT gave N-value of 38 for 30cm penetration.

Layer 5

This layer is weathered and fractured basalt rock and extends average depth interval of 22 m to 29 m below the ground level and has average thickness of 7 m. the average SPT gave N-value of 50 for 30cm penetration.

Layer 6

This layer is decomposed rock (residual soil) and extends average depth interval of 29m to 40m below ground level and has average thickness of 11m. the layer has average SPT gave N-value of 40 for 30cm penetration.

Table 3. 2:soil layercrosection

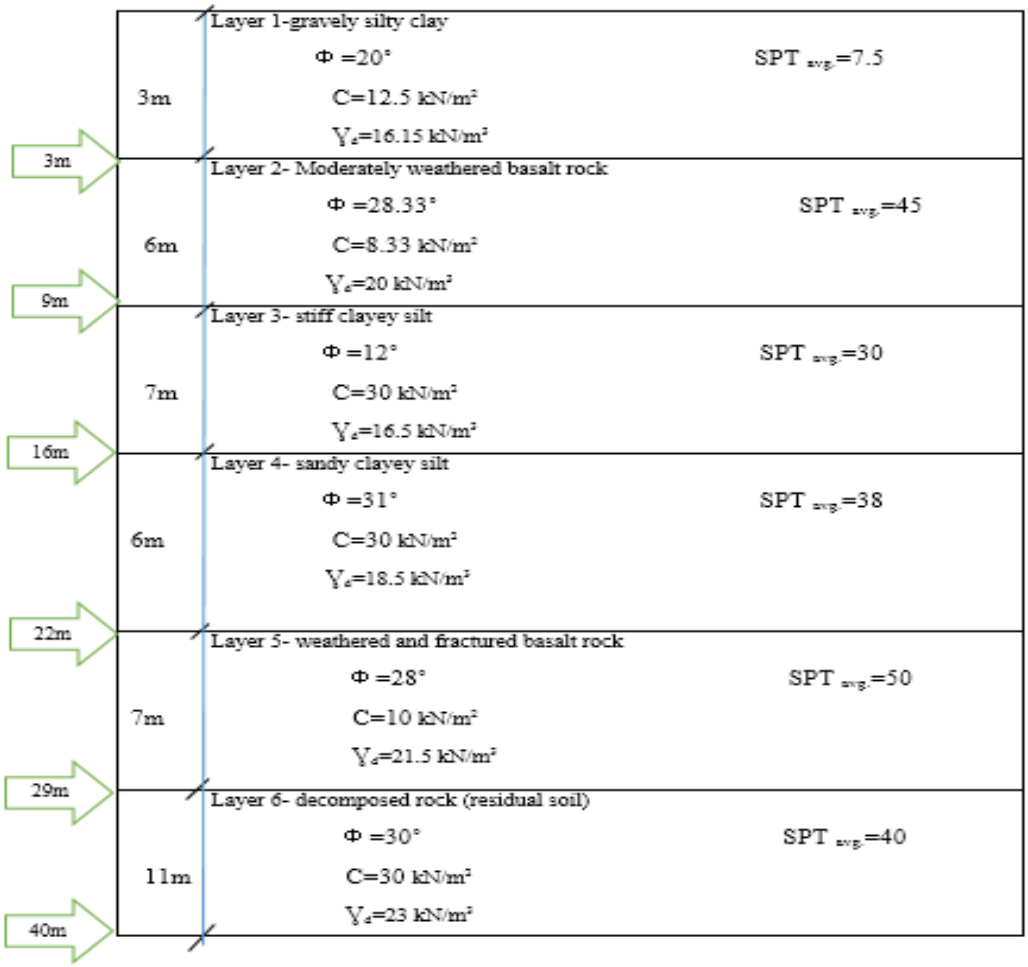

3.2.3. Ground Water Monitoring

During the soil investigation works, water level was monitored daily in order to examine the ground water profile. Static water level measurement was carried out in all boreholes and it was observed in all boreholes at a relatively shallow depth (5.7m in BH1 to 9.50 m in BH4). The static water level in boreholes was recorded daily and is shown on the log sheets.

In order to monitor the ground water level fluctuation of the project site, standpipe piezometer has been installed in borehole BH1. (Best consulting engineers Plc, foundation investigation (2013))

3.3 Soil Strength

The soil strength was determined through in-situ SPT 'N' values with depth below existing ground level. (Best consulting engineers Plc, foundation investigation (2013))

The soil strength/relative density was determined from laboratory tests on undisturbed samples together with empirically related to the SPT-N blow counts and hence, geotechnical designs can be provided.

3.4 Design Parameters

For geotechnical design, the design parameters are correlated and established. Based on the soil investigation carried out, the design parameters recommended for the designs are tabulated in table 3.4.

Table 3. 3: Soil parameters

Parameter	symbol	Unit	Layer 1	Layer 2	Layer 3	Layer 4	Layer 5	Layer 6
Bulk density	γ_w	KN/m^3	16.75	20.83	18.99	19.5	22.0	23.50
Apparent cohesion	c	KN/m^2	12.5	8.33	30	30	10	30
Angle of friction	ϕ	Degree	20	28.33	12	31	28	30
Poisson's ratio	v	-	0.23	0.27	0.25	0.26	0.27	0.25
SPT-N	N	Blows/30cm	7.5	45	30	38	50	40
Young's Modulus	E	KN/m^2	17,500	83,333	45,000	46,500	80,000	20,000
Depth (average)	D	m	0-3	3- 9	9.0 – 16.0	16.0 - 22.0	22.0-29.00	29.00 – 40.00
Moisture content	W	%	2.5	8.33	17	20	15	10
Initial void ratio	e_o	-	0.6	0.4	0.6	0.6	0.5	0.6
Specific gravity	G_s	-	2.675	2.77	2.65	2.68	2.65	2.50
Saturation unit weight	γ_{sat}	KN/m^3	18.25	22.5	18.99	20.50	22.5	23.75
Dry density	γ_d	KN/m^3	16.15	20.0	16.50	18.5	21.5	23.00

3.5 Anchor properties

2 anchor and 1 anchor levels with strands are used, each have been used for the anchoring system. The data for anchor design must be derived from aeromechanical analysis of the shear characteristics of the soil and the strength of the tendon. Bauer's structural engineering have many years of experience in design and can also draw on the results of numerous anchor load tests to aid in correct dimensioning.

In addition, the optimum number, distance length and angle of anchor for any individual site can be determined by continuously updated software packages.

Table 3. 4: Recommended Maximum Allowable Anchor Forces

Maximum allowable anchor forces					
Anchor type	Steel quality (N/mm2)	Steel diameter (mm)	Allowable anchor force acc. DIN 4125		Elastic stretch per KN and m of free length(mm/KNxm)
			Normal earth pressure (KN)	At rest earth pressure (KN)	
Strand Anchor	St 1570/	2xo.6”	251	330	0.018315
	1770	3x0.6”	377	496	0.012210
		4x0.6”	502	661	0.009158
		5x0.6”	628	826	0.007326
		6x0.6”	754	992	0.006105
		7x0.6”	879	1157	0.005233
		8x0.6”	1005	1300	0.004579
		9x0.6”	1130	-	0.004070
		10x0.6”	1256	-	0.003663
		11x0.6”	1300	-	0.003330
Single Bar Anchor	St 835/	32	384	473	0.00604
	1030	36	485	599	0.00477
	St 1080/	26.5	340	388	0.00880
	1230	32	496	563	0.00604
		36	628	723	0.00477

Steel diameter =2*0.6mm

Allowable anchor force DIN 4125

At normal earth pressure =251KN

At rest earth pressure =330KN

Elastic strength per KN and m of free length= 0.018315mm/KNm

Total length of anchor=13m

Anchor angle =15˚

3.6 Wall Properties

In Plaxis2D, real situation can be modelled either by a plane strain or an axisyrnmetric model. In order to predict the field behavior of contiguous walls, the plane strain idealization of continuous wall is reasonable for the purpose of comparative study with diaphragm wall which has been modeled as plane strain.

It is required to idealize the equivalent of plane strain for CBP so that Plaxis2D analysis will be more accurate and represent the actual site condition. Based on the data shown in table 3.4, equivalent thickness has been reduced to account for the spacing of the piles.

3.6.1 Diaphragm wall

Table 3.6 shows the Wall property for Plaxis2D Modeling of Diaphragm Wall.

Table 3. 5: Diaphragm Wall Parameters (Fahmi (2012))

t(mm)	Length (mm)	Fcu (N/mm2)	E(KN/mm2)	A(mm2)	Bending Stiffness, EA(KN/m)	I(mm4)	Flexural Stiffness, EI(KNmm2/m)
600	1000	40	30	600000	18000000	18,000,000,000	0.54E+12
800	1000	40	30	800000	24000000	42666666667	1.28E+12
1000	1000	40	30	1000000	30000000	83333333333	2.5E+12
1200	1000	40	30	1200000	36000000	1.44E+11	4.32E+12
1400	1000	40	30	1400000	42000000	2.28667E+11	6.86E+12

3.6.2. Contiguous Bored pile

In Plaxis2D, real situation can be modeled either by a plane strain or an axisyrnmetric model. In order to predict the field behavior of contiguous walls, the plane strain idealization of continuous wall is reasonable for the purpose of comparative study with diaphragm wall which has been modeled as plane strain. Table 3.7 shows the Wall property for Plaxis2D Modeling of Contiguous Bored Pile Wall.

Table 3. 6: Contiguous Bored Pile Properties (Fahmi (2012))

d(mm)	equivalent thickness	Fcu (N/mm2)	E(KN/mm2)	A(mm2)	Bending Stiffness, EA(KN/m)	I(mm4)	Flexural Stiffness, EI(KNmm2/m)
600	358.14	40	30	358,140	10,744,200	3830000000	1.15E+11
800	511.68	40	30	511,680	15,350,400	11600000000	3.48E+11
1000	665.222	40	30	665,222	19,956,660	24500000000	7.35E+11
1200	821.76	40	30	821,760	24,652,800	46240000000	1.3872E+12
1400	980.417	40	30	980,417	29,412,510	78530000000	2.3559E+12

3.7 Surcharge

The surcharge value should take into account the site conditions and control at site. Site conditions such as loadings from adjacent buildings; vehicles, services, etc. should be taken into consideration in the design. It is prudent to incorporate a minimum surcharge of 10kPa to cater for construction loads and unforeseen circumstances.

3.8 Proposed Scheme

Based on the selection processes for the optimization outlined in the preceding section, diaphragm wall and contiguous board pile wall are adopted for the thesis.

The anticipated excavation for construction is approximately 22m below ground with the proposed scheme, wall is designed to be embedded in the firm to stiff layer. As highlighted earlier, the need for adequate support, embedment and wall stiffness will govern the design, the followings are envisaged to be adopted: -

-Diaphragm wall thickness of 600mm-1400mm

- Contagious bored piles of diameter 600mm to 1400mm

- The Anchorage system will have 2 anchor and 1 anchor, and each anchor have 2*0.6 cable strands.

3.9 Base Model Generation

Typical base model geometry and general dimensions for the study is shown in Figure below. The model is simulated as a plain strain finite element employing 15-noded triangular elements and half of the geometry with a width of 100 meters and depth of 50 meter.

3.10 Justification for all PLAXIS figure output results

The figure below are made for the mere purpose of illustrating the conversation of the coordinate axis of PLAXIS figure output results into a more conventional type of coordinate axis for the intent visualizing the PLAXIS figure output results.

Figure 3.3Geological Sample co-ordinate axis for all PLAXIS figure output results (3m embedment depth)

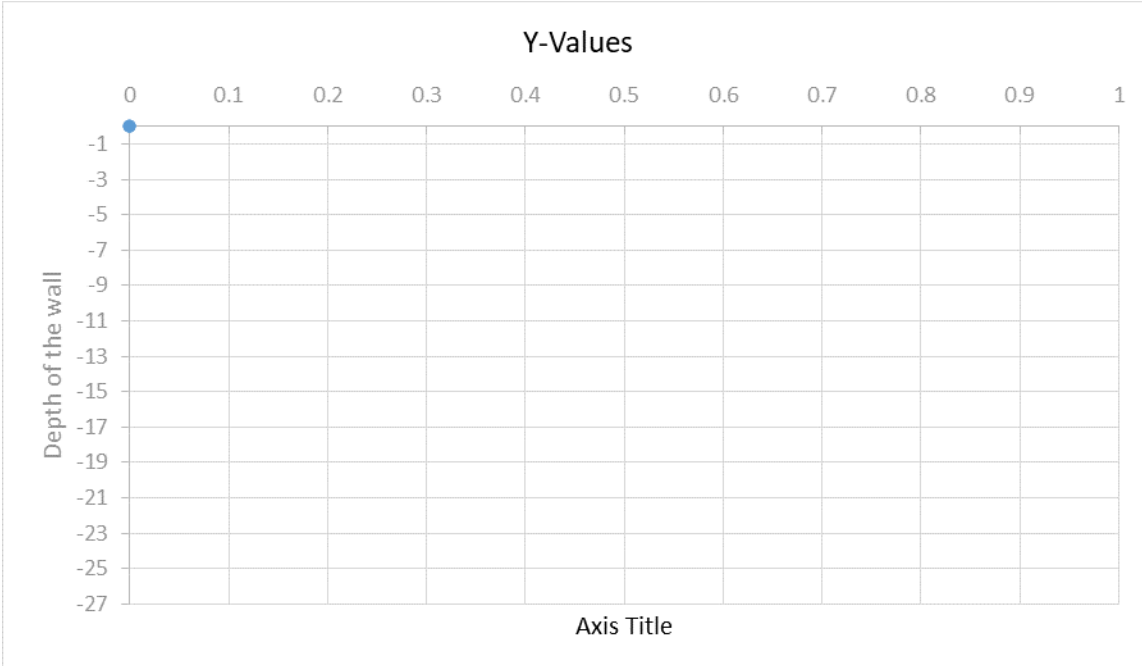

Figure 3.4Geological Sample co-ordinate axis for all PLAXIS figure output results (5 m embedment depth)

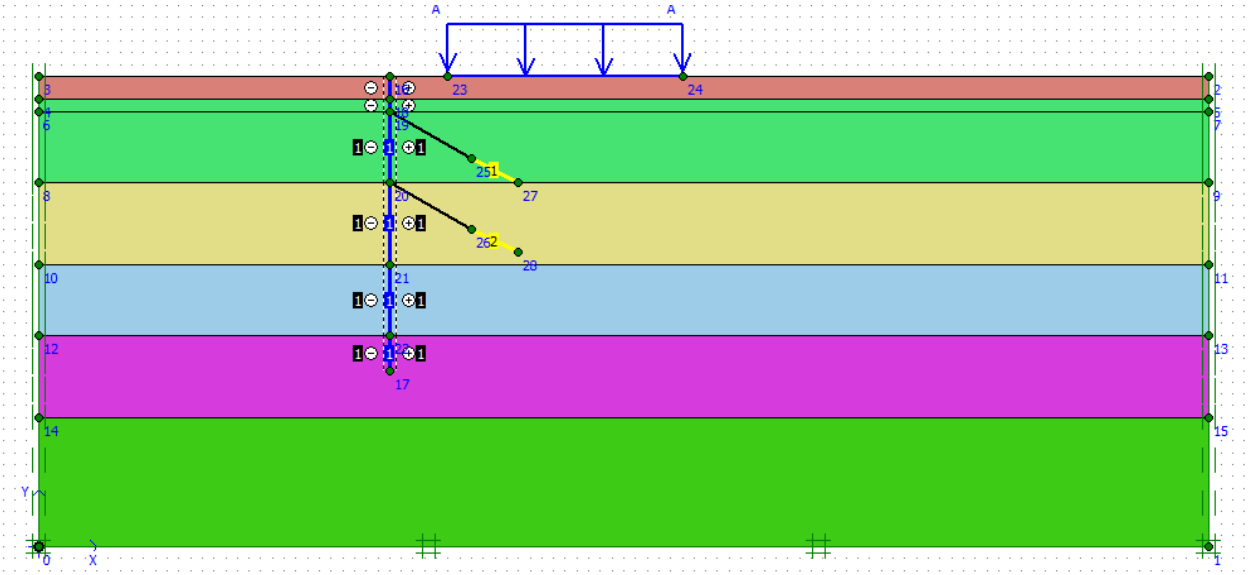

Figure 3.5FE Base Model for 2 Anchor (at 3m and 9m)

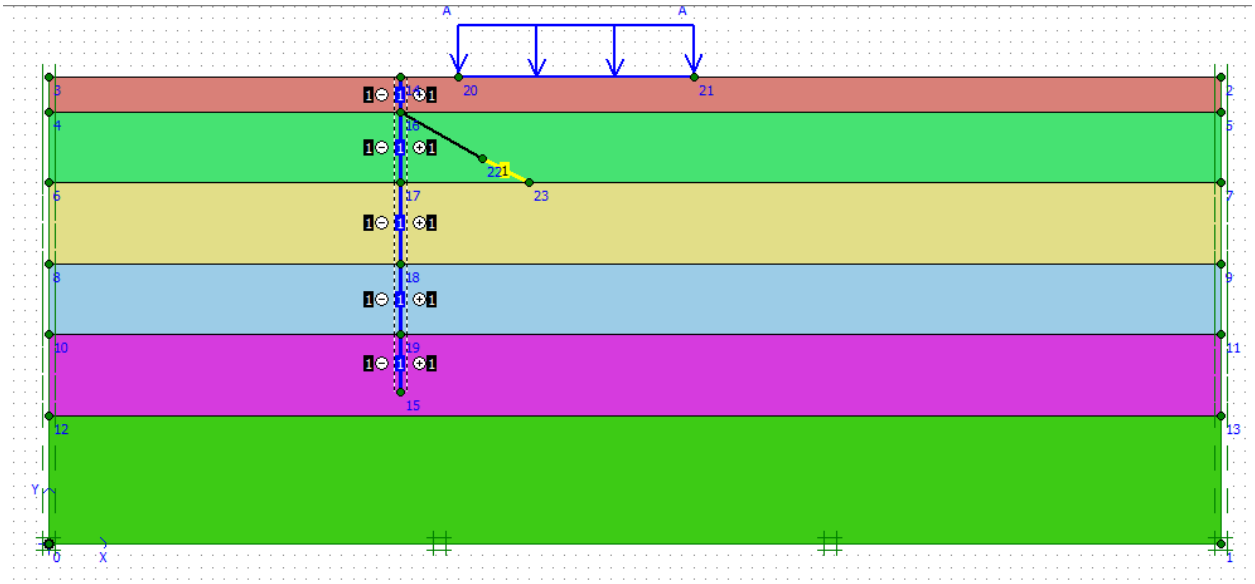

Figure 3.6FE Base Model for Anchor at 3m

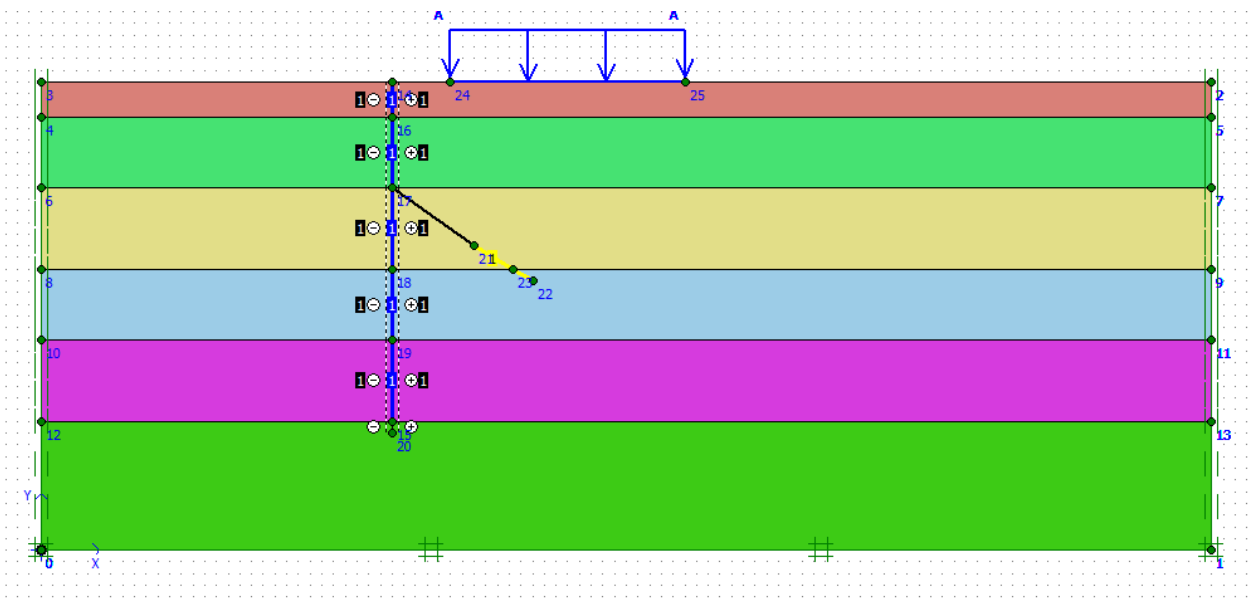

Figure 3.7FE Base Model for Anchor at 9m

Advanced finite element analysis of deep excavations should adopt accurate modeling procedures for geotechnical and structural behavior, e.g.

(i) The geometry of the excavation,

(ii) Detailed retaining structures,

(iii) Correct construction sequence, and

(iv) Reliable material models and input parameters.

The interaction between the soil and the temporary retaining system can be analyzed by using Finite Element Method (FEM) to study the effects of the excavation to the retaining system as well as to the surrounding ground and adjacent buildings. One of the powerful computer programs that use FEM is Plaxis2D to analyses of soil structure interaction problem.

Two dimensional plane strain analysis is used to model the excavation. Finite element mesh is assumed to have the left and right boundaries. The boundaries are assumed to be fixed horizontally but free to move vertically, whereas the bottom boundary was assumed to be fixed in both directions. The in-situ stresses were first generated based on the unit weight and the Ko procedures. After that, the in-situ hydrostatic pore pressures were generated by defining a phreatic line at the assumed water table level in the finite element mesh.

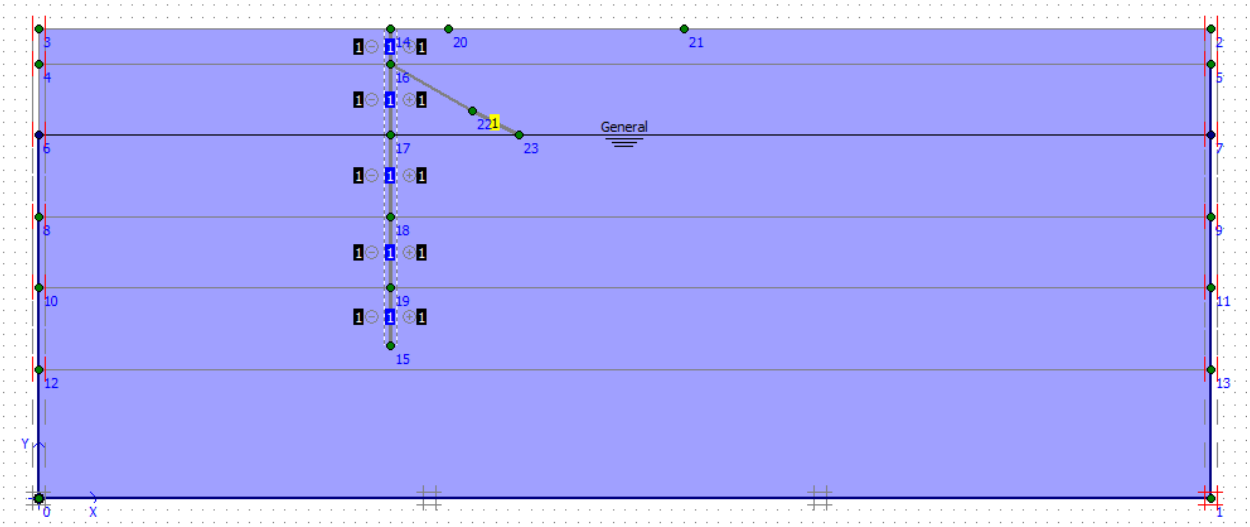

Figure 3.8 FE Base Model, phreatic line at assumed water level

The ground water at the retained earth side was kept at constant level at a depth of 9m below the ground to simulate the excavation. Meanwhile in the excavation side was re-defined to the formation level. This was to reflect the lowering of the ground water to the excavated level

IV. Chapter Four: Analysis of Result and Discussion

4.1. Optimization for Contiguous Bored Pile Walls

4.1.1. Effect of Wall Stiffness

Various size of the wall diameter (600mm-1400mm) for bored pile walls for retaining structure have been adopted for this paper in order to see the effect of the wall stiffness on the lateral wall deflection. In theory, it is expected that deformation of retaining wall decrease with the increase of its stiffness. Stiffness depends on the thickness or diameter of the wall. Based on (BS 8002) recommends, the wall displacement is to be limited to 0.5 % of the wall height. In our case the minimum diameter fulfills the requirement.

In this part of the analysis, the Research concentrated on how change in stiffness of Contiguous bored pile affect the performance of deep excavation at 7m embedment length for 600mm and 800mm diameters, the output from this analysis is presented below.

4.1.1.1 Bending Moment

In order to show the effect of wall stiffness on the Bending moment, diameter 600mm and 800mm have been presented for this paper. In theory, the bending moment of a retaining wall with the increase of its stiffness will increase. The bending stiffness of a beam can be calculated using linear elasticity theory of force displacement relation.

$F = K\Delta X$----------Equation 4.1

Where K is the stiffness of the material and it is given Euler's Bernoulli beam theory. For cylindrical vertical beam of radius r and length L the bending stiffness K is: -

$K = \frac{3}{64}\pi E\frac{D^4}{L^3}$----------Equation 4.2

Where D and L are the diameter and length of the pillar, respectively, and E is the Young's modulus of the material.

The stiffness of any material is highly dependent in the property of the material (elastic modulus) and its geometry (diameter and length in case of cylindrical beam). If the cross-section area which the force applied on (the diameter) increases, there will be distributed over the cross-section area and the stiffness of the structure will be high. Figures 4.1 show the distribution of bending moment of 600mm and 800mm diameter for CBP.

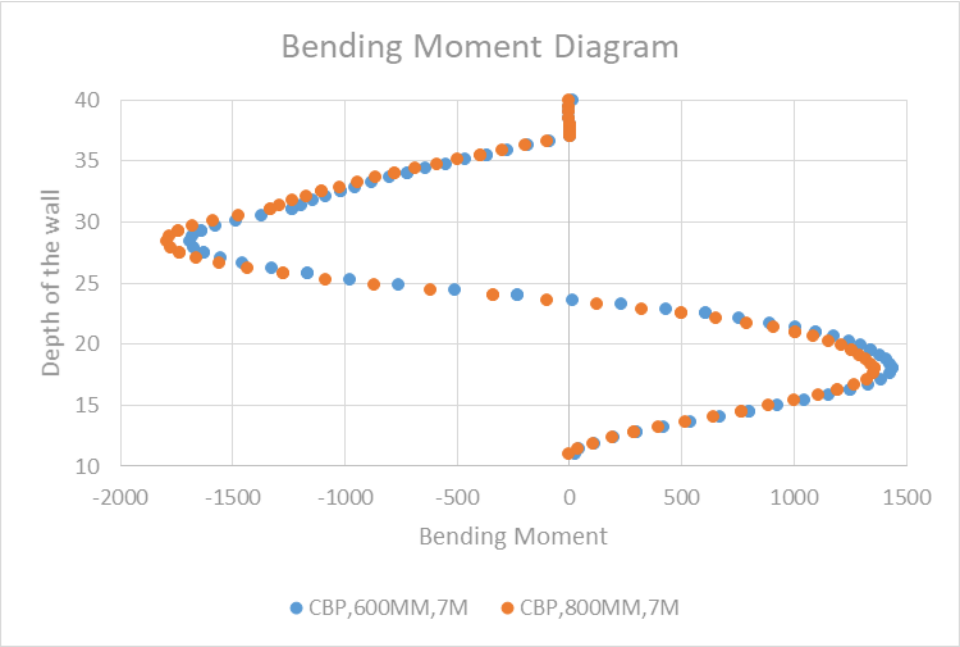

Figure 4.1Bending Moment Diagram for CBP

Figure 4.1 shows the maximum bending moment in contiguous bored piles. It can be seen that the maximum bending moment increased by 0.94 % as the thickness of the wall was increased from 600mm to 800mm for 7m embedment depth, but the percentage is very small. Future diagrams Clearly showed in appendix one.

4.1.1.2 Lateral Wall Deflection

In order to show the effect of wall stiffness on the lateral wall deflection, diameter 600mm and 800mm have been presented for this paper. In theory, the deflection of a retaining wall with the increase of its stiffness will decrease. The stiffness in tension and compression can be calculated using of force deflection relation.

$$K = \frac{F}{\delta}$$ ----------Equation 4.3

$$\delta = \frac{FL}{AE}$$ ----------Equation 4.4

Where F and L are the applied force and length of the pillar, respectively, and E is the Young's modulus of the material. K is the stiffness

The stiffness of any material is highly dependent in the property of the material (elastic modulus) and its geometry (diameter and length in case of cylindrical beam). If the cross-section area which the force applied on (the diameter) increases, there will be distributed over the cross-section area and the stiffness of the structure will be higher. Figures 4.2 show the distribution of lateral wall deflection of 600mm and 800mm for CBP.

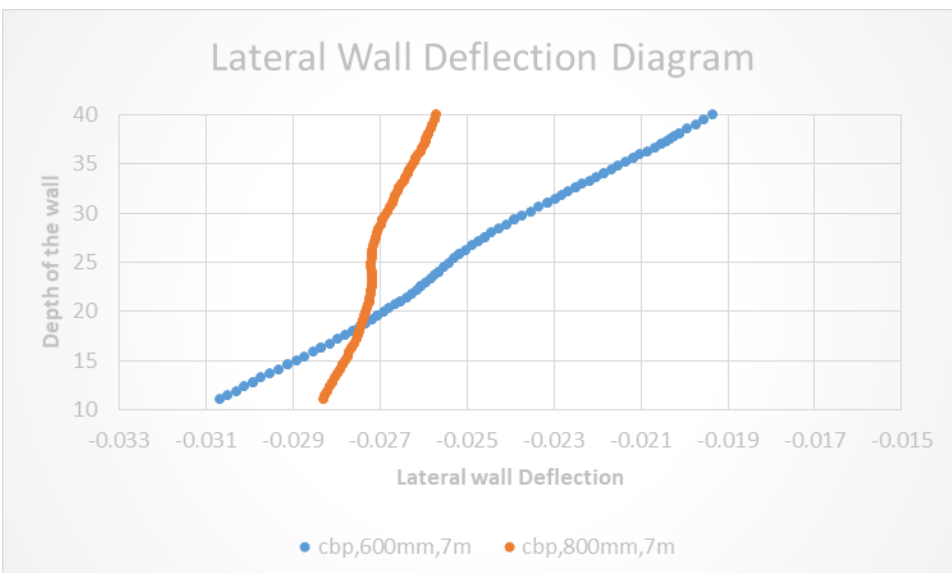

Figure 4.2Lateral Wall Deflection for CBP

Based on Figures 4.2 shows the lateral Wall deflection of the wall decreased as the thickness of the walls was increased from 600mm to 800 mm. It can be seen that the lateral deflection decreases by 0.82 % as the thickness of the wall was increased from 600mm to 800mm for 7m embedment depth, but the percentage is very small. This conclusion meet the idea stated in equations 4.4. Further diagrams Clearly showed in appendix one.

4.1.1.3 Shear Force

To show the effect of wall stiffness on the shear force, diameter 600mm and 800mm have been presented for this paper. In theory, the shear force of a retaining wall with the increase of its stiffness will increase. The shear stress can be calculated using of force cross-section area relation.

$$\tau = \frac{P}{A}$$ ----------Equation 4.5

$$A = \frac{PL}{\delta E}$$ ----------Equation 4.6

$$\delta = \frac{P}{K}$$ ----------Equation 4.7

$$\tau = \frac{PE}{KL}$$ ----------Equation 4.8

Where τ and P are shear stress and applied load , respectively, and

E and K are Young's modulus of the material and stiffness, respectively

From equation 4.8, when the stiffness increases the shear stress increase. since stiffness of any material is highly dependent in the property of the material (elastic modulus) and its geometry (diameter and length in case of cylindrical beam). Figures 4.3 show the distribution of Shear force of 600mm and 800mm for CBP.

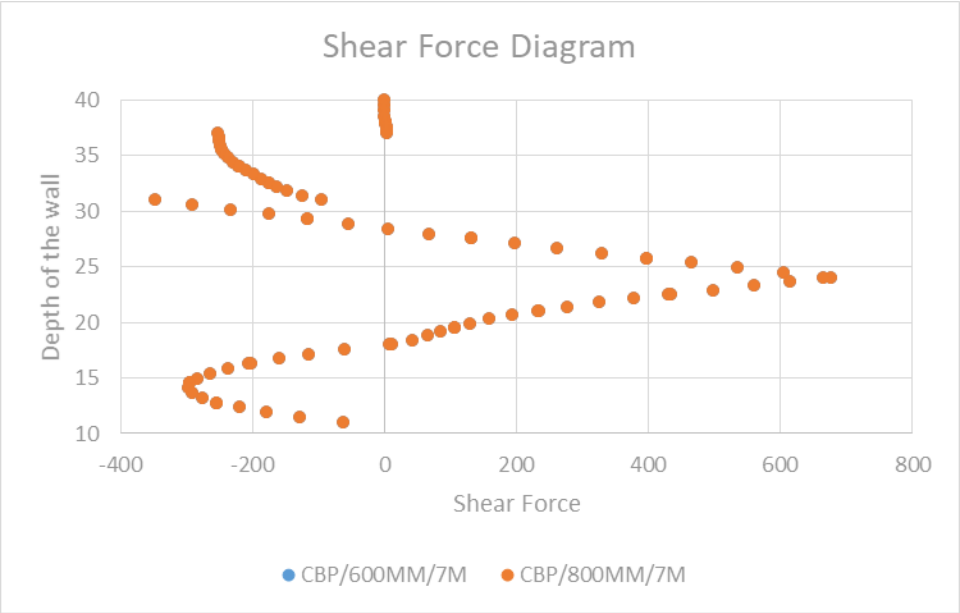

Figure 4. 3shear Force Diagram for CBP

Based on Figure 4.3 show the shear force on CBP decreases as the thickness of the walls is increased from 600mm to 800 mm. The shear force value become 676.78 kN when the thickness of the wall is 600mm. when the thickness become 800mm it decreases from 676.78 kN to 675.95 kN which is a 0.99% decrease for 7m embedment depth, but the percentage is very small. This conclusion meet the ideas stated in equations 4.8. Further diagrams Clearly showed in appendix one.

From the above discussion for the change in wall stiffness in bending moment, lateral wall deflection and shear force and based on BS 8002(which recommend, the wall displacement is to be limited to 0.5% of the wall height) all diameter above 600mm fulfil the requirements. Thus 600mm become the optimum diameter size.

4.1.2 Effect of Wall Embedment Length

In this section, the effect of change in depth of wall embedment on the performance of deep excavation supported by Contiguous bored pile at 600mm diameter for embedment depth (3m -11m) presented.

4.1.2.1 Bending Moment

In order to show the effect of embedment length on the Bending moment, embedment depths (3m -11m) have been presented for this paper. In theory, the bending moment of a retaining wall with the increase of its embedment length will increase. The bending stiffness of a beam can be calculated using equation 4.9.

$M = r \ x \ F$----------Equation 4.9

Where M and r are moment vector and position vector from the reference point, respectively

When the length of material (embedment depth) increase the bending force will be higher due to the moment arm increase. Figures 4.4 show the distribution of bending moment of CBP for embedment depths (3m -11m).

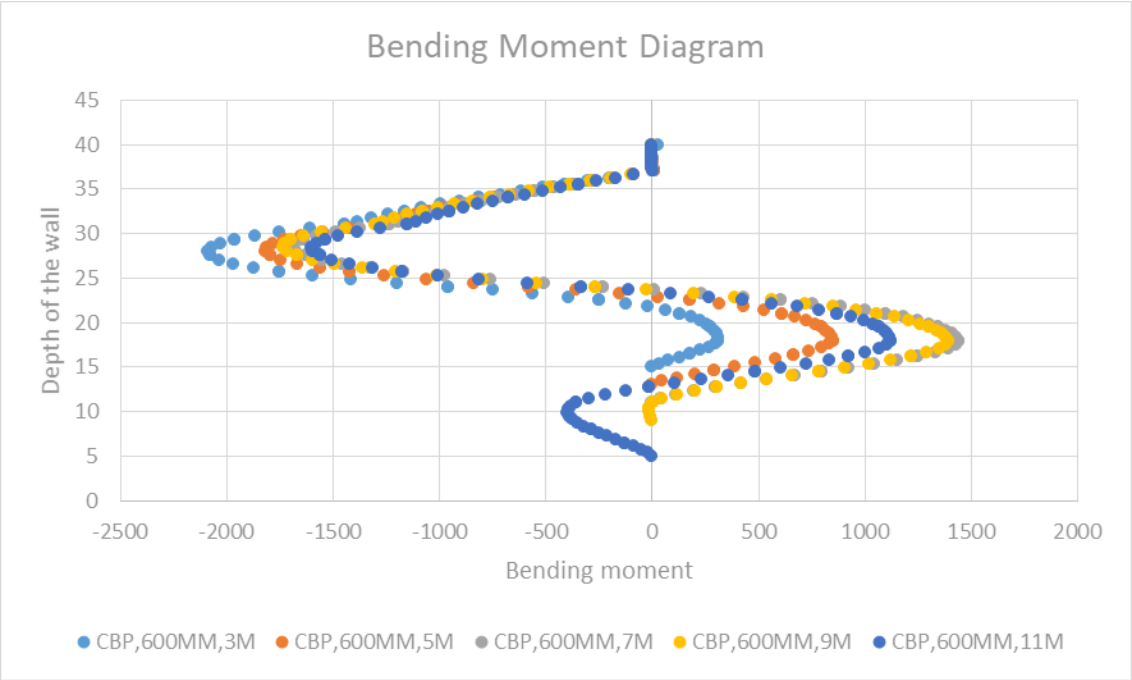

Figure 4.4Bending Moment Diagram for CBP

Figure 4.4 shows the maximum bending moment in the walls increase in response to increase in the depth of wall embedment. For the change of embedment depth from 3m to 5m,7m, 9m and 11m resulted in an increase of 0.87 %, 0.81 %, 0.83% and 0.77% of bending moment respectively for Contiguous Bored Piles wall. but the percentage is very small. This conclusion meet the ideas stated in equations 4.9. Further diagrams Clearly showed in appendix one.

4.1.2.2 Lateral Wall Deflection

In order to show the effect of embedment length on the lateral wall deflection, embedment depths (3m - 11m) have been presented for this paper. In theory, the lateral wall deflection of a retaining wall with the increase of its embedment length will increase. The deflection of a beam can be calculated using equation 4.10.

$$\delta = \frac{FL^3}{3EI}$$ ----------Equation 4.10

Where E is the Young's modulus ,I is the area moment of inertia of the cross-section ,δ is the deflection and L is the length .

When the length of material (embedment depth) increase the deflection will be higher, this clearly shows that deflection is directly proportional to length. Figures 4.5 show the distribution of lateral wall deflection of CBP for embedment depths (3m -11m).

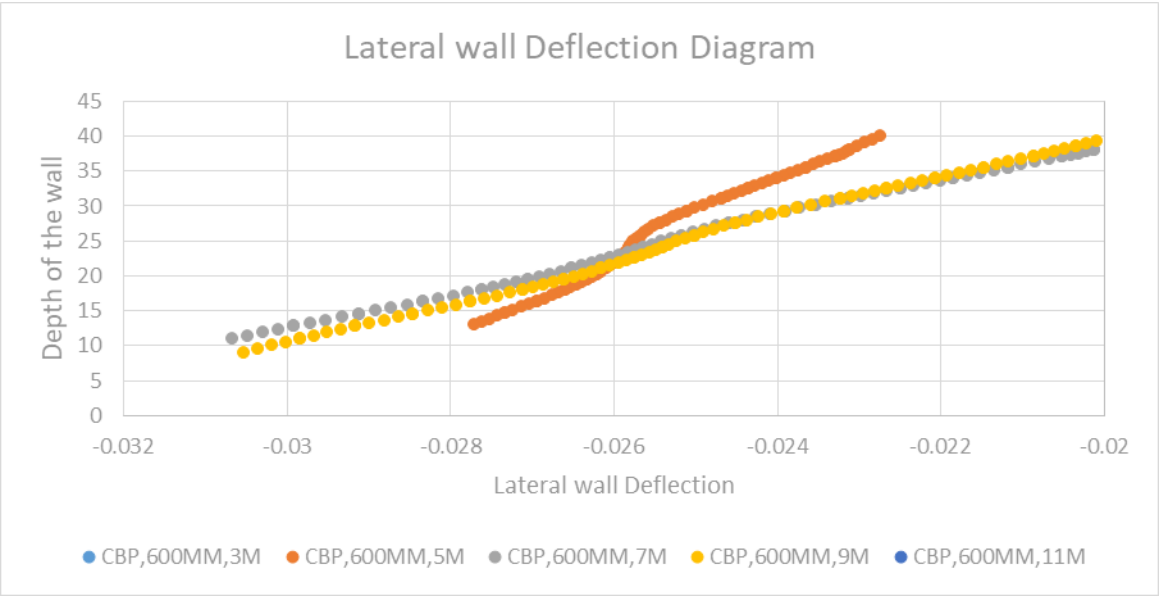

Figure 4.5Lateral Wall Deflection Diagram for CBP

Figure 4.5 shows the lateral wall deflection in the walls increase in response to increase in the depth of wall embedment. For the change of embedment depth from 3m to 5m and 7m resulted in an increase of 0.98 % and 0.94 of lateral wall deflection respectively. But due to skin friction, the lateral wall deflection in the walls decrease in response to increase in the depth of wall embedment, when the embedment depth changes from 3m to 9m and 11m resulted in an increase of 0.98 % and 0.86 of lateral wall deflection respectively for Contiguous Bored Piles wall. but the percentage is very small. Further diagrams Clearly showed in appendix one.

4.1.2.3 Shear Force

In order to show the effect of embedment length on the shear force, embedment depths (3m -11m) have been presented for this paper. In theory, the shear force of a retaining wall with the increase of its embedment length will increase.

Shear force and moment are very closely related to each other. if we take an intensity of load integrated it along the length of the beam, then it will give as shear acting in the beam. If we integrate it again, it will give as the moment value. So shear and moment are related as;

$$V(X) = \frac{dM}{dx}$$ ----------Equation 4.11

Now, because both shear and moment values are directly related to loads acting on the beam, a high shear value directly implies high moment demands on the beam or vice versa. According to equation 4.9, When the length of material (embedment depth) increase the bending force will be higher due to the moment arm increase. This also lead to have high shear force. Figures 4.6 show the distribution of shear force of CBP for embedment depths (3m -11m).

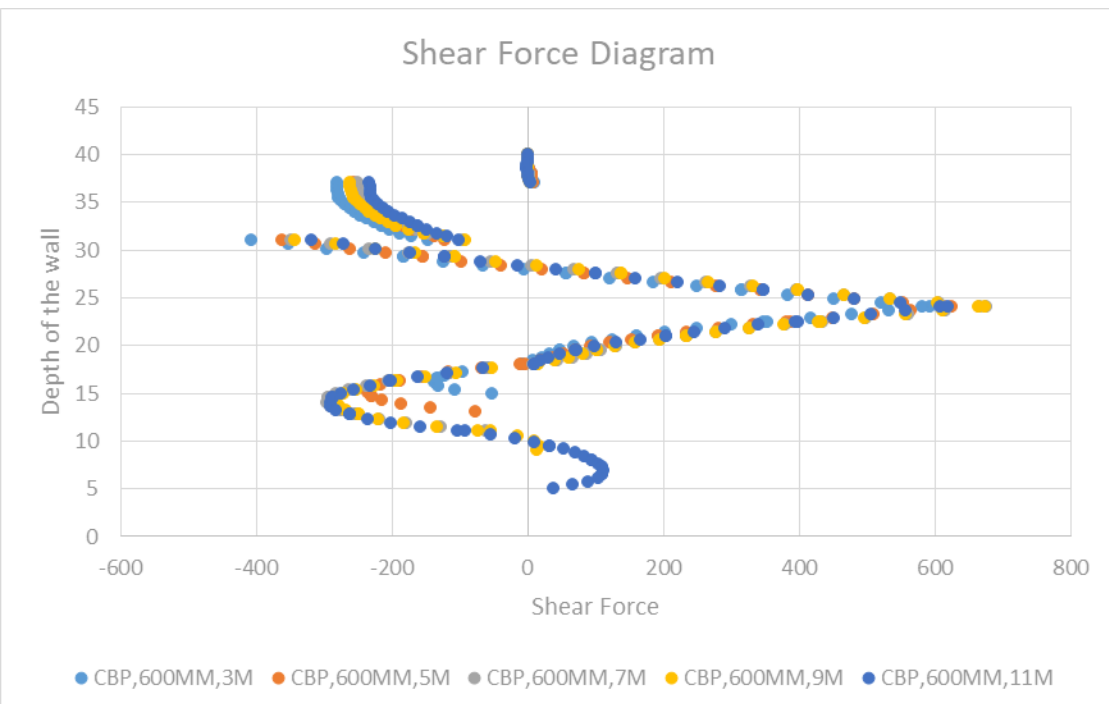

Figure 4.6Shear Force Diagram for CBP

Figure 4.6 shows the shear force in the walls increase in response to increase in the depth of wall embedment. For the change of embedment depth from 3m to 5m and 7m resulted in an increase of 0.95 % and 0.88 of shear force respectively. But due to skin friction, the shear force in the walls decrease in response to increase in the depth of wall embedment, when the embedment depth changes from 3m to 9m and 11m resulted in a decrease of 0.87 % and 0.96 of shear force respectively for Contiguous Bored Piles wall. but the percentage is very small. Further diagrams Clearly showed in appendix one.

From the above discussion for the change in embedment length in bending moment, lateral wall deflection and shear force, based on BS 8002(which recommend, the wall displacement is to be limited to 0.5% of the wall height) and since the adjacent structure of the research area is only road. embedment depth above 7m are not significant. Thus 7m embedment depth become the optimum length.

4.1.3 Effect of Number of Anchor

Its known that to design a deadman anchorage, the designer must be concerned about the depth of burial of the deadman and its distance behind the wall. In order to maximize the capacity of a deadman, the burial must be at a sufficient distance behind the wall to allow the deadman to develop its full passive resistance without conflicting with the active zone behind the wall.When a load is applied to a deadman, the anchorage resists through the development of a passive pressure wedge.

The capacity of the anchorage is defined in terms of passive pressure principles, and as an example, the unit capacity of the anchorage in a cohesion less material is: -

$P = Kp\frac{d}{2}$----------Equation 4.12

where ‘d’ is the depth of burial of the anchorage.

Tiebacks, whether they are anchored in soil (soil anchors) or rock (rock anchors) are designed so that they develop their capacity in friction along some portion of their length. While past practice at times relied on belled ends of drilled anchors and/or anchor plates to develop a passive cone of resistance, current thinking holds that most anchors will develop a frictional load along a defined length.

In this section, the effect of Number of anchors when it became 1 anchor or 2 anchors and also effect of anchor location due to embedment depth on the performance of deep excavation supported by Contiguous bored pile at 600mm diameter for embedment depth 7m presented.

4.1.3.1 Bending Moment

In order to show the effect of Anchor on the Bending moment, the optimum size from the above discussion (diameter 600mm with embedment depth 7m) have been presented for this paper. Theoretically when the number of anchor increase bending moment decrease.

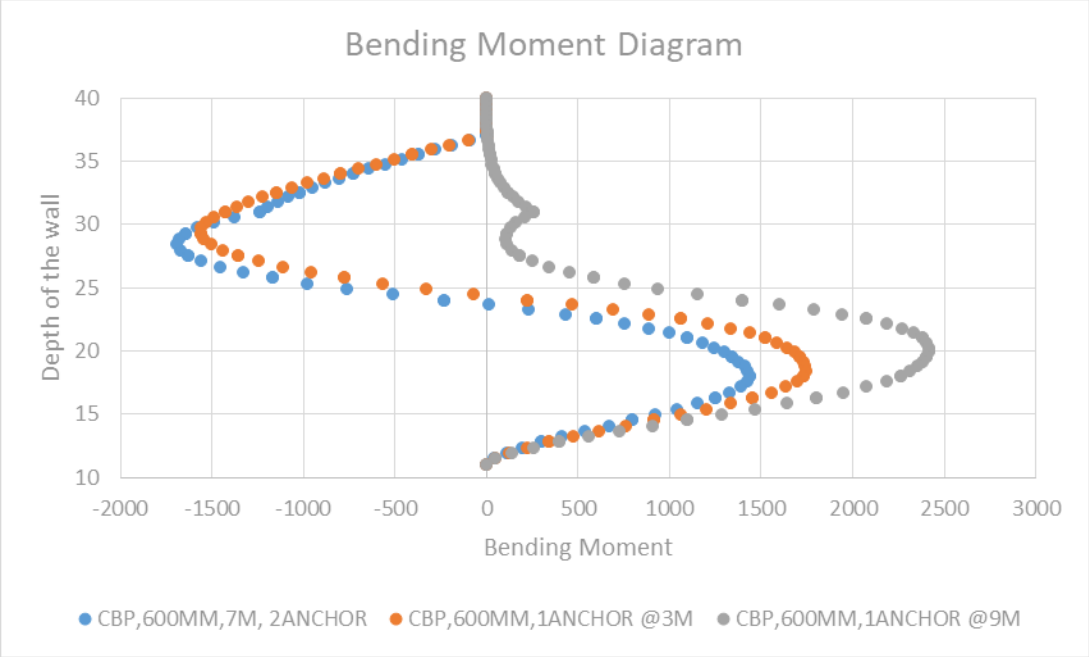

Figure 4.7Bending Moment Diagram for CBP

Figure 4.7 shows the maximum bending moment in contiguous bored piles. It can be seen that the maximum bending moment increased by 0.97 % as the no of anchor wall was decrease from 2 Anchors to 1Anchor. similarly, due the counter balance moment, maximum bending moment increased by 0.72 % as the anchor location change from 3m to 9m embedment depth. but the percentage is very small. This results meet the theoretical concept which discussed earlier. Future diagrams Clearly showed in appendix one.

4.1.3.2 Lateral Wall Deflection

In order to show the effect of Anchor on the lateral wall deflection, the optimum size from the above discussion (diameter 600mm with embedment depth 7m) have been presented for this paper. similar to the bending moment it was expected that, when the number of anchor increase Lateral wall deflection decrease.

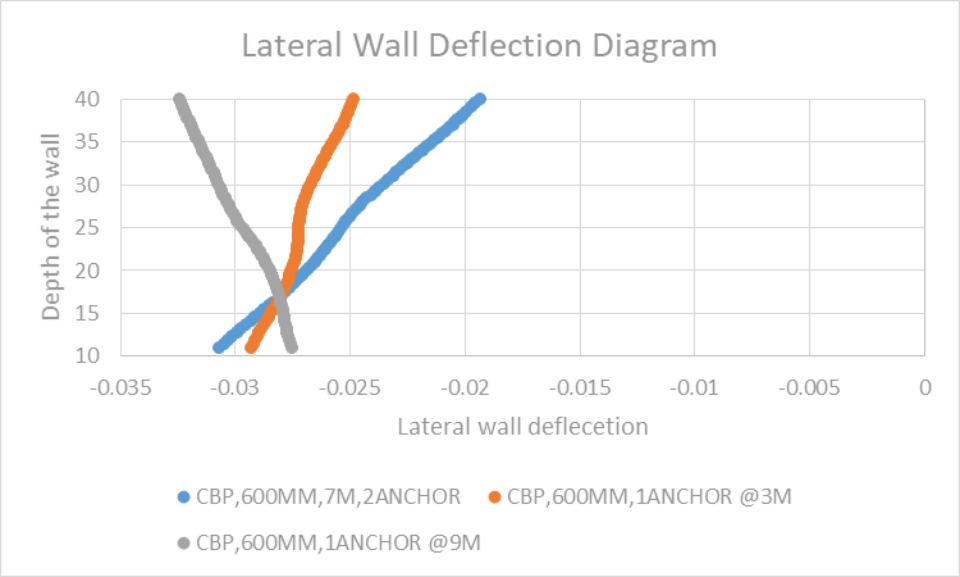

Figure 4.8: Lateral Wall Deflection for CBP

Figure 4.8 shows the lateral Wall deflection decrease by 0.98 % as the no of anchor wall was decrease from 2 Anchors to 1Anchor. but, the lateral Wall deflection increased by 0.97 % as the anchor location change from 3m to 9m embedment depth. but the percentage is very small. Future diagrams Clearly showed in appendix one.

From the above discussion for the change of number of anchorage, when the embedment depth increases the number of anchor decrease this is because we consider it like fixed support, while the depth decrease we consider only rotational failure. Also when the depth is increase passive resistance is higher.

When we consider using of 1 anchor, when the location is at embedment depth of 3m the deflection is smaller than that when it locates at embedment depth 9m, this is due to the capping effect. From this for our research area since we have capping effect and the only adjacent structure is road., 1 anchorage at depth of 3m is suitable.

4.2. Optimization for Diaphragm Walls.

4.2.1. Effect of Wall Stiffness

Various size of the wall thickness (600mm-1400mm) for Diaphragm walls for retaining structure have been adopted for this paper in order to see the effect of the wall stiffness on the lateral wall deflection. As Discussed Previously, theoretically it is expected that deformation of retaining wall decrease with the increase of its stiffness. Stiffness depends on the thickness or diameter of the wall. Based on (BS 8002) recommends, the wall displacement is to be limited to 0.5 % of the wall height. In our case the minimum diameter fulfills the requirement.

In this part of the analysis, the Research concentrated on how change in stiffness of Diaphragm wall affect the performance of deep excavation at 7m embedment length for 600mm and 800mm thickness, the output from this analysis is presented below.

4.2.1.1 Bending Moment

In order to show the effect of wall stiffness on the Bending moment, thickness 600mm and 800mm have been presented for this paper. In theory, the bending moment of a retaining wall with the increase of its stiffness will increase. The bending stiffness of a beam can be calculated using linear elasticity theory of force displacement relation. Using equation 4.1 and 4.2

The stiffness of any material is highly dependent in the property of the material (elastic modulus) and its geometry. If the cross-section area which the force applied on increases, there will be distributed over the cross-section area and the stiffness of the structure will be high. Figures 4.9 show the distribution of bending moment of 600mm and 800mm thickness for DW.

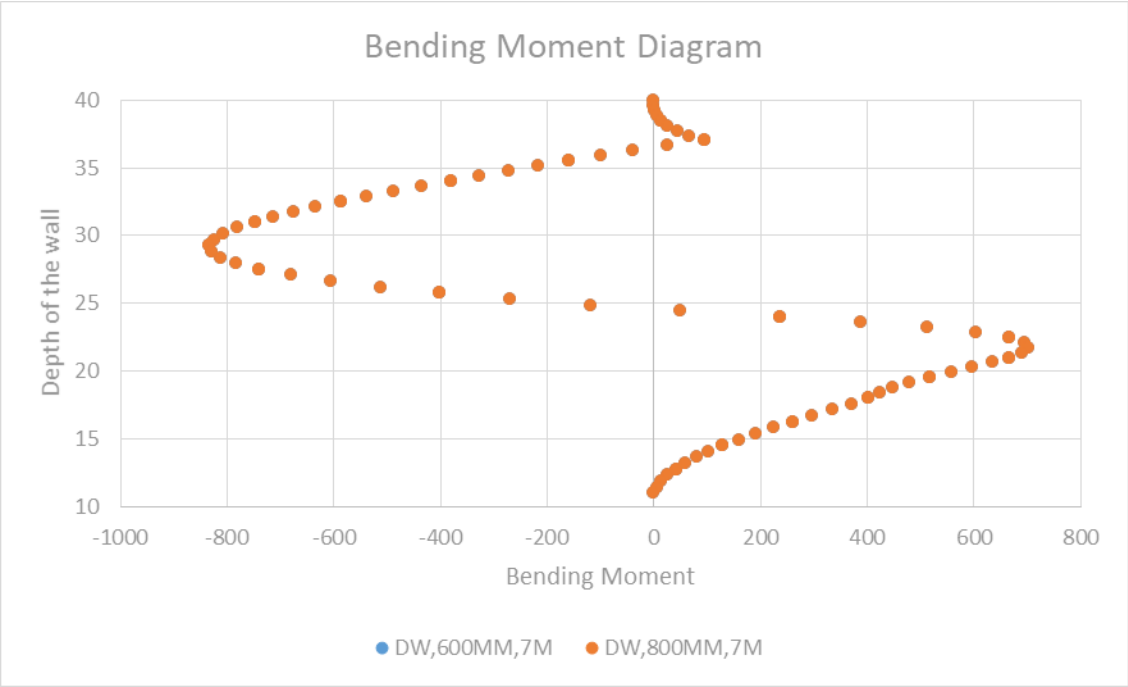

Figure 4.9 Bending Moment Diagram for DW

Figure 4.9 shows the maximum bending moment in Diagram wall. It can be seen that the maximum bending moment increased by 0.84 % as the thickness of the wall was increased from 600mm to 800mm for 7m embedment depth, but the percentage is very small. Future diagrams Clearly showed in appendix one.

4.2.1.2 Lateral Wall Deflection

In order to show the effect of wall stiffness on the lateral wall deflection, thickness 600mm and 800mm have been presented for this paper. In theory, the deflection of a retaining wall with the increase of its stiffness will decrease. The stiffness in tension and compression can be calculated using of force deflection relation. Using equation 4.3 and 4.4

As discussed earlier, stiffness of any material is highly dependent in the property of the material (elastic modulus) and its geometry. If the cross-section area which the force applied increases, there will be distributed over the cross-section area and the stiffness of the structure will be higher. Figures 4.10 show the distribution of lateral wall deflection of 600mm and 800mm for DW.

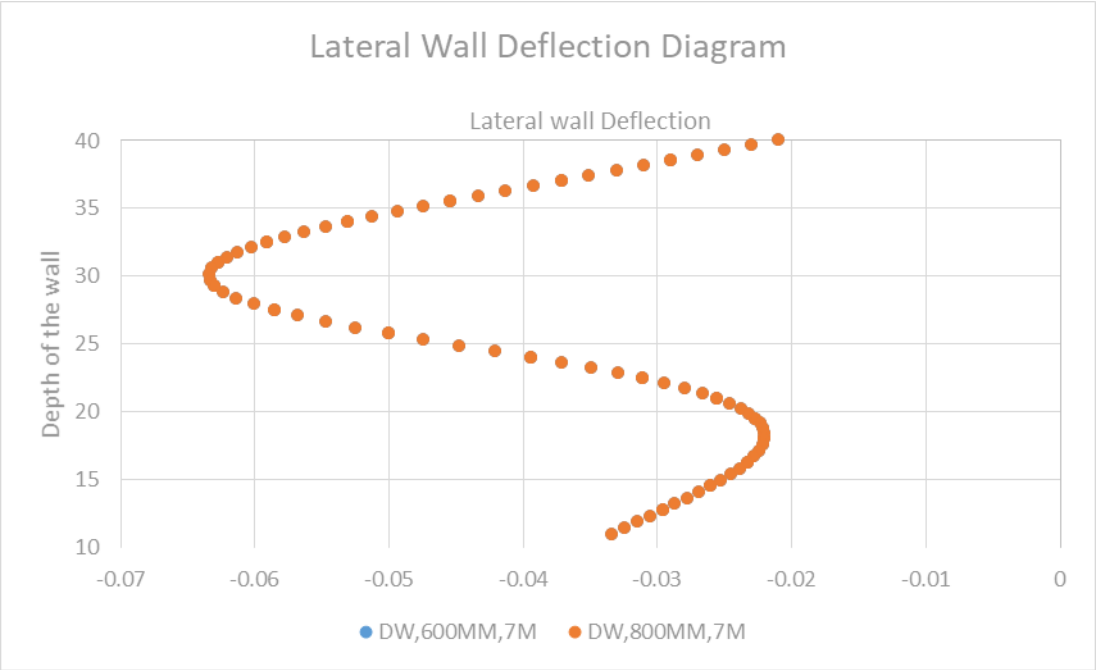

Figure 4.10 Lateral Wall Deflection for DW

Based on Figures 4.10 shows the lateral Wall deflection of the wall decreased as the thickness of the walls was increased from 600mm to 800 mm. It can be seen that the lateral deflection decreases by 0.77 % as the thickness of the wall was increased from 600mm to 800mm for 7m embedment depth, but the percentage is very small. This conclusion meet the idea stated in equations 4.4. Further diagrams Clearly showed in appendix one.

4.2.1.3 Shear Force

To show the effect of wall stiffness on the shear force, thickness 600mm and 800mm have been presented for this paper. In theory, the shear force of a retaining wall with the increase of its stiffness will increase. The shear stress can be calculated using of force cross-section area relation.

From equation 4.8, when the stiffness increases the shear stress increase. since stiffness of any material is highly dependent in the property of the material (elastic modulus) and its geometry. Figures 4.11 show the distribution of Shear force of 600mm and 800mm for DW.

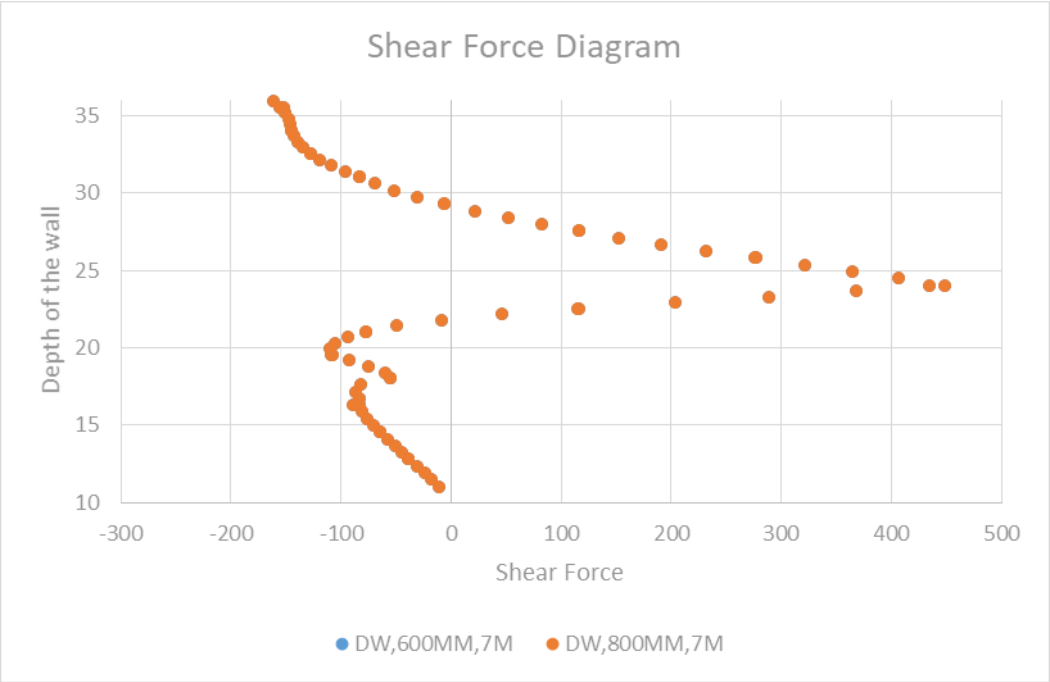

Figure 4.11 shear Force Diagram for DW

Based on Figure 4.11 show the shear force on DW increase as the thickness of the walls is increased from 600mm to 800 mm. The shear force value become 449.23kN when the thickness of the wall is 600mm. when the thickness become 800mm it decreases from 449.23kN to 468.12 kN which is a 0.96 % increase for 7m embedment depth, but the percentage is very small. Further diagrams Clearly showed in appendix one.

From the above discussion for the change in wall stiffness in bending moment, lateral wall deflection and shear force and based on BS 8002(which recommend, the wall displacement is to be limited to 0.5% of the wall height) all diameter above 600mm fulfil the requirements. Thus 600mm become the optimum thickness size.

4.2.2 Effect of Wall Embedment Length

In this section, the effect of change in depth of wall embedment on the performance of deep excavation supported by Diagram wall at 600mm thickness for embedment depth (3m -11m) presented.

4.2.2.1 Bending Moment

In order to show the effect of embedment length on the Bending moment, embedment depths (3m -11m) have been presented for this paper. In theory, the bending moment of a retaining wall with the increase of its embedment length will increase. The bending stiffness of a beam can be calculated using equation 4.9.

When the length of material (embedment depth) increase the bending force will be higher due to the moment arm increase. Figures 4.12 show the distribution of bending moment of DW for embedment depths (3m -11m).

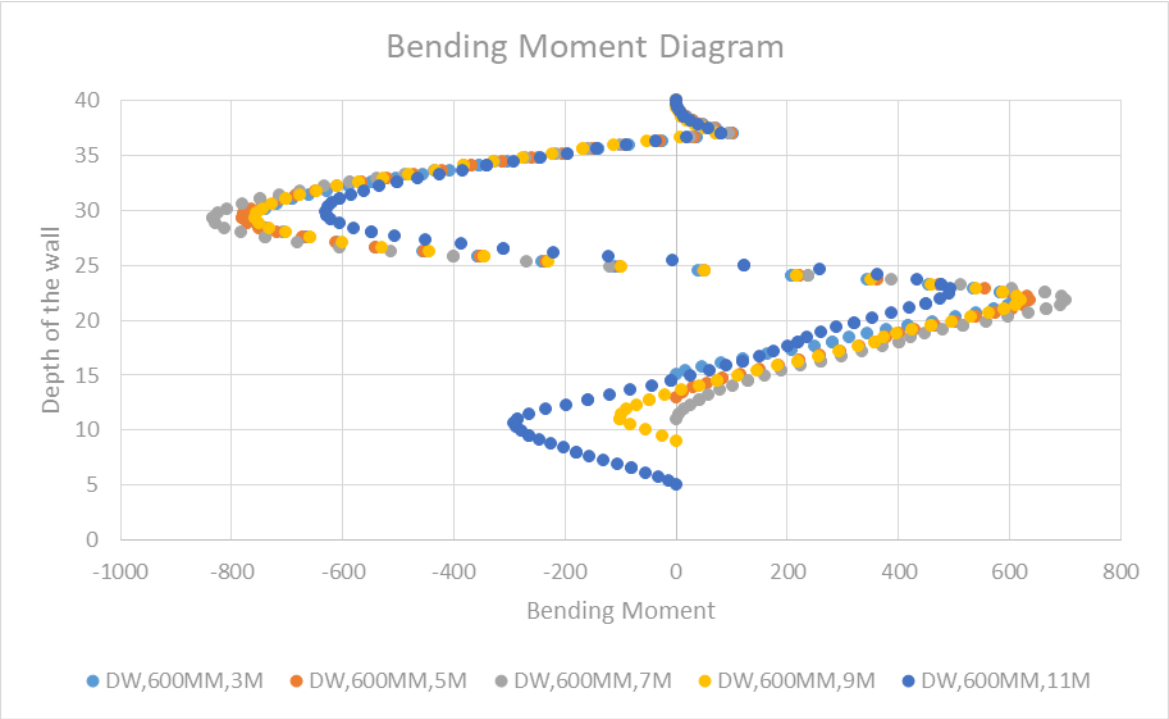

Figure 4.12 Bending Moment Diagram for DW

Figure 4.12 shows the maximum bending moment in the walls decreases in response to increase in the depth of wall embedment. For the change of embedment depth from 3m to 5m and 7m resulted in a decrease of 0.97 % and 0.91 of bending moment respectively. But due to skin friction, the maximum bending moment in the walls increase in response to increase in the depth of wall embedment, when the embedment depth changes from 3m to 9m and 11m resulted in an increase of 0.99 % and 0.83 of bending moment respectively for Diaphragm wall. but the percentage is very small. Further diagrams Clearly showed in appendix one.

4.2.2.2 Lateral Wall Deflection

In order to show the effect of embedment length on the lateral wall deflection, embedment depths (3m - 11m) have been presented for this paper. In theory, the lateral wall deflection of a retaining wall with the increase of its embedment length will increase. The deflection of a beam can be calculated using equation 4.10.

When the length of material (embedment depth) increase the deflection will be higher, this clearly shows that deflection is directly proportional to length. Figures 4.13 show the distribution of lateral wall deflection of DW for embedment depths (3m -11m).

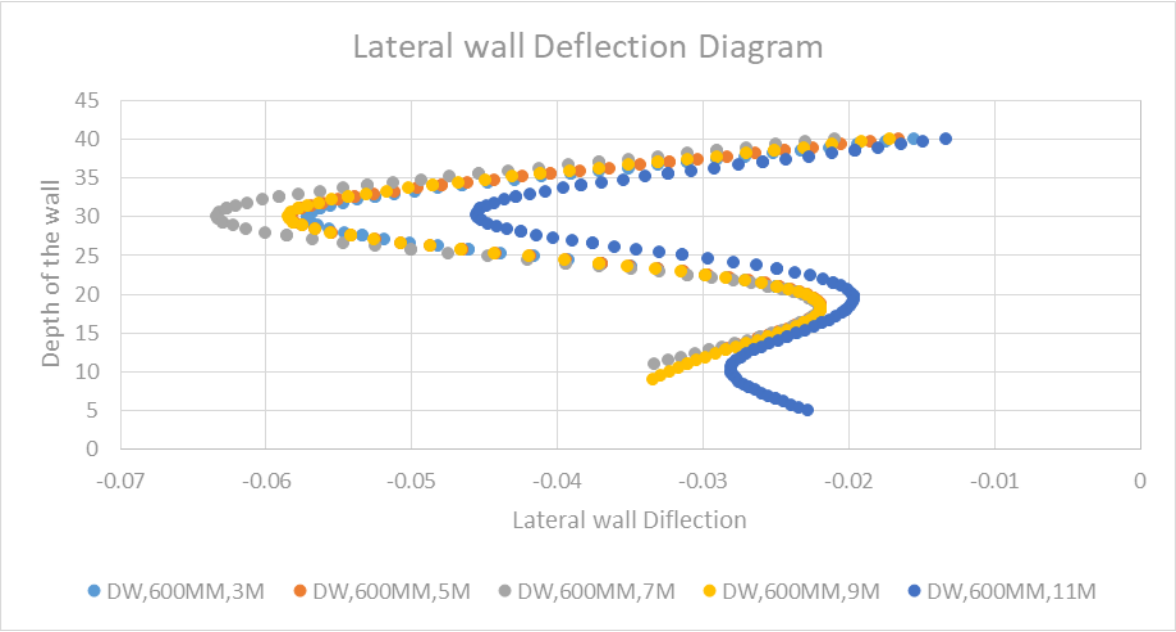

Figure 4.13 Lateral Wall Deflection Diagram for DW

Figure 4.13 shows the lateral wall deflection in the walls increase in response to increase in the depth of wall embedment. For the change of embedment depth from 3m to 5m and 7m resulted in an increase of 0.99 % and 0.93 of lateral wall deflection respectively. But due to skin friction, the lateral wall deflection in the walls decrease in response to increase in the depth of wall embedment, when the embedment depth changes from 3m to 9m and 11m resulted in a decrease of 0.99 % and 0.80 of lateral wall deflection respectively for Diaphragm wall. but the percentage is very small. Further diagrams Clearly showed in appendix one.

4.2.2.3 Shear Force

In order to show the effect of embedment length on the shear force, embedment depths (3m -11m) have been presented for this paper. In theory, the shear force of a retaining wall with the increase of its embedment length will increase.

Shear force and moment are very closely related to each other. if we take an intensity of load integrated it along the length of the beam, then it will give as shear acting in the beam. If we integrate it again, it will give as the moment value. So shear and moment are related it can describe as written in equation 4.11.

Now, because both shear and moment values are directly related to loads acting on the beam, a high shear value directly implies high moment demands on the beam or vice versa. According to equation 4.9, When the length of material (embedment depth) increase the bending force will be higher due to the moment arm increase. This also lead to have high shear force. Figures 4.14 show the distribution of shear force of DW for embedment depths (3m -11m).

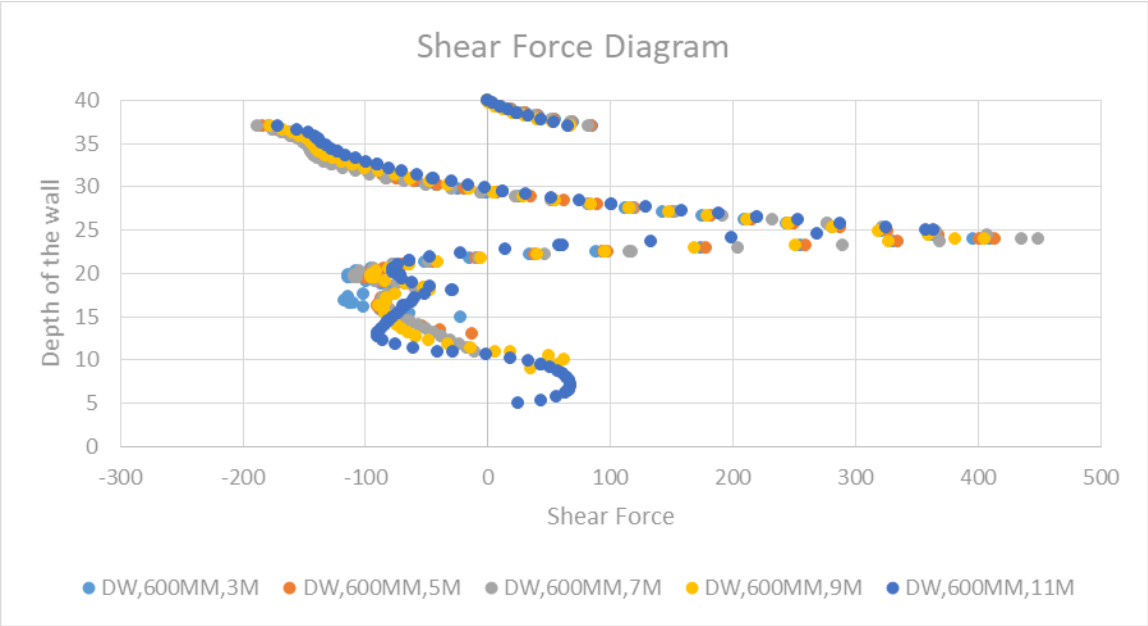

Figure 4.14 Shear Force Diagram for DW

Figure 4.14 shows the shear force in the walls increase in response to increase in the depth of wall embedment. For the change of embedment depth from 3m to 5m and 7m resulted in an increase of 0.99 % and 0.91 of shear force respectively. But due to skin friction, the shear force in the walls decrease in response to increase in the depth of wall embedment. When the embedment depth changes from 3m to 9m and 11m resulted in a decrease of 0.99 % and 0.89 of shear force respectively for Diaphragm wall. but the percentage is very small. Further diagrams Clearly showed in appendix one.

From the above discussion for the change in embedment length in bending moment, lateral wall deflection and shear force, based on BS 8002(which recommend, the wall displacement is to be limited to 0.5% of the wall height) and since the adjacent structure of the research area is only road. embedment depth above 7m are not significant. Thus 7m embedment depth become the optimum length.

4.3 Cost Analysis

In this part, the Research concentrated on the comparison and selection of minimum cost. From the above discussions on the effect of stiffness, embedment depth and anchor ,the optimum section was selected,

thus the optimum section is diameter 600mm with 7m embedment depth for CBP and thickness 600mm with embedment depth of 7m for DW with one anchor was selected.

The cost analysis (unit rate) of the walls is prepared per meter. The unit rate for contiguous and diaphragm walls is taken from the current Ethiopian construction condition whereas drilling unit rate of the diaphragm wall, due to local unavailability, is adopted from international market.

N.B.: All prices are expressed here after are in **ETB (Ethiopian Birr)** and are net prices which are subject to 15% VAT. Furfure cost analysis attached in Appendix 2.

Table 4. 1: contiguous Board PileWall BOQ Shoring Works with thickness 600mm

Item No.	Description	Unit	Total Qty	Unit Price	Total Price
1	Drilling Equipment Mobilization	Lump sum	1	156,329.16	156,329.16
2	Drilling Equipment Demobilization	Lump sum	1	78,704.16	78,704.16
3	Anchoring, shotcreting and grouting machine mobilization	Lump sum	1	26,869.87	26,869.87
4	Anchoring shotcreting and grouting machine demobilization	Lump sum	1	26,869.87	26,869.87
5	Drilling of pile apex.dia 600mm piles	M	29	3846.37	111,544.73
6	Reinforcement cage installation	Kg	1224	51.95	63586.80
7	Piling Concrete Installation	m3	33	2735.54	90,272.82
8	Installation of Temporary Grouted Anchors	M	39	2,474.93	96,522.27
9	Stressing and Proof testing of Anchors	No.	3	2,197.89	6,593.67
10	Shotcreting reinforcement cage installation	Kg	168	65	10,920.00
11	Shotcreting (15 cm thickness)	m2	29	2853.54	82,752.66
TOTAL					750,966.01
VAT (15%)					112,644.90
GRAND TOTAL					863,610.91

Table 4. 2: Diaphragm Wall BOQ shoring Works with thickness 600mm

Item No.	Description	Unit	Total Qty.	Unit Price	Total Price
			Quantity		
1	Drilling Equipment Mobilization	Lump sum	1	171,962.08	171,962.08
2	Drilling Equipment Demobilization	Lump sum	1	86,574.58	86,574.58
3	Anchoring, shotcreting and grouting machine mobilization	Lump sum	1	26,869.87	26,869.87
4	Anchoring shotcreting and grouting machine demobilization	Lump sum	1	26,869.87	26,869.87
5	Drilling cost	m3	33	1,400.00	46,200
6	Reinforcement cage installation	Kg	1224.00	51.95	63,586.80
7	Piling Concrete Installation	m3	33	2735.54	90,272.82
8	Installation of Temporary Grouted Anchors	M	39	2,474.93	96,522.27
9	Stressing and Proof testing of Anchors	No.	3	2,197.89	6,593.67
10	Bentonite and Cement	m2	468	42	19,656.00
TOTAL					635,107.96
VAT (15%)					95,266.19
GRAND TOTAL					730,374.15

Table 4. 3:

summary of cost Analysis

No	Item	CBP (Birr)	DW (Birr)
1	Direct cost Analysis for pilling	17,660	9,267.755
2	Summary of BOQ for concrete work	139,551.90	119,840.29
3	Summary of BOQ for Shoring works	863,610.91	730,374.15
Total		1,020,822.81	859,482.195

V. Chapter Five: Conclusion and Recommendation

5.1 Conclusion

The primary goal of this thesis was to study the effects of Diaphragm and Contiguous bored pile retaining walls for deep excavation in terms of wall deflections and cost incurred. The effects of wall stiffness, embedment depth and no of Anchors have been investigated for that purpose in detail.

It is known that increasing in the wall stiffness will result in less wall deflection and the ground surface movement. However, it is only to some extent because stiffer wall tempts larger bending moment. Thus, more reinforcement is needed and this will result in less economical design. Hence by extending the embedment depth of the wall it will give significant reduction in lateral wall deflection and also the ground surface movement at the retained side.

The Finite element results shows for both Diaphragm and contiguous bored pile walls, an increase in stiffness (size of the wall), decrease displacement decrease.BS 8002 recommends, the wall displacement is to be limited to 0.5% of the wall height. Because of this those wall sections above 600mm fulfill the requirement.

Similarly, when increasing the embedment depth, the deflection increase, However, it is only to some extent because of wall friction deflection decrease when embedment depth increases. Since the adjacent structure in the research area is road, embedment depth require is at a shallow depth of 7m is enough.

Finally based on comparison of cost incurred, Diaphragm wall require minimum cost for installation than contiguous bored pile walls.

Based on the results of this Research the optimized wall type for the selected site is Diaphragm wall with thickness of 600mm with embedment depth of 7m.

5.2 Recommendation

As mentioned earlier, in our country especially in Addis Ababa the most common type of retaining wall for deep excavation is Contiguous bored pile wall. Based on the results of this Research ,the optimized wall type for the selected site is Diaphragm wall with thickness of 600mm with embedment depth of 7m.

5.3 Recommendation for Further Studies

All the analysis performed in this study assumed that there is no dynamic effect of wall installation. Thus, to simulate an actual condition at a site and to get more accurate result in terms of ground movement the wall installation effect need to be considered.

All the analysis in this study also performed by using plane strain analysis (2D). For future study shall be performed to incorporate the 3D effects, such studies can account for cases with shorter wall dimensions, that deviate from plane strain condition.

VI. References

1. Arora,J.(2004).*Introduction to Optimum Design (2nd Edition ed.)*. Amsterdam: Elsevier Academic Press.
2. Ashok V. M, Dr. Babu Kurian, Merin Mathews, and Anu James(2016)*Section Optimization of Diaphragm Wall.*International Journal for Research in Applied Science & Engineering Technology (IJRASET)
3. Braja M. Das (1997). *Advanced Soil Mechanics.* California State University.
4. Brinkgreve, R., Broere, W., & Waterman, D. (2004). *PLAXIS 2-D Professional Version 8.0 - User's Manual.* PLAXIS b.v., The Netherlands.
5. BS 8002, (1994). *Code of practice for earth retaining structures. London:* Bristish Standards Institution
6. Christopher,A.C.(2004).*Simulation Modeling Hand Book*-A Practical
7. Clough, G., & Tsui, Y. (1974). Performance of Tied-Back Walls in Clay. (ASCE, Ed.) *Journal of Geotechnical Engineering Division, 10* (12), 1259-1273.
8. Clough, G. W., and Hansen, L. A. 1981. "Clay anisotropy and braced wall behavior." J. Geotech. Eng. Div., Am. Soc. Civ. Eng., 1077, 893–913
9. Clough, G. W., E. M. Smith and B. P. Sweeney (1989). Movement control of excavation support systems by iterative design. ASCE conference on current principles and practices on foundation and engineering. New York, ASCE. **Vol.2:** 869-884.
10. Clough, G. W. and T. D. O'Rourke (1990). *Construction induced movements of insitu walls*. ASCE Conference on Design and Performance of Earth Retaining Structures. Cornell University, Ithaca, New York**:** 439-470.
11. Finno, R. J. and L. S. Bryson (2002). "*Response of building adjacent to stiff excavation support system in soft clay*." Journal of Performance of Constructed Facilities **16**(1): 10-20.
12. Finno, R. J., & Harahap, I. S. (1991). "*Finite element analyses of HDR-4 excavation.* Journal of Geotechnical Engineering", *117*(10), 1590-1609. https://doi.org/10.1061/(ASCE)0733-9410 (1991) 117 : 10(1590)

13. Hashash, M. (1992). *Analysis of Deep Excavation in Clay.* MIT, Dept. of Civil Engineering. Cambridge, MA.

14. Hashash, Y. M. A. and A. J. Whittle (1996). "*Ground movement prediction for deep excavations in soft clay*." Journal of Geotechnical and Geoenvironmental Engineering **122**(6): 474-486.
15. Institution of Structural Engineers. 1975. Design and Construction of Deep Basements. Institution of Structural Engineers. London.

16. Lim, A., C. Y. Ou and P. G. Hsieh (2010). "Evaluation of clay constitutive models for analysis of deep excavation under undrained conditions." Journal of GeoEngineering **5**(1): 9-20.
17. Mana, A. I. and G. W. Clough (1981). "Prediction of movements for braced cuts in clay." Journal of the Geotechnical Engineering Division **107**(6): 759-777.
18. Muhammed Fahimi Bin Johan(2012). "*Optimization of Retaining Wall in Deep Excavation for Basement Work"*. Faculty of Civil Engineering, Malaysia.
19. Ouand Shiau (1998).*Analysis of the corner effect on excavation behaviors.*Canadian Geotechnical Journal 35(3):532-540

20. Ou, C., Hsieh, P., & Chion, D. (1993). Characteristics of ground surface settlement during excavation. *Canadian Geotechnical Journal, 30* (5), 758-767.
21. Peck, R. (1969). Deep excavations and tunneling in soft ground. *Proceedings of the 7th International Conference on Soil Mechanics*, (pp. 225-290).
22. R.J. Jardine, D.M.Potts, A.S Fourie and J. B Surland (1984) ."Studies of the Influence of Non-Liner Stress –Strain Characteristics in Soil-Structure Interaction." London Géotechnique 36(3):377-396 ·
23. Teferra, A. (1992). *Foundation Engineering.* Addis Ababa: Addis Ababa University Press.
24. Teferra, A., & Leikun, M. (1999). *Soil Mechanics.* Addis Ababa: Addis Ababa University Press.
25. Telford,J.K.(2007).*A Brif introduction to Design of Experiments*.(J.hopkins,Ed.)APL Technical Digest,27.
26. Terzaghi, K. (1943). Theoretical Soil Mechanics. New York, John Wiley & Son.

27. Venkata Ramasubbarao GODAVARTHI, Dineshbabu MALLAVALLI, Ramya PEDDI, Neelesh KATRAGADDA, and Prudhvikrishna MULPURU(2011)*Contiguous Pile Wall as a Deep Excavation Supporting System.*SRK Institute of Technology, Enikepadu-521 108, Vijayawada, Andhra Pradesh, India.
28. Wanchai Teparaksa and Jirat Teparaksa (2019).*Comparison of diaphragm wall* movement *prediction and field performance for different construction techniques.* Faculty of Civil Engineering, Thailand.

VII. Appendix-One

Additional Results

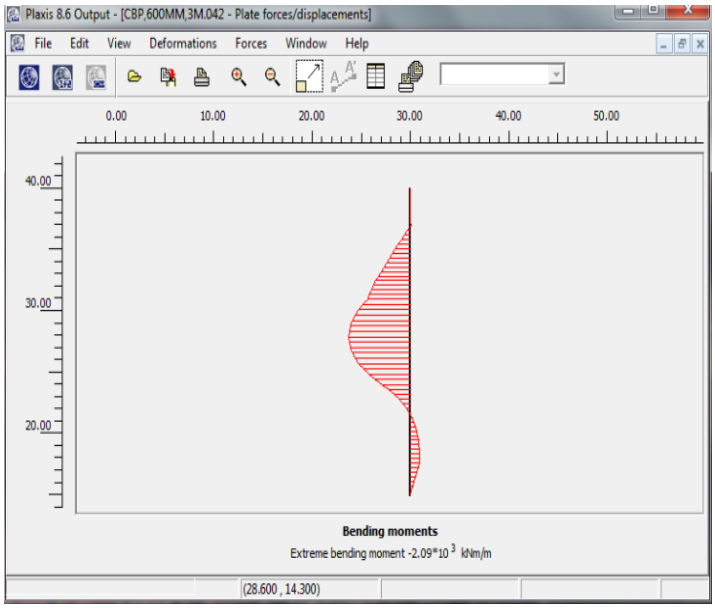

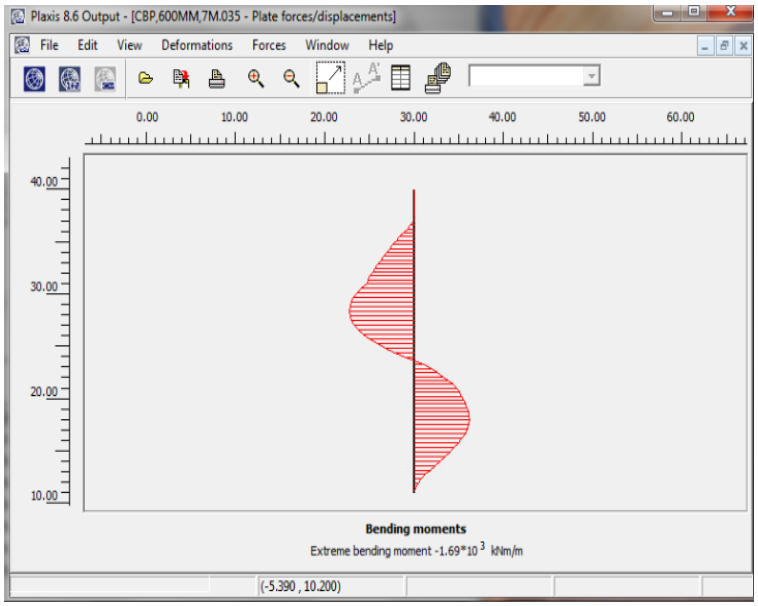

(a) (b)

Figure 7.1 Bending Moment Diagram of CBP for 600mm diameter (a) 3m depth& (b) 5m depth

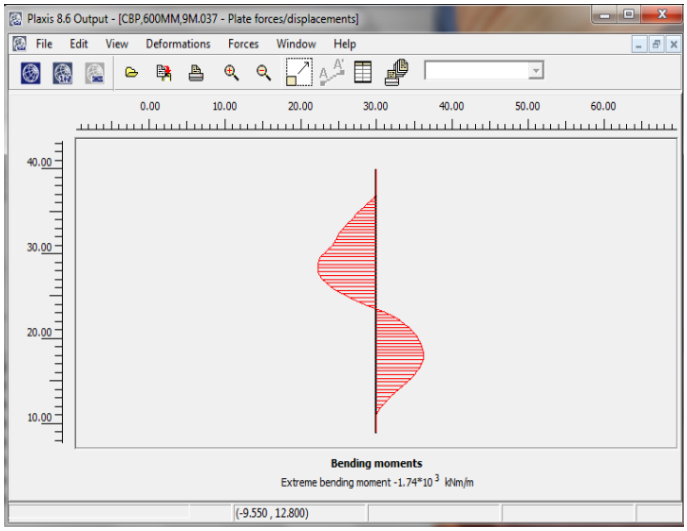

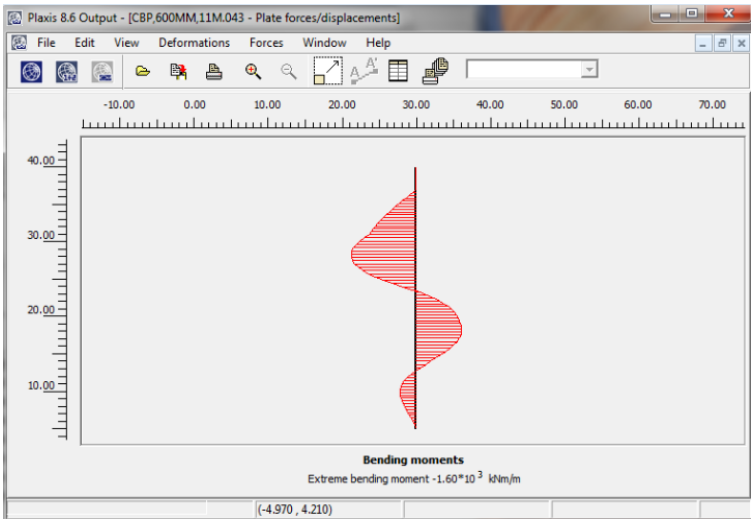

(a) (b)

Figure 7.2Bending Moment Diagram of CBP for 600mm diameter (a) 9m depth& (b) 11m depth

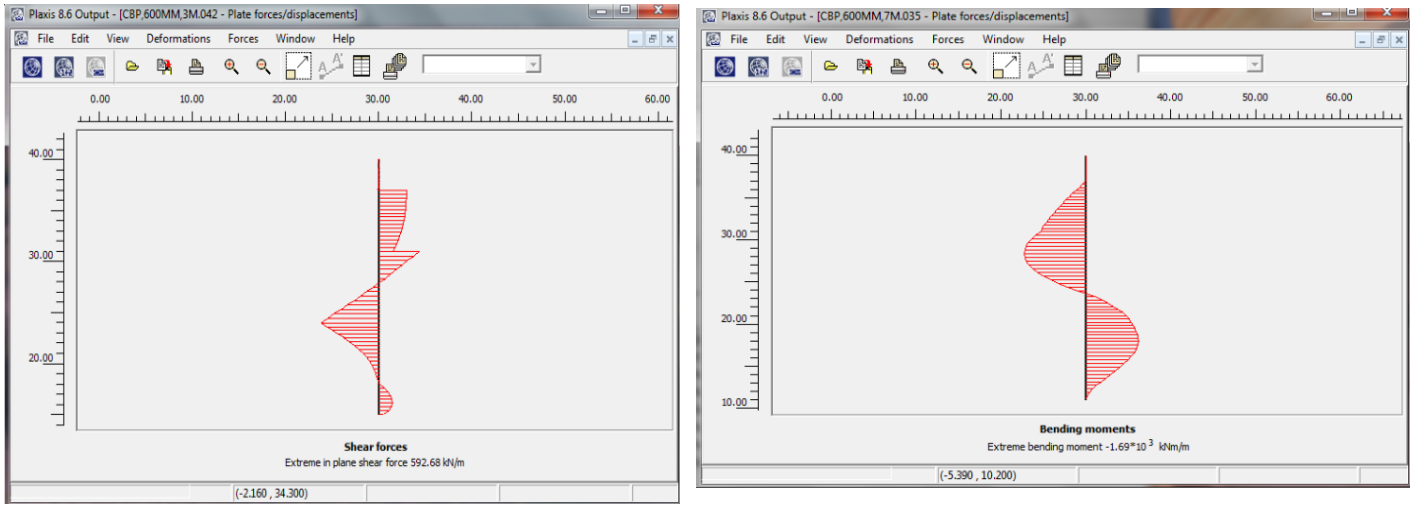

(a) (b)

Figure 7.3 shear force Diagram of CBP for 600mm diameter (a) 3m depth& (b) 7m depth

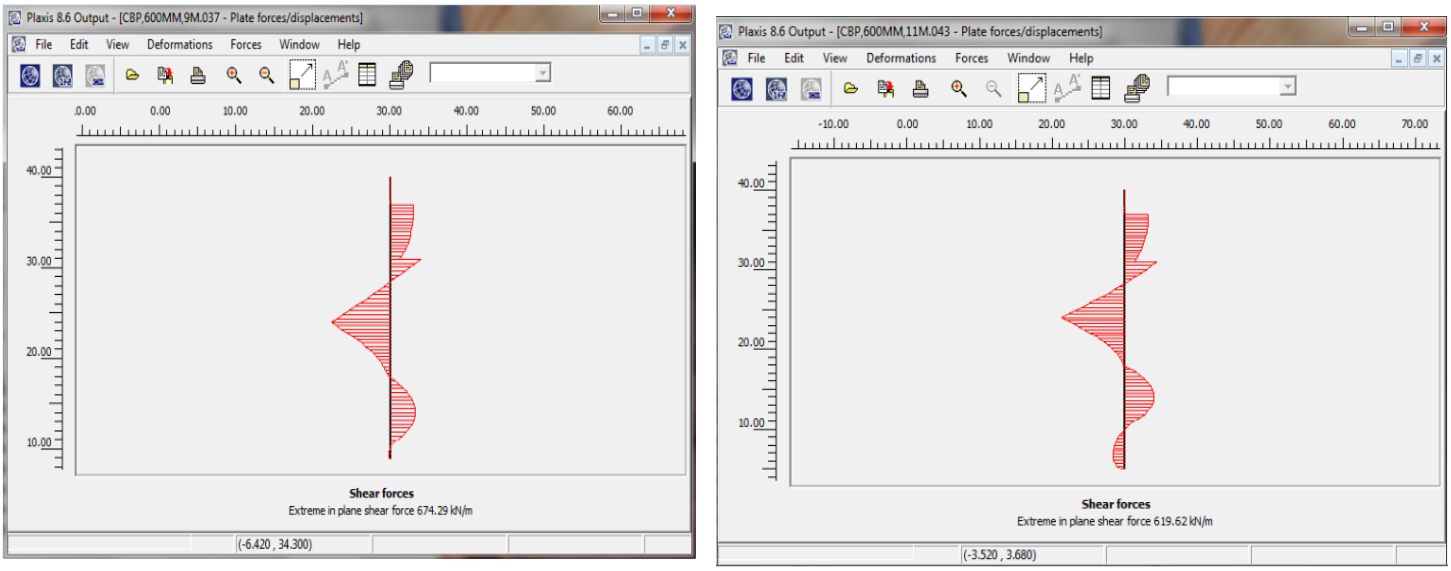

Figure 7.4shear force Diagram of CBP for 600mm diameter (a) 9m depth& (b) 11m depth

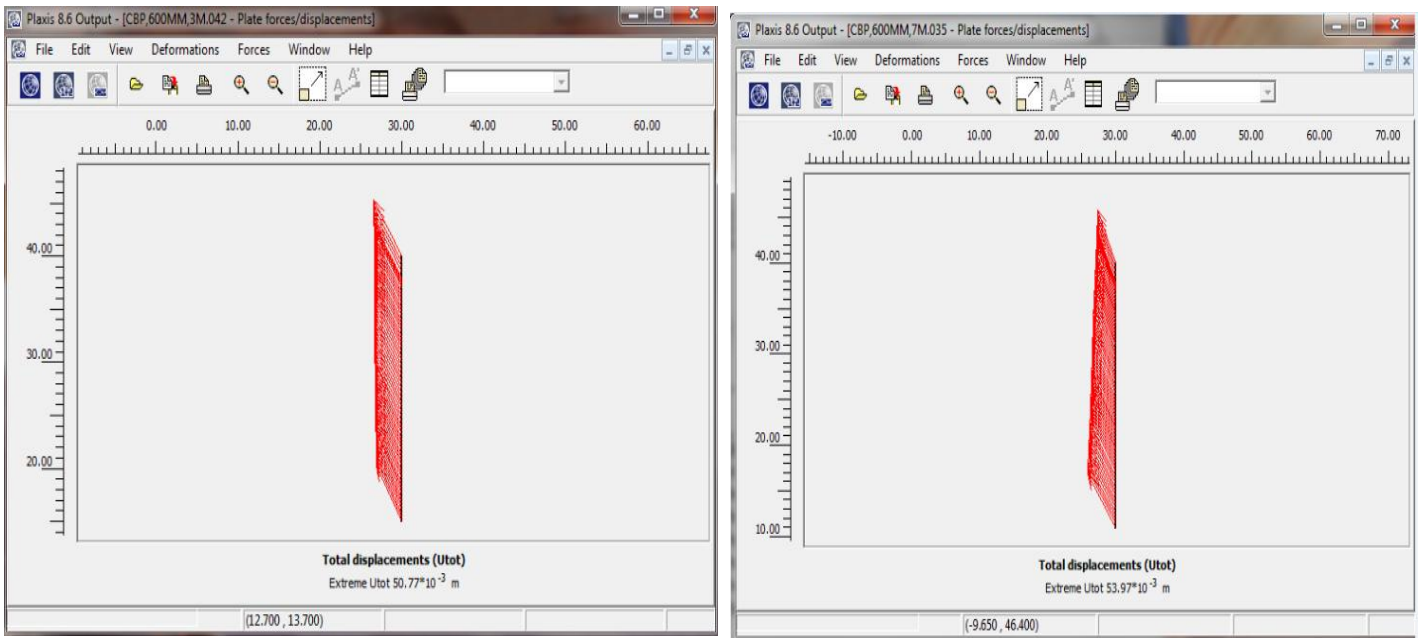

(a) (b)

Figure 7.5Lateral wall deflection Diagram of CBP for 600mm diameter (a) 3m depth& (b) 7m depth

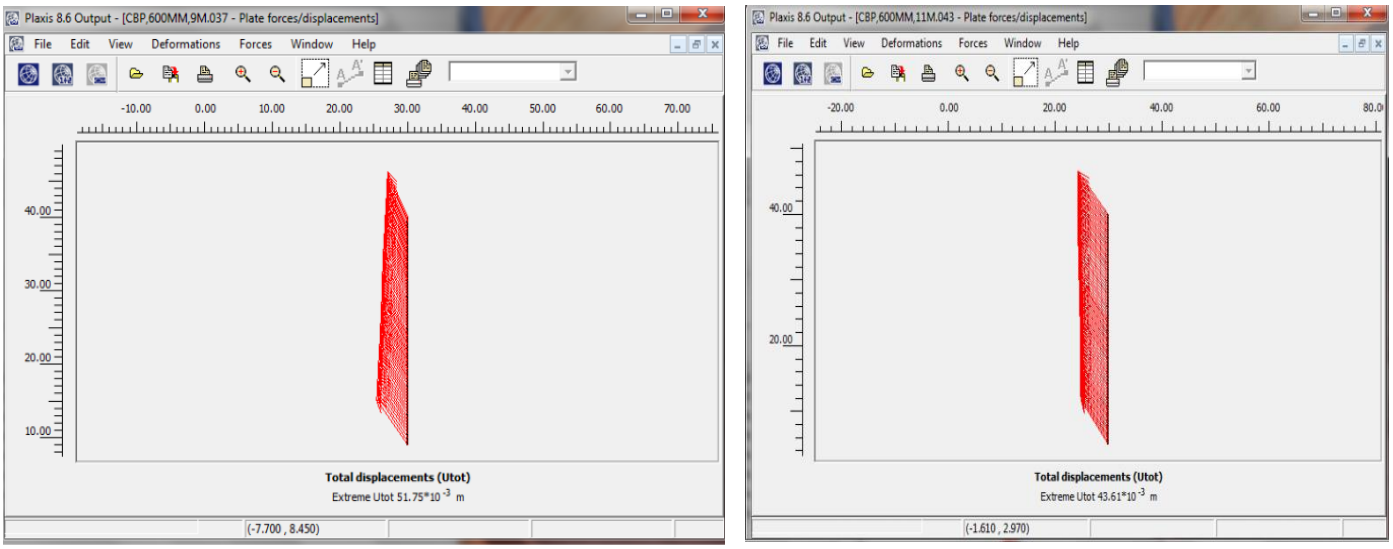

(a) (b)

Figure 7.6Lateral wall deflection Diagram of CBP for 600mm diameter (a) 9m depth& (b) 7m depth

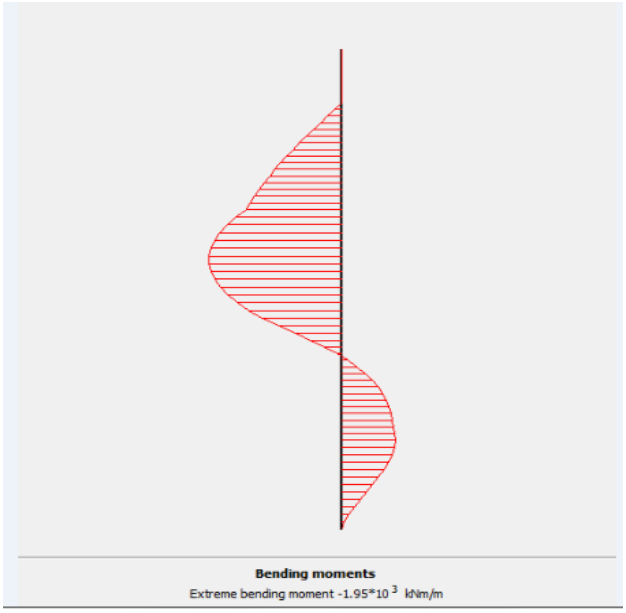

(a)

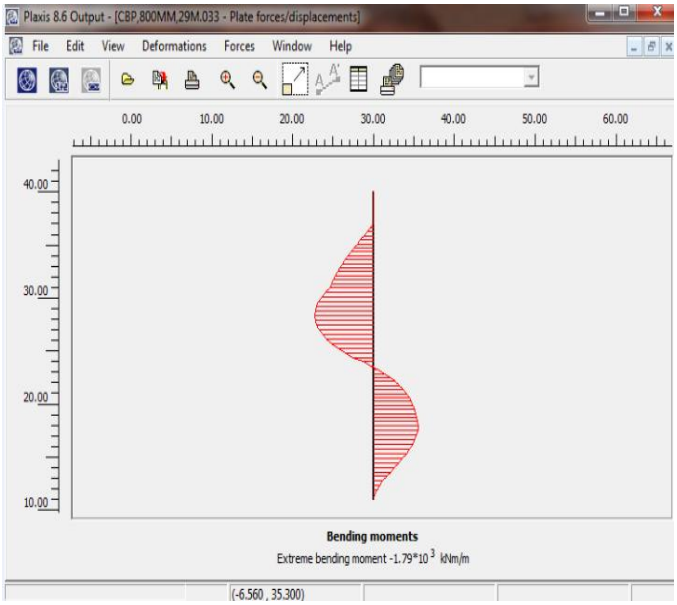

(b)

Figure 7.7Bending Moment Diagram of CBP for 800mm diameter (a) 5m depth& (b) 7m depth

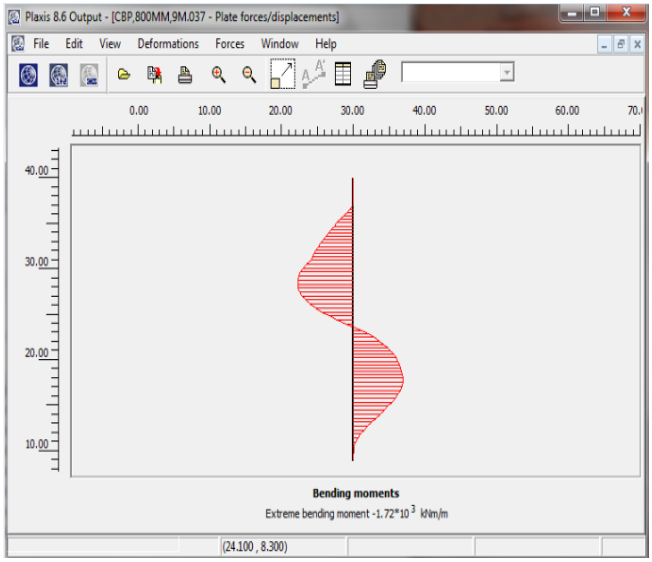

(a)

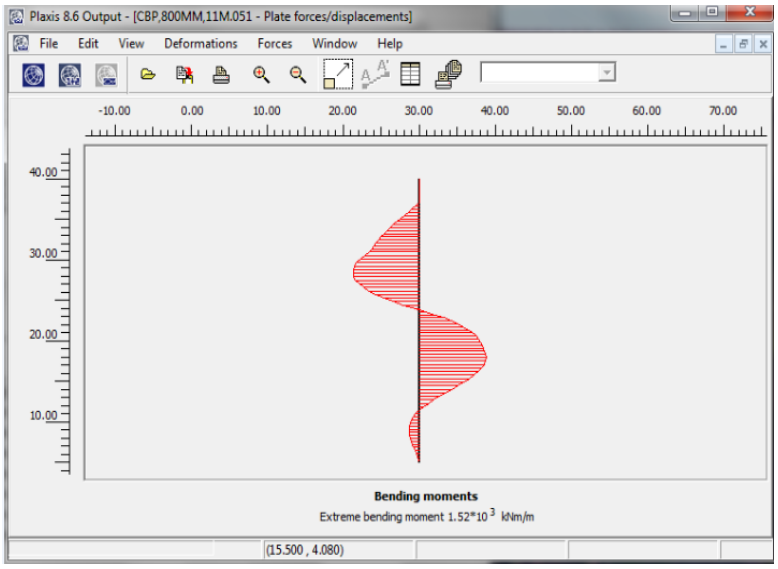

(b)

Figure 7.8Bending Moment Diagram of CBP for 800mm diameter (a) 9m depth& (b) 11m depth

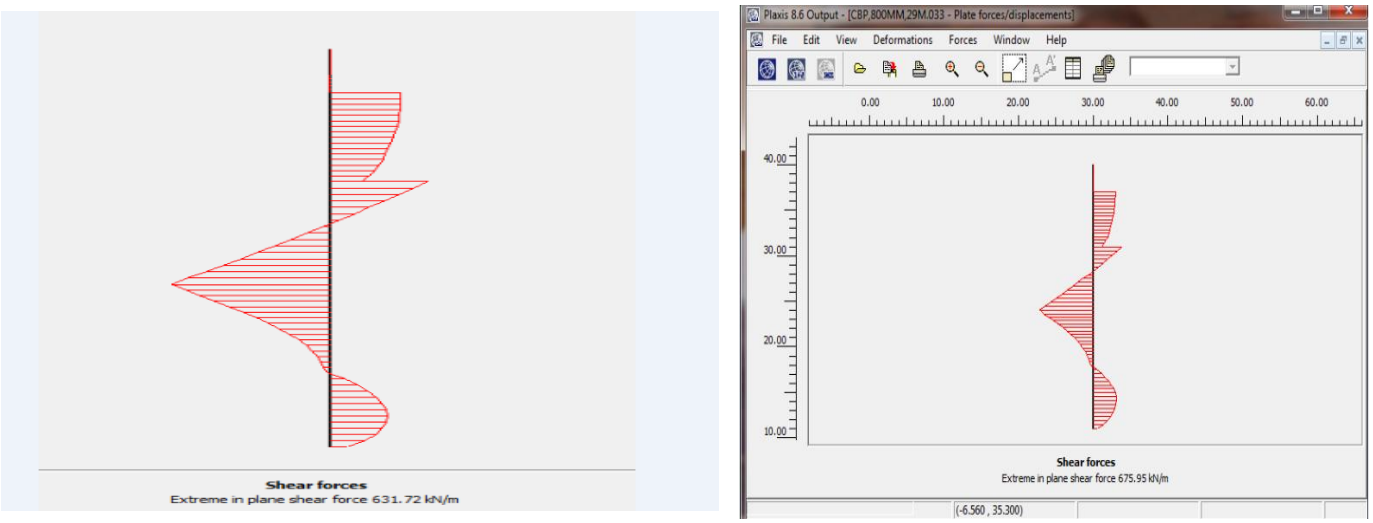

(a) (b)

Figure 7. 9shear force Diagram of CBP for 800mm diameter (a) 5m depth& (b) 7m depth

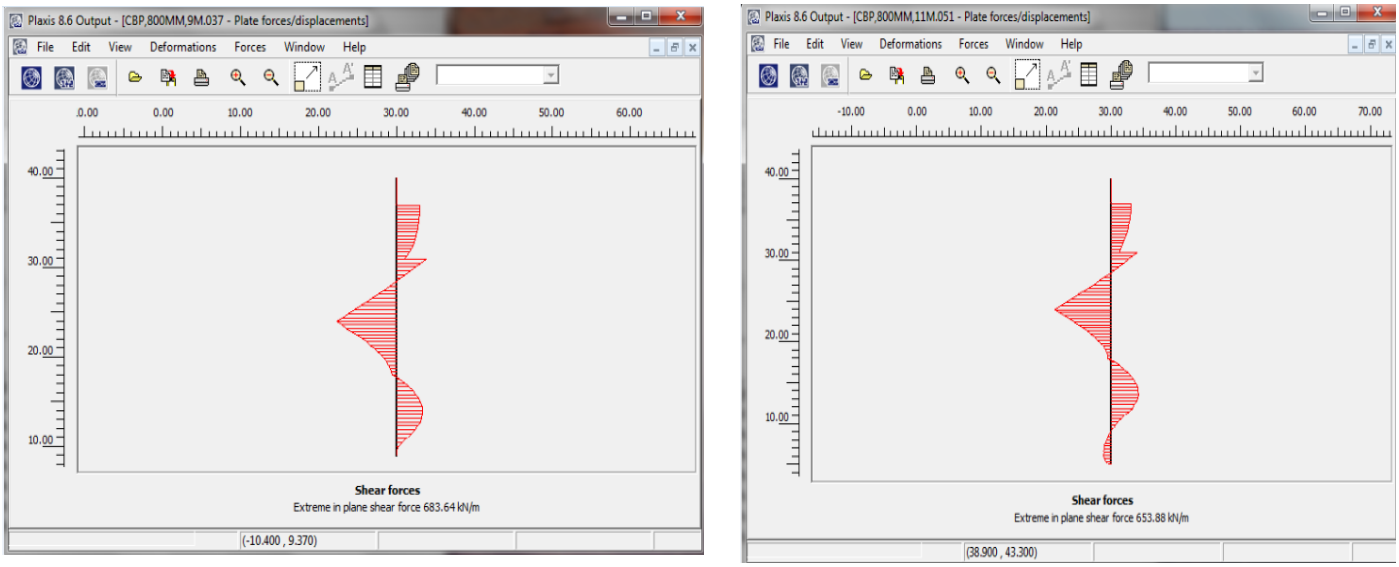

(a) (b)

Figure 7. 10 shear force Diagram of CBP for 800mm diameter (a) 9m depth& (b) 11m depth

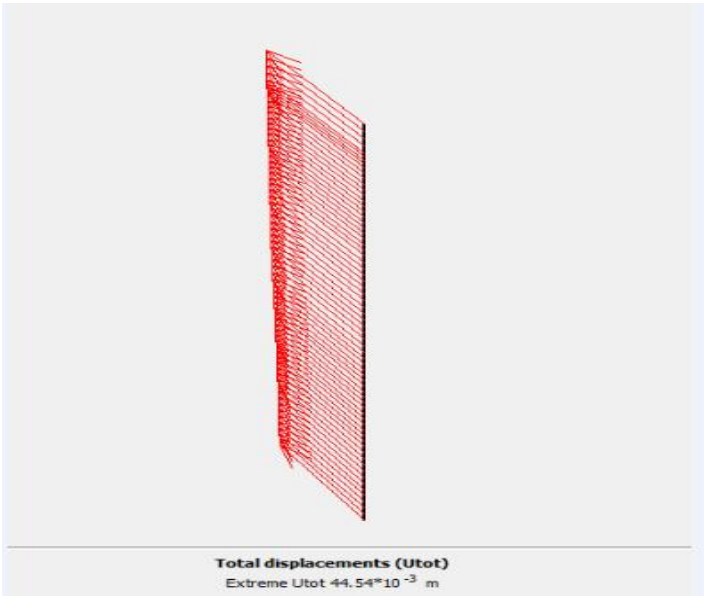

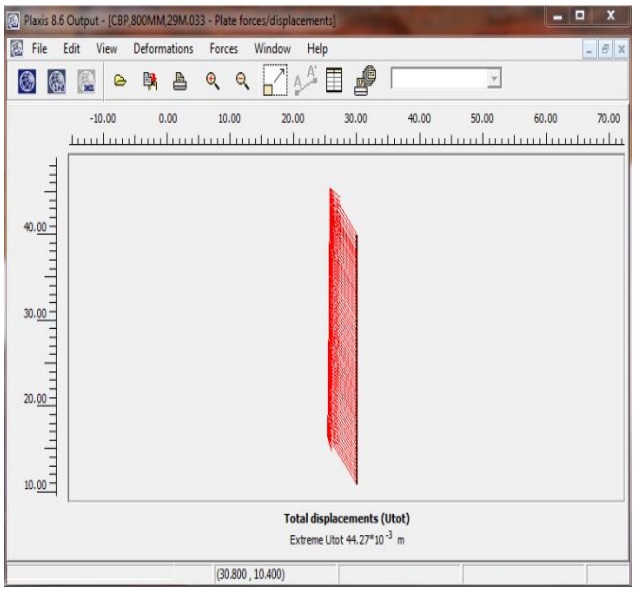

(a) (b)

Figure 7. 11Lateral wall deflection Diagram of CBP for 800mm diameter (a) 5m depth& (b) 7m depth

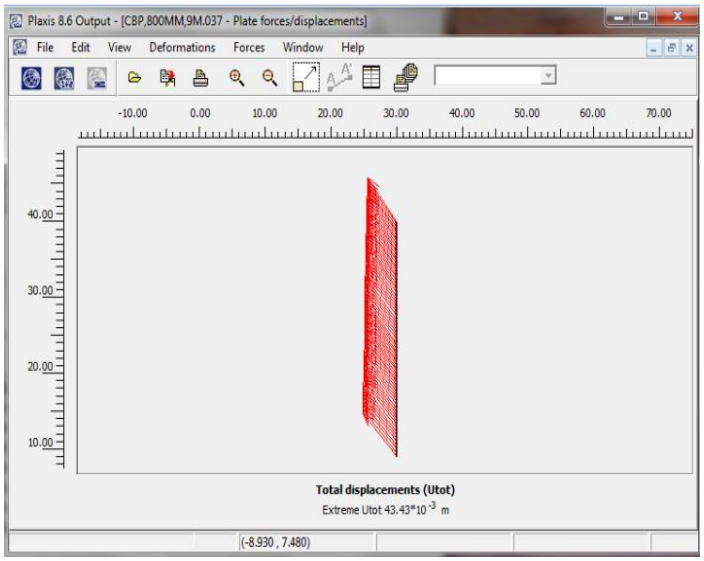

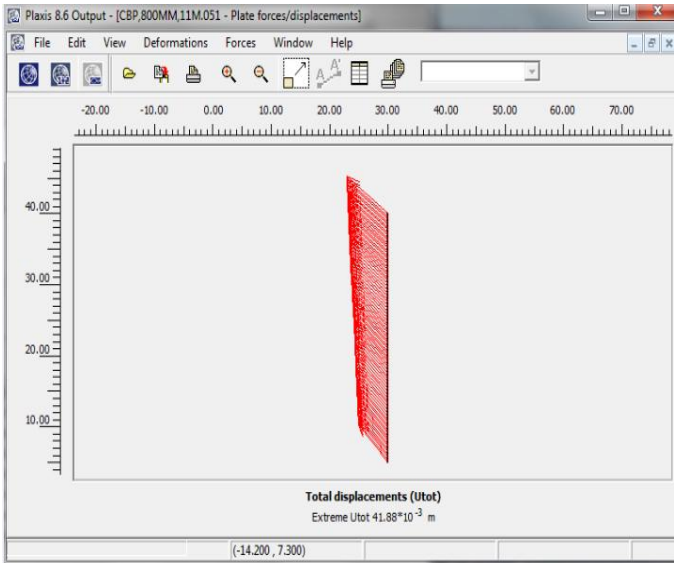

(a) (b)

Figure 7. 12Lateral wall deflection Diagram of CBP for 800mm diameter (a) 9m depth& (b) 11m depth

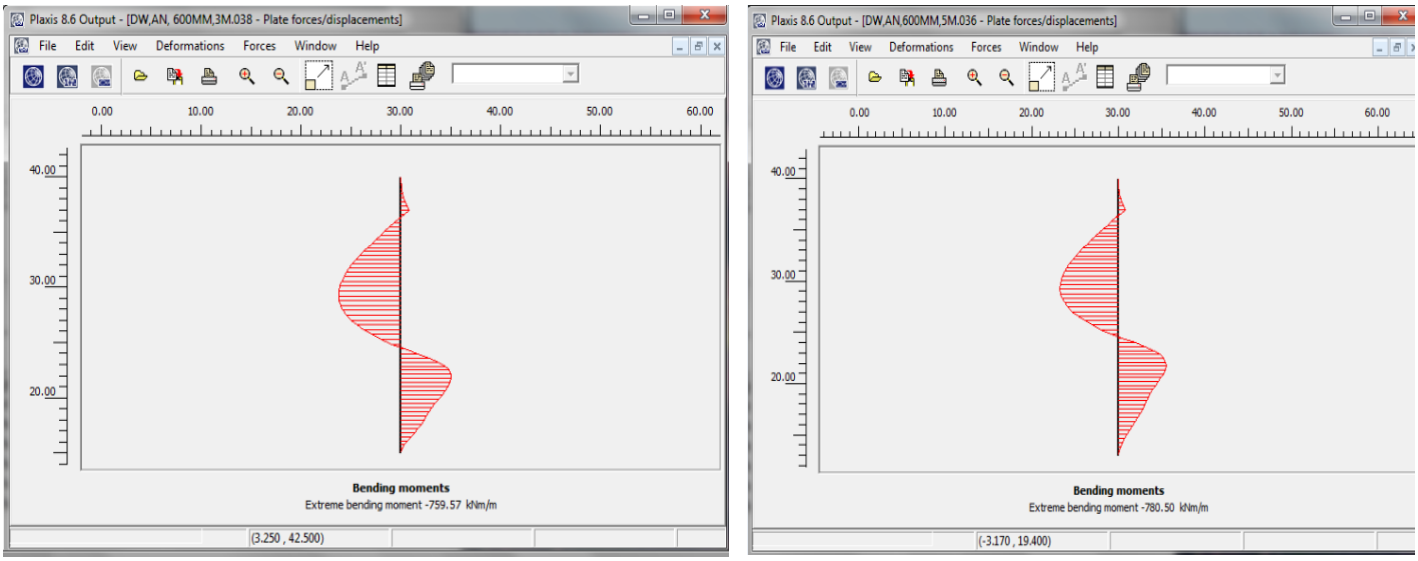

(a) (b)

Figure 7.13Bending Moment Diagram of DW for 600mm diameter (a) 3m depth& (b) 5m depth

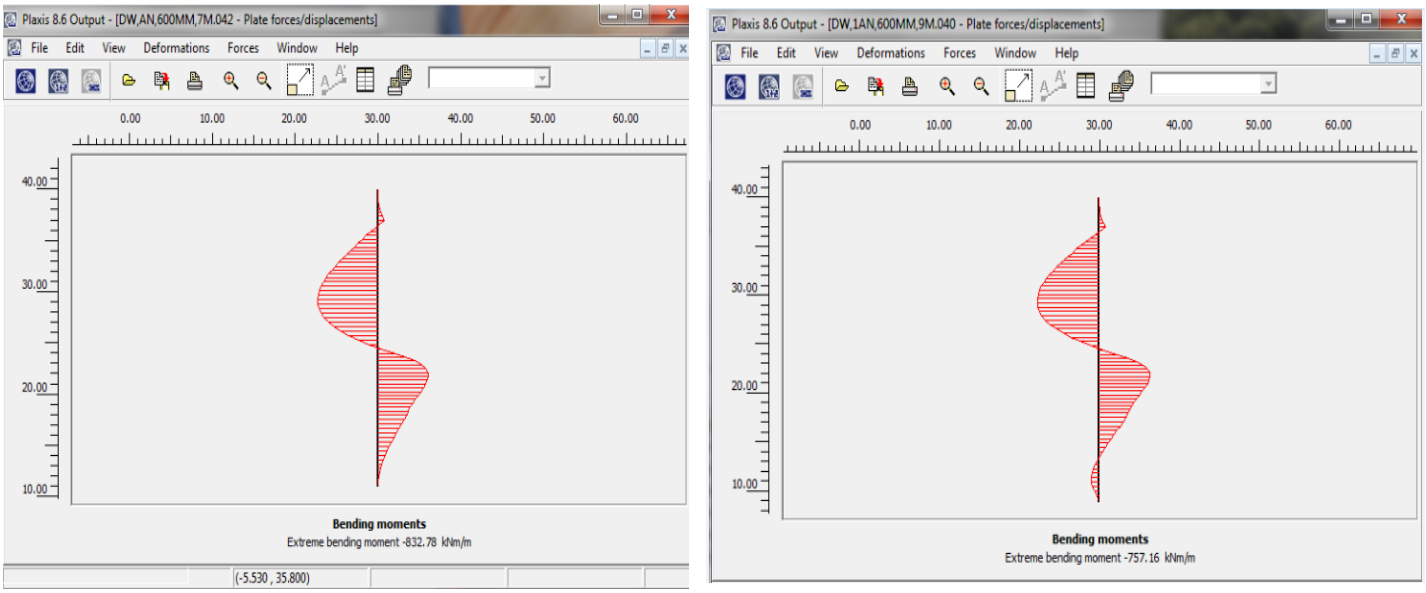

(a) (b)

Figure 7.14Bending Moment Diagram of DW for 600mm diameter (a) 7m depth& (b) 9m depth

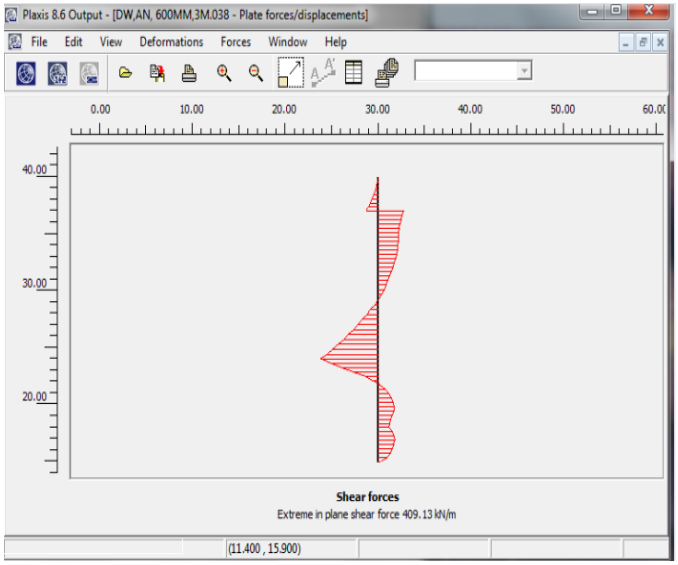

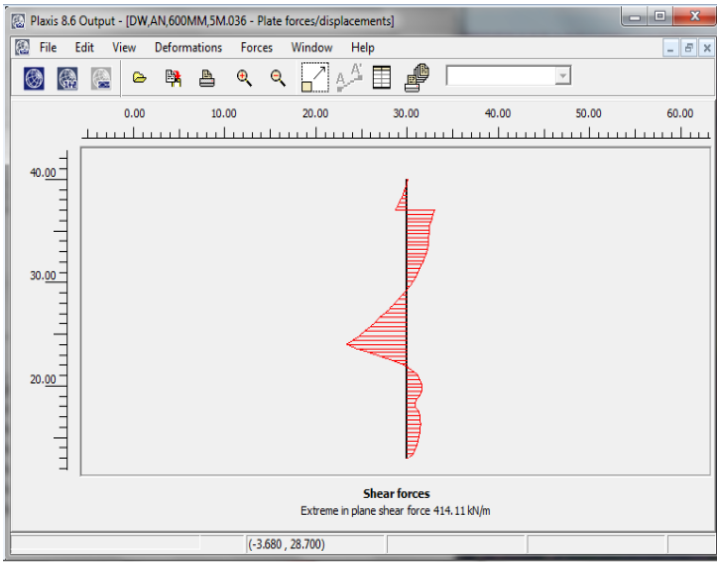

(a)(b)

Figure 7.15shear force Diagram of DW for 600mm diameter (a) 3m depth& (b) 5m depth

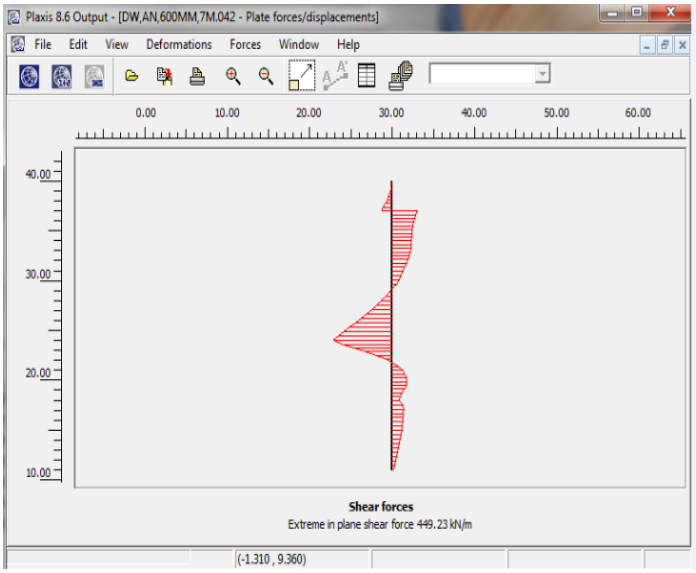

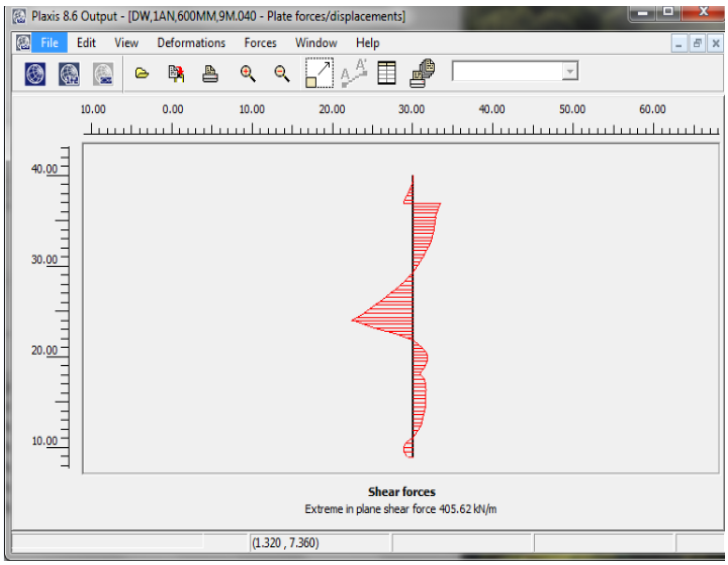

(a) (b)

Figure 7.16 shear force Diagram of DW for 600mm diameter (a) 7m depth& (b) 9m depth

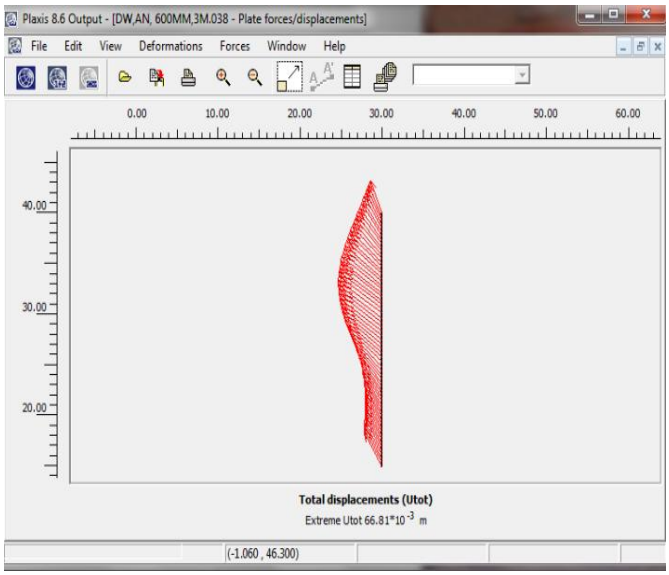

(a)

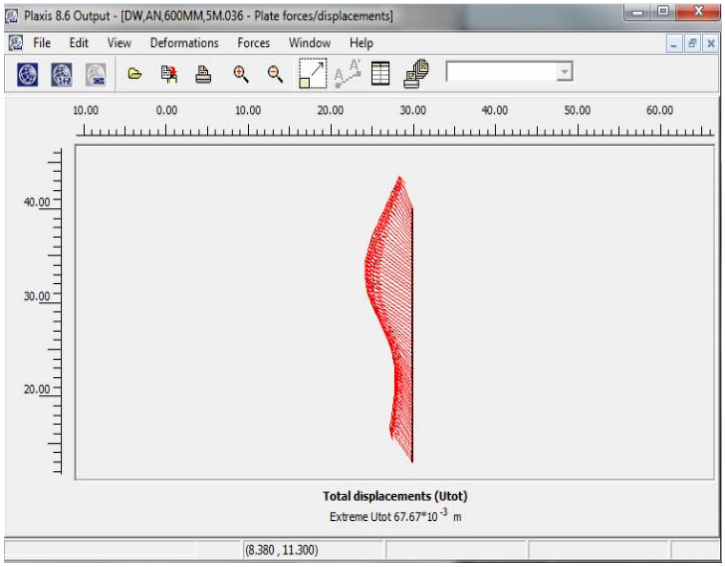

(b)

Figure 7. 17Lateral wall deflection Diagram of DW for 600mm diameter (a) 3m depth& (b) 5m depth

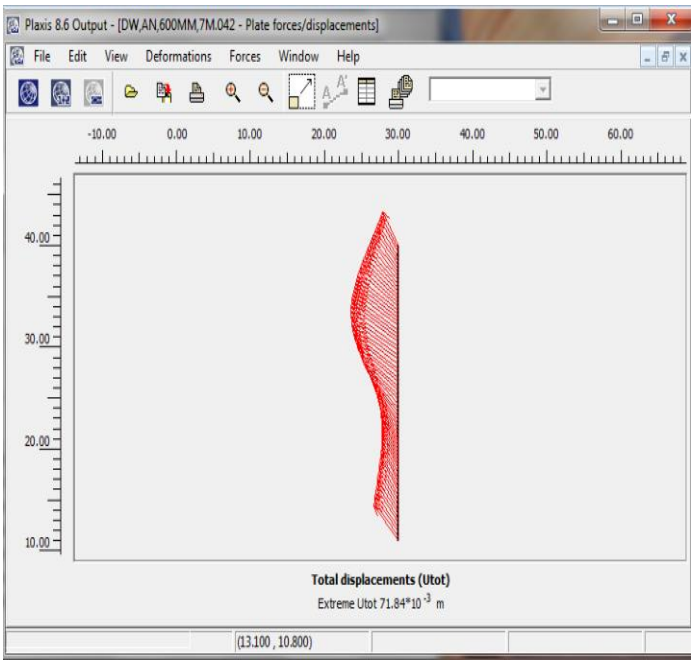

(a)

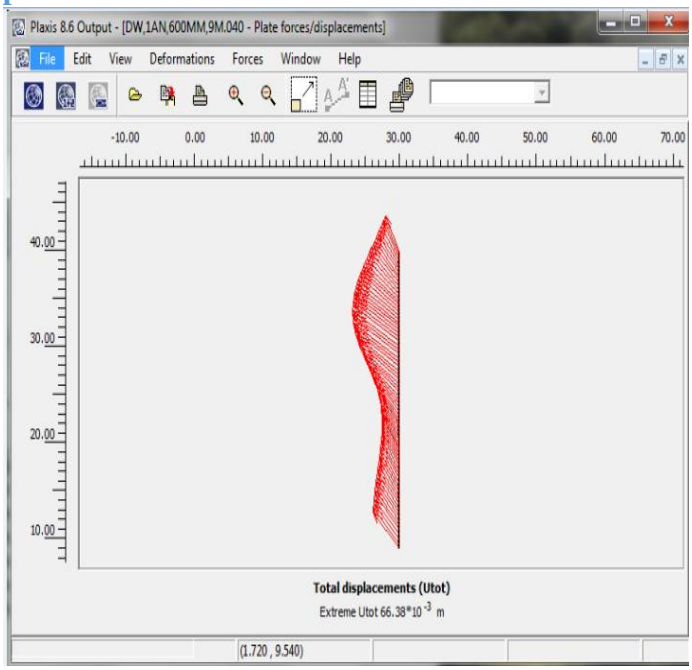

(b)

Figure 7.18Lateral wall deflection Diagram of DW for 600mm diameter (a) 7m depth& (b) 9m depth

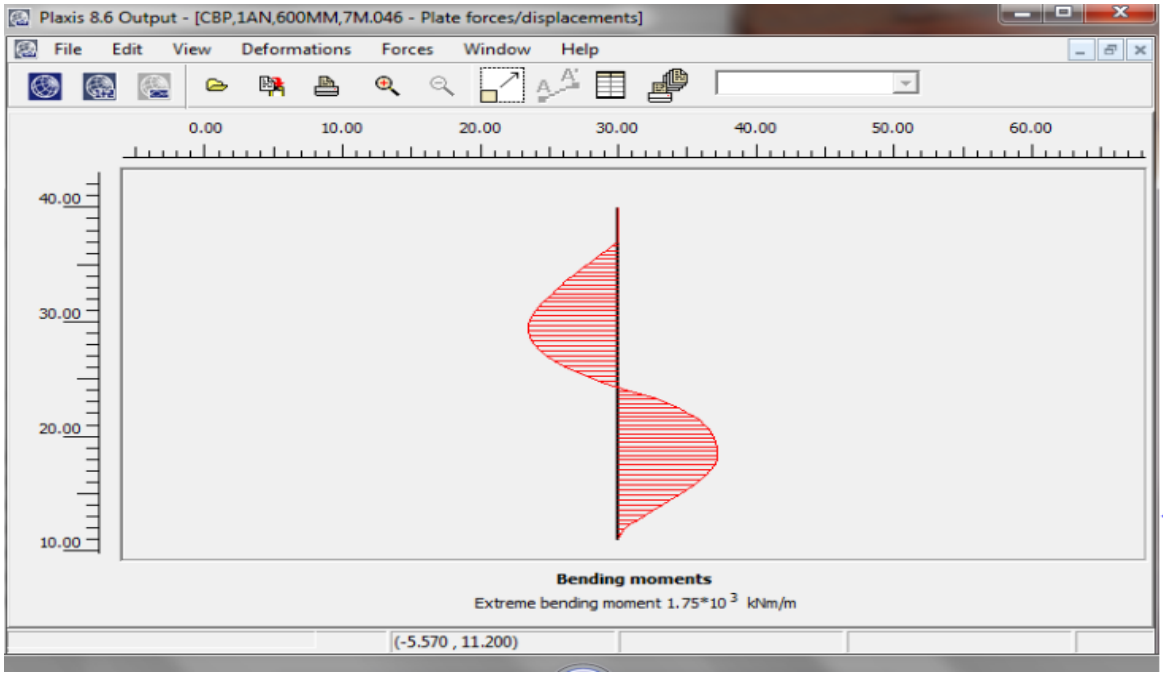

Figure 7.19 Bending Moment Diagram of CBP for 1Anchor @ 3m

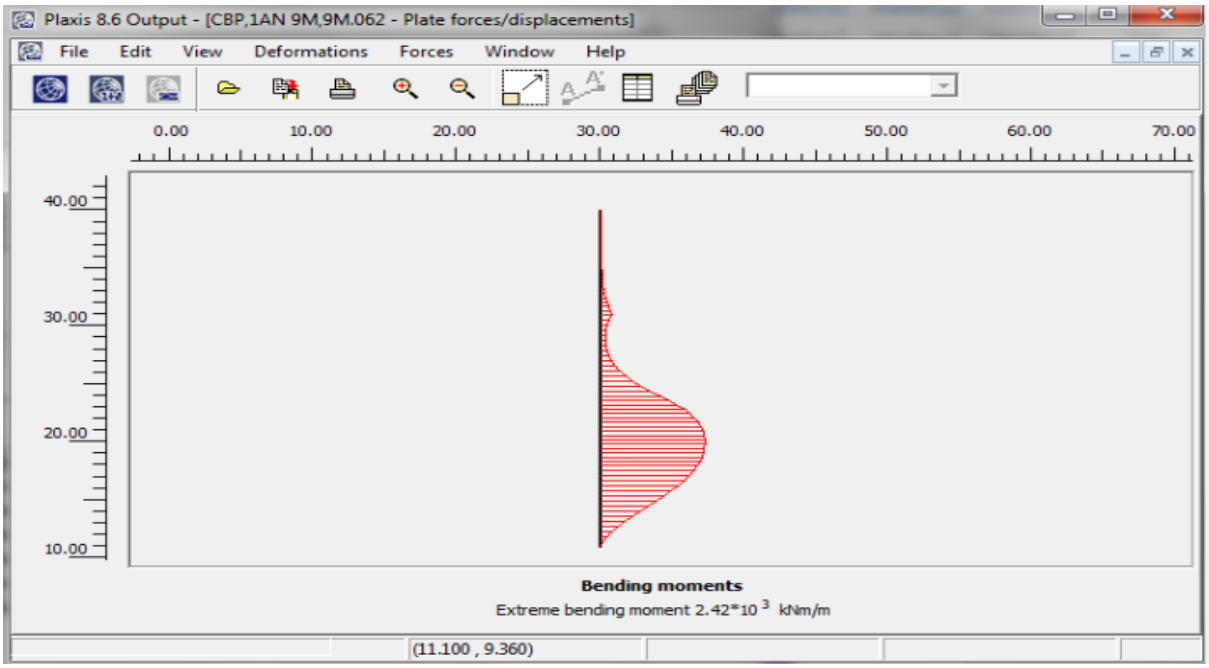

Figure 7.20Bending Moment Diagram of CBP for 1Anchor @ 9m

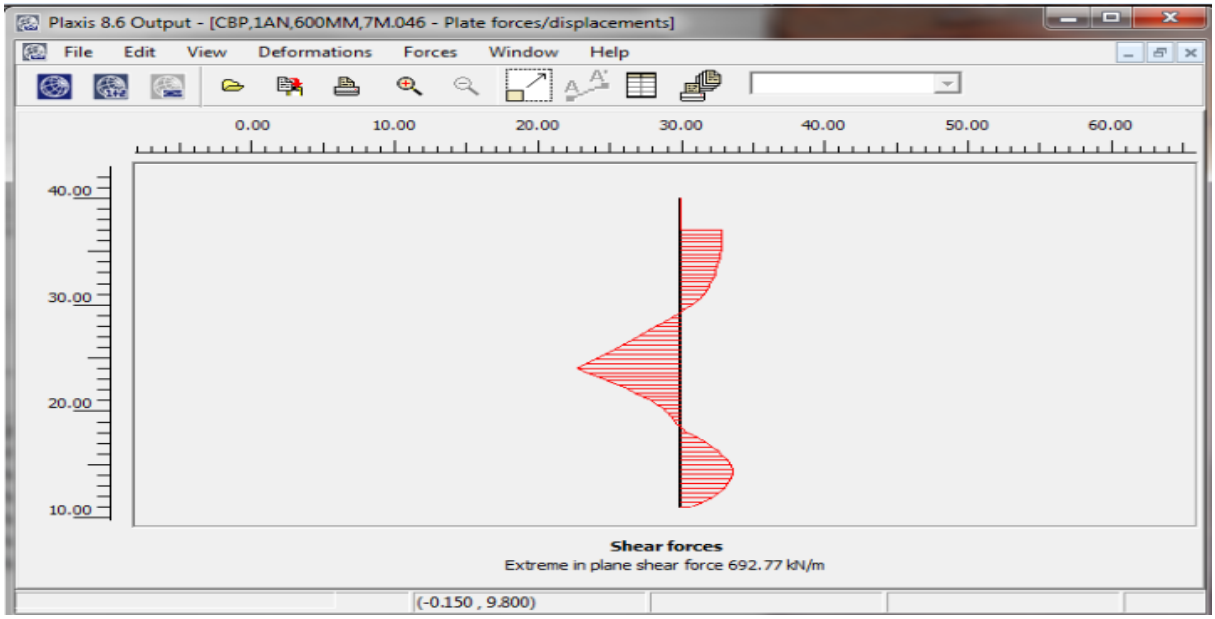

Figure 7.21Shear Force Diagram of CBP for 1Anchor @ 3m

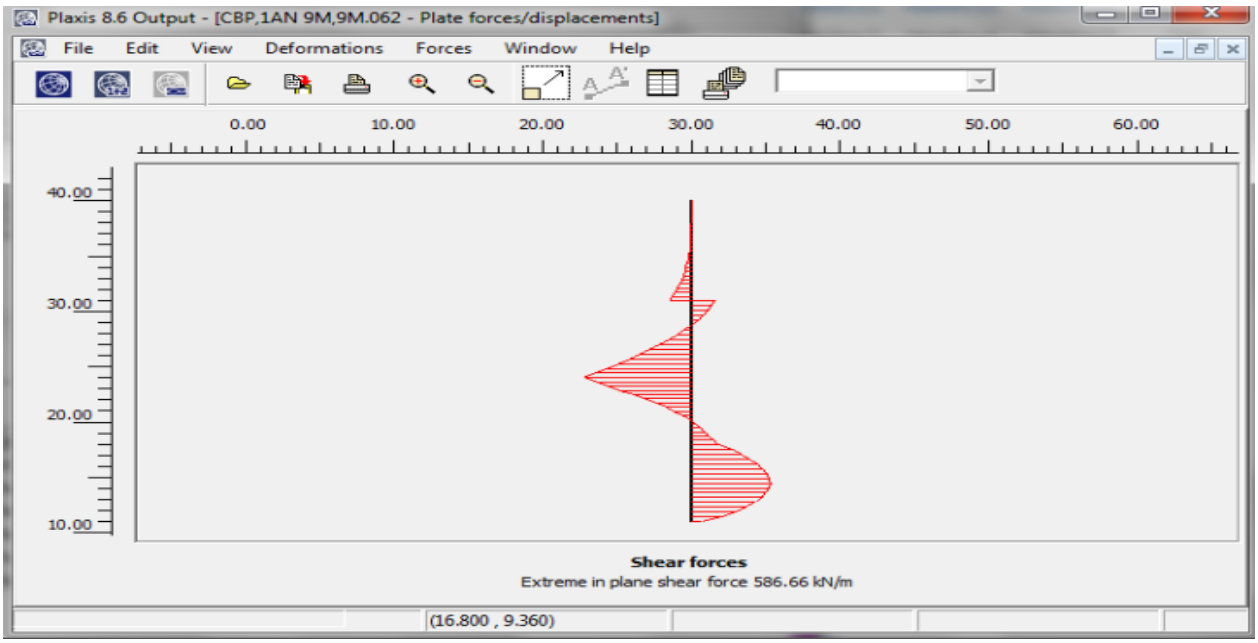

Figure 7.22Shear Force Diagram of CBP for 1Anchor @ 9m

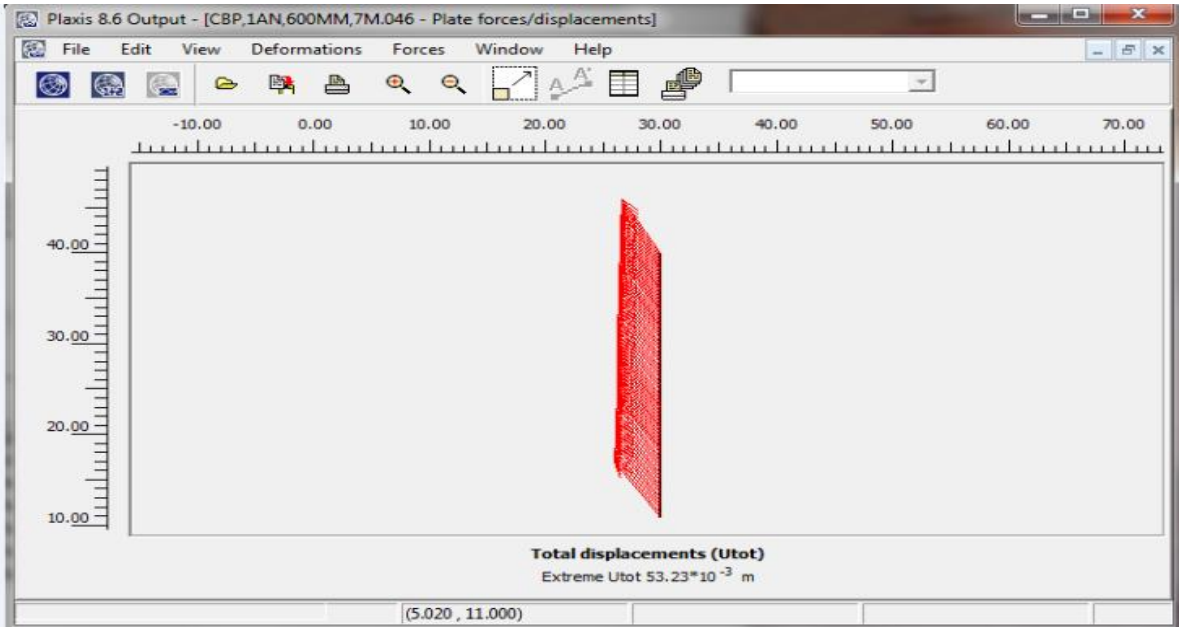

Figure 7.23Lateral Wall Deflection Diagram of CBP for 1Anchor @ 3m

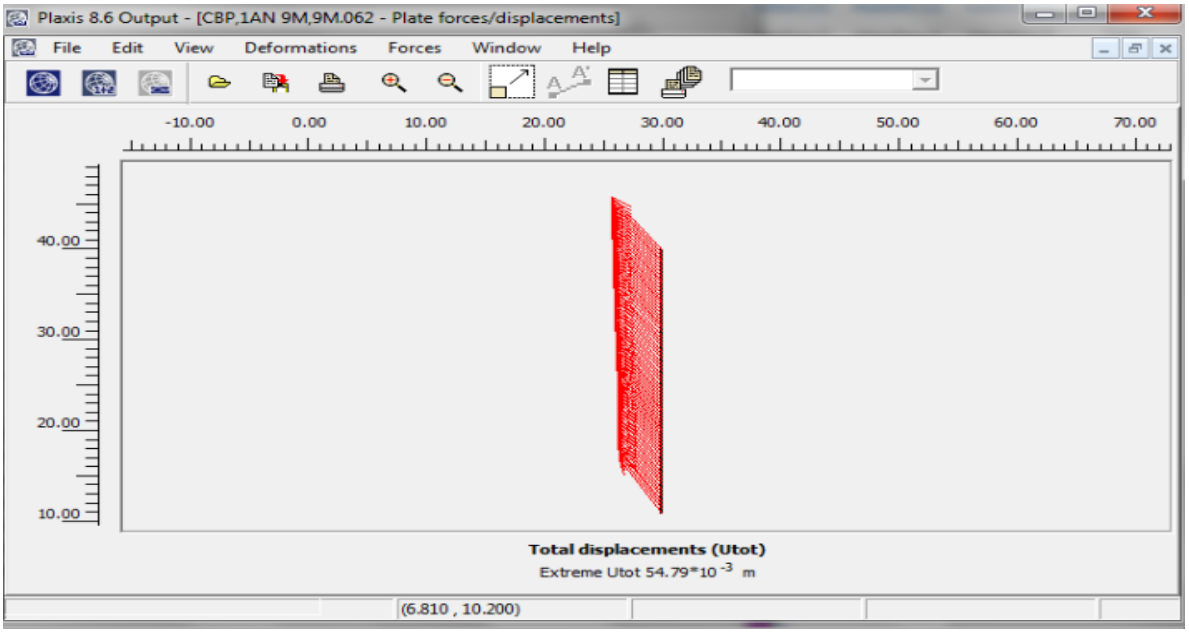

Figure 7.24Lateral Wall Deflection Diagram of CBP for 1Anchor @ 9m

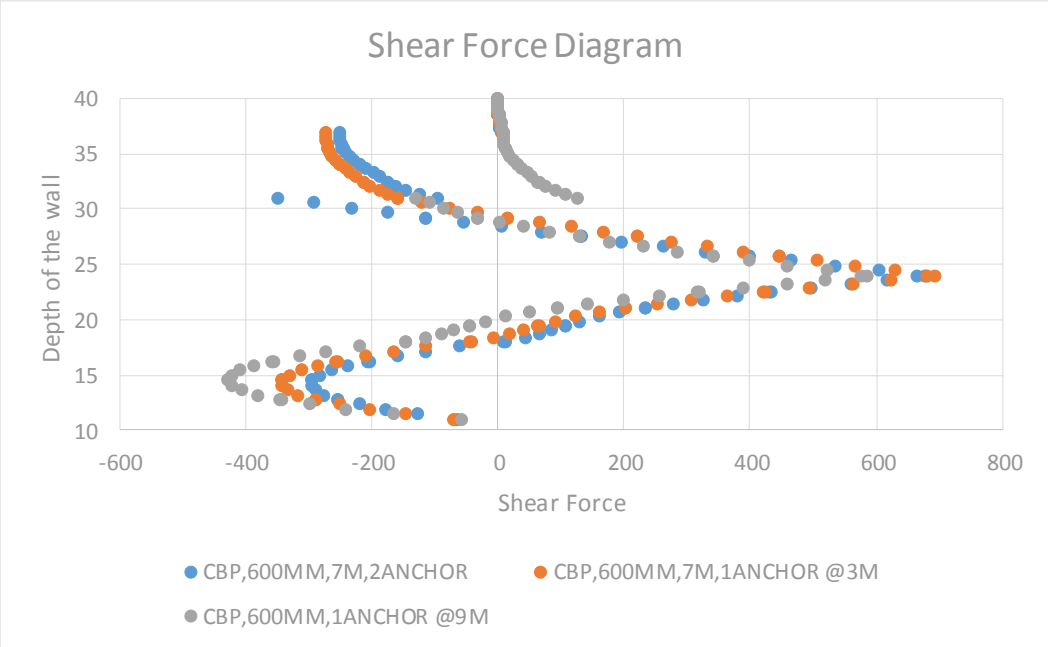

Figure 7.25Shear Force Diagram of CBP for 600mm diameter

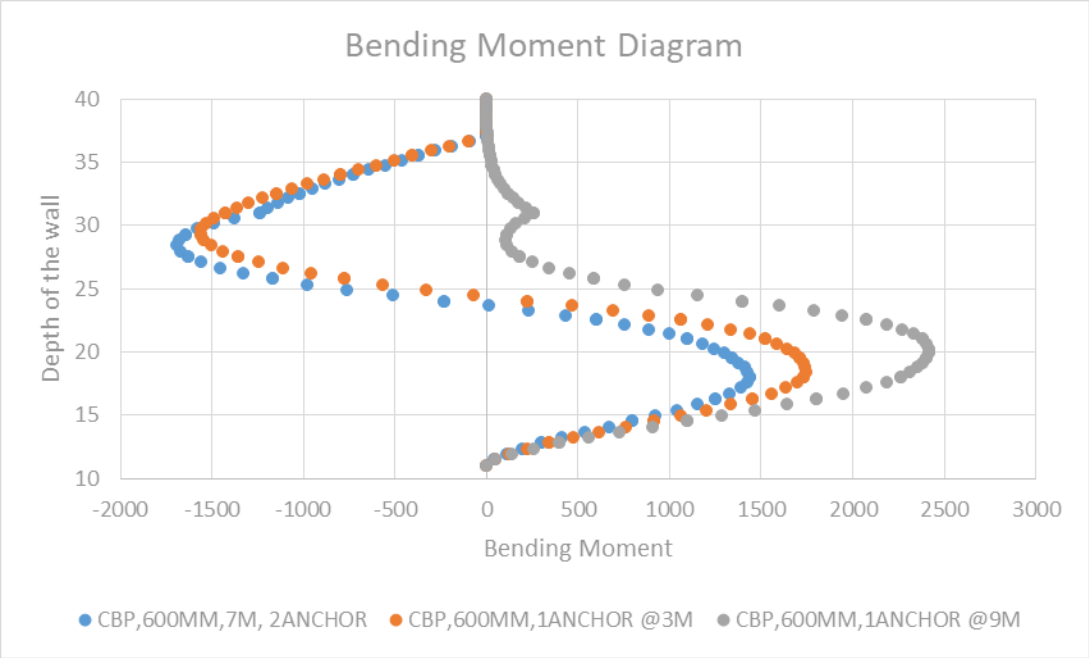

Figure 7.26 Bending Moment Diagram of CBP for 600mm diameter

VII. Appendix-Two

Unit cost breakdown for cost analysis

In this section, additional table related to unit rate (cost break down) for those different walls (DW and CBP) are presented in order to estimate the cost that each walls worth.

Table 7. 1: Direct Cost Analysis of contiguous Board Pile wall pilling work sheet one

DIRECT COST ANALYSIS SHEET

PROJECT: ZEMEN BANK S.C.

DESCRIPTION: Diameter 600mm pile - Boring in all soil formations

ITEM: LABOR HRLY OUTPUT / QUIPMENT HRLY OUTPUT

QUANTITY: RESULTANT 3.50 mL

MATERIAL COST

type of material	unit	qty	rate	cost/um
Core Barrel Teeth	no.	17161	500.00	139.34
Auger & Bucket Teeth	no.	14199	950.00	134.34
TOTAL				273.69
material unit cost				273.69

LABOR COST

labor by trade	No	UF	indvd hrly cost	hourly cost
Site Engineer	1	1/3	67.31	22.44
Foreman	1	1	57.69	57.69
Operator	2	1	182.69	365.38
Front man	1	1	19.23	19.23
Mechanic	2	1	120.19	240.38
Electrician	1	1	120.19	120.19
Welder	2	1	81.49	162.98
Helpers	5	1	8.75	43.75
Surveyor	1	1	72.12	72.12
TOTAL				1,104.17
manpower unit cost				315.48

EQUIPMENT COST

type of equipment	No.	UF	hrly rental rate	hourly cost
Drilling Rig	1.00	1	4,500.00	4,500.00
Excavator	1.00	0	1,100.00	-
Welding Machir	2.00	1	185.00	370.00
Casing	1.00	1	200	200.00
Water pump	1.00	1	26.16	26.16
Dump truck	1.00	0	300.00	-
Hand tools	10.00	1	1.00	10.00
TOTAL				5,106.16
equipment unit cost				1,458.90

DIRECT COST OF WORK ITEM: 2,048.07 ETB/m

REMARK & ASSUMPTIONS

Table 7. 2: Direct Cost Analysis of contiguous Board Pile wall pilling work sheet two

DIRECT COST ANALYSIS SHEET

PROJECT	ZEMEN BANK S.C.	LABOR HRLY OUTPUT	
DESCRIPTION		EQUIPMENT HRLY OUTPUT	
ITEM		RESULTANT	3.50 m3
QUANTITY			

MATERIAL COST

type of material	unit	qty	rate	cost/un
cement	qtls	4.00	275.00	1,100.00
sand	m3	0.52	620.00	322.40
aggregate	m3	0.78	450.00	351.00
Waste & shrinkage	%	10%	1.00	177.34
TOTAL				1,950.74

LABOR COST

labor by trade	No	UF	indxd hrly cost	hourly cost
Concrete Forman	1	1/3	38.46	12.82
Operator I	1	1/3	48.08	16.03
Laborers	20	1/3	8.75	58.33
TOTAL				87.18

EQUIPMENT COST

type of equipment	No.	UF	hrly rental rate	hourly cost
Car mixer	1.00	1	750.00	750.00
Trimie Pipe	1.00	1	200.00	200.00
tools	3.00	1	1.00	3.00
Crane	1.00	1	1,400.00	1,400.00
TOTAL				2,353.00

material unit cost	1,950.74	manpower unit cost	24.91	equipment unit cost	672.29

DIRECT COST OF WORK ITEM 2,647.93 ETB/m³

REMARK & ASSUMPTIONS

Page 5

Table 7. 3: Direct Cost Analysis of contiguous Board Pile wall pilling work sheet three

DIRECT COST ANALYSIS SHEET

PROJECT	ZEMEN BANK S.C.	LABOR HRLY OUTPUT	
DESCRIPTION	Reinforcement Cage Production & Installation	EQUIPMENT HRLY OUTPUT	
ITEM		RESULTANT	25.00 kg
QUANTITY			

MATERIAL COST

type of material	unit	qty	rate	cost/un
reinforcement bar	kg	1.05	40.00	42.00
Black wire	kg	0.01	25.00	0.25
TOTAL				42.25

LABOR COST

labor by trade	No	UF	indxd hrly cost	hourly cost
Bar bender forman	1	1/8	31.25	3.91
Bar bender III	1	1	31.25	31.25
Daily labourer	3	1	31.25	93.75
TOTAL				128.91

EQUIPMENT COST

type of equipment	No.	UF	hrly rental rate	hourly cost
Cutting Machine	1.00	0.13	5.02	0.63
Bending machine	1.00	0.13	2.61	0.33
tools	1.00	1.00	1.00	1.00
Crane	1.00	1.00	36.84	36.84
TOTAL				38.80

material unit cost	42.25	manpower unit cost	5.16	equipment unit cost	1.55

DIRECT COST OF WORK ITEM 48.96 ETB/kg

REMARK & ASSUMPTIONS: Hourly rental rate of crane for this case = 1400 Birr per hr/700kg(avg. weight of the steel cage)*25(production output)

Page 6

Table 7. 4: contiguous Board Pile wall Bill of Quantity Concrete work

NO	Description	Unit	Qty	Rate	Amount
	CBP				
	1. Concrete work				
	1.1 Reinforced concret in c-25 with minimum cement content of 360kg/ m3 . Cast in to formwork and vibrated around reinforcement (reinforcement and formwork measured separetely)				
	a) pile circle column				
	d=29m	m3	29	2853.54	82,752.66
	1.2 shootcreat	m3	1.375	2622.36	3,605.25
	Steel reinforcement according to structural drawing ,price including cutting bending & placing in position & tying wires				
	a) dia 8 deformed bar	kg	45.76	51.95	2,377.31
	d) dia 10 deformed bar	kg	472.8622	51.95	24,566.00
	e)dia 16 deformed bar	kg	505.29	51.95	26,250.68
	total carried to summary				139,551.9

Table 7. 5: Direct Cost Analysis of Diaphragm wall pilling work sheet one

DIRECT COST ANALYSIS SHEET

PROJECT	ZEMEN BANK S.C.	LABOR HRLY OUTPUT	
DESCRIPTION		EQUIPMENT HRLY OUTPUT	
ITEM		RESULTANT	3.50 m3
QUANTITY			

MATERIAL COST

type of material	unit	qty	rate	cost/un
cement	qtls	4.00	275.00	1,100.00
sand	m3	0.52	620.00	322.40
aggregate	m3	0.78	450.00	351.00
Waste & shrinkage	%	10%	1.00	177.34
TOTAL				1,950.74
material unit cost				1,950.74

LABOR COST

labor by trade	No	UF	indxd hrly cost	hourly cost
Concrete Forman	1	1/3	38.46	12.82
Operator I	1	1/3	48.08	16.03
Laborers	20	1/3	8.75	58.33
TOTAL				87.18
manpower unit cost				24.91

EQUIPMENT COST

type of equipment	No.	UF	hrly rental rate	hourly cost
Car mixer	1.00	1	750.00	750.00
Trimie Pipe	1.00	1	200.00	200.00
tools	3.00	1	1.00	3.00
Crane	1.00	1	1,400.00	1,400.00
TOTAL				2,353.00
equipment unit cost				672.29

DIRECT COST OF WORK ITEM 2,647.93 ETB/m³

REMARK & ASSUMPTIONS

Page 5

Table 7. 6: Diaphragm Wall BOQ shoring Works with thickness 600mm

Item No.	Description	Unit	Total Quantity	Unit Price	Total Price
1	Drilling Equipment Mobilization	Lump sum	1	171,962.08	171,962.08
2	Drilling Equipment Demobilization	Lump sum	1	86,574.58	86,574.58
3	Anchoring, shotcreting and grouting machine mobilization	Lump sum	1	26,869.87	26,869.87
4	Anchoring shotcreting and grouting machine demobilization	Lump sum	1	26,869.87	26,869.87
5	Drilling cost	m3	33	1,400.00	46,200
6	Reinforcement cage installation	Kg	1224.00	51.95	63,586.80
7	Piling Concrete Installation	m3	33	2735.54	90,272.82
8	Installation of Temporary Grouted Anchors	M	39	2,474.93	96,522.27
9	Stressing and Proof testing of Anchors	No.	3	2,197.89	6,593.67
10	Bentonite and Cement	m2	468	42	19,656.00
TOTAL					635,107.96
VAT (15%)					95,266.19
GRAND TOTAL					730,374.15

Table 7. 7: Diaphragm wall Bill of Quantity concrete work

	DW				
	1. Concrete work				
	1.1 5cm thick lean concrete class C-5				
	lean concrete pile coiumn	m2	2	108.25	216.50
	1.2 Reinforced concret in c-25 with minimum cement content of 360kg/ m3 . Cast in to formwork and vibrated around reinforcement (reinforcement and formwork measured separetely)				
	shear wall				
	t=0.60	m3	24.17445	2735.54	66,130.16
	1.3 Provide cut and fix in position sawn zigba wood or equivalent formwork				-
	t=0.60	m2	167.4	319.56	53,493.63
	total carried to summary				**119,840.29**

Table 7. 8: CBP Shoring pile Concrete Take-off

			CBP
			1.concrete
			1.1 Reinforced concret in c-25 with minimum cement content of 360kg/ m3 . Cast in to formwork and vibrated around reinforcement (reinforcement and formwork measured separately)
			a) pile circle column
			v=3.14r2*h
			d=22m
2	0.5		
	29		
		29	m3
			1.2 shootcreat
	2.5		
	11		
	0.05		
		1.375	m3

Table 7. 9: Diaphragm Wall Shoring pile Concrete Take-off

			DW
			1. Concrete work
			1.1 5cm thick lean concrete class C-5
			lean concrete pile coiumn
	2.5		
	0.8		
		2	m2
			1.2 Reinforced concret in c-25 with minimum cement content of 360kg/ m3 . Cast in to formwork and vibrated around reinforcement (reinforcement and formwork measured separetely)
			shear wall
			t=0.60
	22		
	2.5		
	0.6		
		33	m3
			1.3 Provide cut and fix in position sawn zigba wood or equivalent formwork
			t=0.60
	22		
	6.2		
		136.4	m2